

UNCLASSIFIED

AD NUMBER
AD863519
NEW LIMITATION CHANGE
TO Approved for public release, distribution unlimited
FROM Distribution authorized to U.S. Gov't. agencies and their contractors; Administrative/Operational Use; 01 OCT 1969. Other requests shall be referred to Naval Postgraduate School, Monterey, CA.
AUTHORITY
NPS ltr 1 Oct 1971

THIS PAGE IS UNCLASSIFIED

AD 863519

United States Naval Postgraduate School



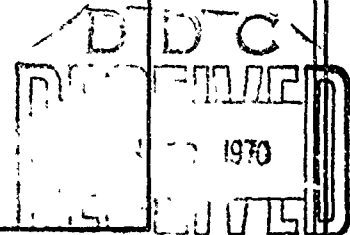
AN INVESTIGATION OF THE EFFECTS OF ACCELERATION
ON THE BURNING RATES OF SOLID PROPELLANTS

by

D. W. NETZER, R. C. BATES

W. BRINGHURST, JR., M. J. BULMAN

1 October 1969



Reproduced by the
CLEARINGHOUSE
for Federal Scientific & Technical
Information Springfield Va 22151

A

This document is subject to special export controls and each transmittal to foreign government or foreign nationals may be made only with prior approval of the Naval Postgraduate School, Monterey, California 93940 (Code 023).

DISCLAIMER NOTICE

THIS DOCUMENT IS BEST QUALITY PRACTICABLE. THE COPY FURNISHED TO DTIC CONTAINED A SIGNIFICANT NUMBER OF PAGES WHICH DO NOT REPRODUCE LEGIBLY.

NAVAL POSTGRADUATE SCHOOL
Monterey, California

Rear Admiral R. W. McNitt, USN
Superintendent

R. F. Rinehart
Academic Dean

ABSTRACT:

The acceleration sensitivity of aluminized and nonmetallized composite and double-base propellants were investigated. A review of previous experimental findings and current analytical models was also conducted.

Ten composite propellants were tested to accelerations of 100G and pressures of 1000 psia to determine the effects of AP crystal size, base burning rate, pressure, the form of the molten metal on the burning propellant surface, and temperature on the acceleration sensitivity. The most dominant factor influencing acceleration sensitivity was found to be the base burning rate. The weight and form of the molten metal on the burning surface were found to be important at low accelerations. At high accelerations, the form of the molten metal was found to have more effect on augmentation than the weight. Burn time (web thickness) was also found to have a pronounced effect on the augmentation.

The experimental data were compared with current analytical models and qualitative agreement was obtained. A change was proposed for the nonmetallized analytical model which yielded better agreement with the experimental data.

An investigation was conducted to determine the cause(s) for the differences in burning rate augmentation data reported by various investigators. Strand length (burn time) was found to be the dominant factor.

Lead and copper additives commonly found in double-base propellants were found to decrease the burning rate with increasing acceleration. Burning rate instability was also obtained at high accelerations. The addition of aluminum increased the burning rate at any given acceleration.

This task was supported by: Naval Ordnance Systems Command
ORD-032-135/551-1/F009-06-01



David W. Netzer
Assistant Professor

Approved by:


R. W. Bell, Chairman
Department of Aeronautics

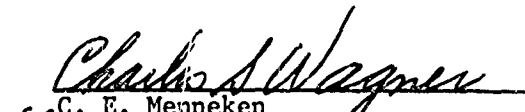

for C. E. Menneken
Dean of Research Administration

TABLE OF CONTENTS

Section		Page
I	INTRODUCTION	9
II	REVIEW OF PAST INVESTIGATIONS.	10
	Analytical	10
	Experimental	16
III	PURPOSE OF INVESTIGATION	20
IV	EXPERIMENTAL EQUIPMENT AND PROCEDURES.	21
V	METHOD OF INVESTIGATION AND PROPELLANTS.	23
	General Discussion	23
	Propellants.	23
	Method of Investigation.	25
VI	EXPERIMENTAL RESULTS AND DISCUSSION.	27
	General Discussion	27
	Effects of Strand Cross-Section and Length	28
	Nonmetallized Composite Propellants.	34
	Aluminized Composite Propellants	42
	Double-Base Propellants.	53
VII	CONCLUSIONS.	55
VIII	FUTURE INVESTIGATIONS.	58
	REFERENCES	59
	FIGURES.	62
	DISTRIBUTION LIST.	107

LIST OF TABLES

Table		Page
I	Composite Propellant Formulations	24
II	Double-Base Propellant Formulations	24
III	UTX Propellant Data With 0.6 in. Strand Length.	29
IV	UTX Propellant Data With 2.0 in. Strand Length.	30
V	Effect of Acceleration on b and n in the Equation $\dot{r} = bP^n$	45

LIST OF FIGURES

Figure		Page
1	NPS Centrifuge	62
2	Combustion Bomb and Strand Holder.	63
3	Typical Pressure-time Trace.	64
4	Ammonium Perchlorate Size Distribution	65
5	Comparison of Burning Rate Data for UTC Control Propellant (Adapted from Reference 8).	66
6	Effect of Strand Cross-section on Burning Rate Augmentation of Nonaluminized Composite Propellant (N-1) at 500 psia	67
7	Effect of Strand Cross-section on Burning Rate Augmentation of Aluminized Composite Propellant (N-7) at 500 psia	68
8	Effect of Strand Cross-section on Residue Formation of Aluminized Composite Propellant (N-7) at 500 psia . .	69
9	Effect of Strand Length on Burning Rate Augmentation of Nonaluminized Composite Propellant (N-1) at 500 psia	70
10	Effect of Strand Length on Burning Rate Augmentation of Aluminized Composite Propellant (N-7) at 500 psia . .	71
11	Effect of Strand Length on Residue Formation of Aluminized Composite Propellant (N-7) at 500 psia. . . .	72
12	Effect of Temperature on Burning Rate Augmentation of Nonaluminized Composite Propellant (N-1) at 500 psia . .	73
13	Effect of Pressure on Burning Rate Augmentation of Nonmetallized Composite Propellant (N-1)	74
14	Effect of Pressure on Burning Rate Augmentation of Nonmetallized Composite Propellant (N-3)	75
15	Effect of AP Size and \dot{r}_0 On Burning Rate Augmentation of Nonmetallized Composite Propellants at 500 psia . . .	76
16	Effect of \dot{r}_0 on Burning Rate Augmentation of Nonmetallized Composite Propellants at 500 psia (90 μ AP)	77

Figure		Page
17	Effect of AP Size on Burning Rate Augmentation of Nonmetallized Composite Propellants at 500 psia	78
18	Critical Particle Diameter versus Acceleration at 500 psia.	79
19	Comparison of Stokes' versus Non-Stokes' Theory with Experiment for P410 Propellant.	80
20	Comparison of Stokes' versus Non-Stokes' Theory with Experiment for P411 Propellant.	81
21	Effect of Temperature on Burning Rate Augmentation of Aluminized Composite Propellant (N-7) at 500 psia . . .	82
22	Effect of Pressure on Burning Rate Augmentation of Aluminized Composite Propellant (N-7)	83
23	Effect of Pressure on Residue Formation of Aluminized Composite Propellant (N-7).	84
24	Effect of Pressure on Burning Rate Augmentation of Aluminized Composite Propellant (N-6)	85
25	Effect of Pressure on Residue Formation of Aluminized Composite Propellant (N-6).	86
26	Effect of AP Size and \dot{r}_0 on Burning Rate Augmentation of Aluminized Composite Propellants at 500 psia.	87
27	Effect of AP Size and \dot{r}_0 on Residue Formation of Aluminized Composite Propellants at 500 psia.	88
28	Post-Fire Residue	89
29	Effect of \dot{r}_0 on Burning Rate Augmentation of Aluminized Composite Propellants at 500 psia.	90
30	Effect of \dot{r}_0 on Residue Formation of Aluminized Composite Propellants at 500 psia	91
31	Effect of AP Size on Burning Rate Augmentation of Aluminized Composite Propellants at 500 psia.	92
32	Effect of Aluminum, N-1 versus N-6.	93
33	Effect of Aluminum, N-2 versus N-7.	94
34	Effect of Aluminum, N-3 versus N-8.	95
35	Effect of Aluminum, N-4 versus N-9.	96
36	Effect of Aluminum, N-5 versus N-10	97

Figure		Page
37	Comparison of Crowe Model With Experimental Data at 500 psia	98
38	Comparison of Crowe Model With Experimental Data - Catalyzed Propellants at 500 psia	99
39	Comparison of Crowe Model With Experimental Data - Effect of Base Burning Rate at 500 psia	100
40	Comparison of Crowe Model With Experimental Data - Propellant N-7 at 1000 psia	101
41	Comparison of Crowe Model With Experimental Data - Propellant N-6 at 1000 psia	102
42	Effect of Acceleration on \dot{r}/\dot{r}_0 of Double-Base Propellants	103
43	Effect of Acceleration on Residue Formation of Double-Base Propellant at 265 psia.	104
44	Effect of Acceleration on \dot{r}/\dot{r}_0 of Aluminized Double-Base Propellant.	105
45	Effect of Acceleration on Residue Formation of Aluminized Double-Base Propellant	106

LIST OF SYMBOLS

Latin Symbols

AP	ammonium perchlorate
a	major diameter of agglomerate in UTC model, acceleration
A	area
b	burning rate constant ($\dot{r} = bP^n$)
C	centigrade
d	AP particle diameter
f	fraction of combustion energy release transferred to the propellant surface, Sturm model
F_d	drag force
Fe	iron
F_g	acceleration force
g	standard acceleration due to gravity
G	acceleration/g
h_c	energy released by combustion of AP oxidizer particles, Sturm model
h_v	energy required to heat up and vaporize a unit mass of propellant, Sturm model
J	fraction of small AP oxidizer particle mass released by decomposition on the propellant surface, Sturm model
k	constant
n	burning rate pressure exponent ($\dot{r} = bP^n$)
O	oxygen
P_c, P, p	pressure
PBAN	polybutadiene - acrylonitrile
\dot{r}_a	burning rate at acceleration α and pressure P
\dot{r}_0	burning rate at zero acceleration and pressure P
r_s	equivalent sphere radius of agglomerate
R	gas constant
Re	Reynolds number

Latin Symbols

T temperature
V velocity
W metal content, UTC model
W₀ propellant small AP oxidizer loading weight percentage, Sturm model

Greek Symbols

α acceleration in G
 μ viscosity, micron
 ρ density

Subscripts

d AP particle
g gas
p metal particle in UTC model, otherwise designates propellant
s propellant in UTC model

INTRODUCTION

The need to investigate the effects of acceleration on the burning rates of solid propellants has been discussed in some detail in the published literature [1, 2, 3, 4, 5].¹ In brief, high acceleration environments have been found to cause significant changes in motor operating pressure, propellant burn time, propellant burning characteristics, and overall performance.

Several investigators have analytically investigated the effects of acceleration on the burning rates of aluminized and nonmetallized composite propellants [2, 5, 6, 7, 8]. In addition, there are currently four facilities experimentally investigating the same effects; The United Technology Center, The NASA Langley Research Center, The Atlantic Research Corporation, and the Naval Postgraduate School.

NASA-LRC uses a centrifuge-mounted combustion bomb. The propellant slab employed has a burning surface 4" x 6" and a web thickness of 0.5 inches. Experiments have been conducted at accelerations up to 300g and at pressures as high as 2000 psia [1, 9, 10]. Extinguishment studies have also been conducted.

Experiments at UTC have been made with acceleration levels up to 600g and pressures up to 1250 psia. These experiments were conducted in a small rocket motor utilizing an internally burning propellant grain. The propellant grain was a nominal 7 inches long, with an outside diameter of 4.5 inches and a web thickness of 0.6 inches. Recent photographic studies have also been made using strand burners in a centrifuge mounted combustion bomb [2,3, 8].

The Atlantic Research Corporation [11] has also recently undertaken a photographic investigation of internally burning grains subject to acceleration fields up to 2000g and pressures as high as 50 atm.

¹Numbers in brackets refer to Reference list on page 59.

The test facility at the NPS consists of a combustion bomb mounted on a centrifuge. Experiments have been limited to propellant strands with cross sections up to 1.0 inch by 1.0 inch and with lengths up to 5 inches. Experiments have been conducted with accelerations as high as 2000 g and pressures as high as 1500 psia [4, 5, 12, 13, 14, 15, 16].

Each of the above methods can be effectively employed to parametrically study acceleration induced burning rate augmentation. Each method has its advantages and disadvantages and care must be taken when comparing the various results which have been obtained.

REVIEW OF PAST INVESTIGATIONS

Analytical

To date, the only analytical model that shows some promise for explaining many aspects of the acceleration induced burning rate augmentation of metallized composite propellants is due to Crowe, et al. [8]. The model considers the opposing forces of acceleration and pressure on the aluminum or aluminum oxide agglomerates on the propellant surface. The agglomerates are considered to burn on the propellant surface in pits and propellant vaporization holds the agglomerates slightly off the surface. The main mechanism for burning rate augmentation is considered to be the increased heat conduction through the hot particle and the laminar outflowing gases below the particle. The following equation for augmented burning rate is derived in Reference 8;

$$\frac{\dot{r}_a}{r_o} = 2 \left[\frac{r_s}{a} \left\{ \frac{\rho_p P_c \alpha}{r_s} \right\}^{1/4} \frac{k^1}{\rho_s r_o (1-W)} - 0.2 \right] + 1 \quad (1)$$

a = major diameter of agglomerate
 g = standard acceleration due to gravity
 k = constant
 P_c = chamber pressure
 \dot{r}_a = burning rate at acceleration a and pressure P_c
 \dot{r}_0 = burning rate at $0g$ and P_c
 r_s = equivalent sphere radius of agglomerate
 W = metal content
 α = acceleration in G
 ρ_s = propellant density
 ρ_p = particle density

The dependence of augmentation on pressure, base burning rate, and acceleration given by Equation 1 is in qualitative agreement with many experimental findings. The model has the obvious limitation of not allowing the prediction of the agglomerate size which may be a function of almost all of the propellant physical characteristics and operating parameters (AP size, \dot{r}_0 , propellant burn time, pressure, etc.). Even with this rather severe limitation, the model demonstrates that in the case of distinct metal agglomerates, local heat conduction through the hot particles causes a significant portion of the increase in burning rate observed for aluminized composite propellants subjected to acceleration forces.

Rather than proposing a new analytical model, Northam and Lucy [1, 9, 10] have correlated their experimental findings by expanding Vieille's law ($\dot{r} = bP^n$) to include the effects of acceleration on b and n . This method does give a working expression for a given propellant but does not help to explain any of the physical mechanisms involved.

There have been two analytical models proposed for the augmentation of nonmetallized composite propellants. Glick [7] has proposed an extension to Summerfield's [17] granular diffusion flame model to include acceleration effects. The model failed to correlate the experimental data of Anderson and Reichenbach [4]. King and McHale [11] have also discussed the limitations of this model.

Sturm [5,15] has also proposed a model for nonmetallized composite propellants containing ammonium perchlorate (AP) crystals. Sturm extended Fenn's [18] "phalanx flame" model for the burning of composite propellants to include acceleration effects. It was assumed that when the small AP crystals in a bi-modal mix become exposed at the surface, they rapidly become "unattached" to the surface. The "phalanx flame" was considered to have proceeded completely around the AP-binder interface of these smaller crystals before appreciable decomposition had taken place. In 0g conditions, these small "unattached" crystals are carried away from the surface by the evolving gases. This process causes an oxidizer depletion and a corresponding reduction in burning rate. As the acceleration field is increased above the 0g condition these small crystals begin to be held on the surface - increasing the burning rate. A small AP crystal is considered to remain on the surface until decomposition reduces its size to the point where the drag force becomes greater than the acceleration force. The AP crystal size where the acceleration and drag forces are equal was called the critical particle size. The acceleration force on a particle is given by

$$F_g = \frac{\pi d^3 \rho_d a}{6} \quad (2)$$

where d = particle diameter

ρ_d = particle density

a = acceleration

Assuming Stokes' flow, the drag force on a spherical particle is given by

$$F_D = 3\pi\mu_g dV_g \quad (3)$$

where μ_g = gas viscosity

V_g = gas velocity

From continuity

$$\rho_g A_g V_g = \rho_p A_p V_p \quad (4)$$

where A_g = gas flow area

A_p = propellant burn area

V_p = propellant burn rate

ρ_p = propellant density

ρ_g = gas density

For propellant strands enclosed in rigid inhibitors, $A_p = A_g$ and $V_p = \dot{r}$ = propellant burn rate normal to the surface. Thus, Equation 4 becomes

$$V_g = \frac{\rho_p \dot{r}}{\rho_g} \quad (5)$$

Assuming a perfect gas

$$\rho_g = \frac{P}{R_g T} \quad (6)$$

Equating Equations 2 and 3, and substituting Equations 5 and 6 yields the critical particle diameter, d_c .

$$d_c = \left[\frac{18\mu_g \rho_p \dot{r} R_g T}{P \rho_d^2} \right]^{1/2} \quad (7)$$

Thus, for a given propellant formulation

$$d_c \propto \left[\frac{\dot{r}}{Pa} \right]^{1/2} \quad (8)$$

Allowing for the increased heat release at the surface due to the retention of AP crystals at higher than 0g acceleration, Sturm [5] derived the following equation for burning rate augmentation.

$$\frac{\dot{r}}{\dot{r}_0} = \frac{1}{1 - \frac{w_0 f h_c J}{h_v}} \quad (9)$$

where f = fraction of combustion energy release transferred to the propellant surface

h_c = energy released by decomposition of AP oxidizer particles and the subsequent combustion with fuel per unit mass of small AP oxidizer consumed.

h_v = energy required to heat up and vaporize a unit mass of propellant

J = fraction of small AP oxidizer particle mass released by decomposition on the propellant surface ($0 < J < 1$)

\dot{r} = propellant burning rate at a given pressure and acceleration

\dot{r}_0 = propellant burning rate at the given pressure and zero acceleration

w_0 = mass fraction of small AP oxidizer in propellant

The main limitation of the model (as noted by Sturm) is that f , h_c , J , and h_v are unknown functions of acceleration, pressure, and/or propellant composition. Equation 9 may be written as

$$\frac{\dot{r}}{\dot{r}_0} = \frac{1}{1 - \eta f J} \quad (10)$$

where $\eta = \frac{w_0 h_c}{h_v}$

Sturm [5, 15] has reasoned from the analytical expression for augmentation (Equation 9) of nonmetallized composite propellants that: 1) burning rate is insensitive to accelerations less than the threshold acceleration (the threshold acceleration corresponds to the acceleration which makes the largest AP crystal in the fine cut just equal to the critical particle diameter); 2) burning rate increases with acceleration above the threshold acceleration as increased amounts of AP are prevented from leaving the surface; 3) burning rate reaches a constant, maximum value at high accelerations where all the AP is consumed on the surface; 4) burning rate augmentation increases with increasing pressure; 5) burning rate augmentation increases with increasing mass fraction of fine cut AP; and 6) burning rate augmentation decreases with increasing base burning rate.

In Equation 10, η was assumed to be only a function of propellant composition. Sturm reasoned from the Summerfield and Fenn theories that f should vary proportionally with the one-third power of pressure. J varies with acceleration through the critical particle diameter. J is assumed to be zero at zero acceleration since at this acceleration all of the small AP oxidizer crystals are assumed to leave the surface. By specifying d_{critical} , J may be determined. All of the particles in the smaller cut of AP oxidizer crystals are assumed to be consumed on the surface until their diameters become equal to the chosen d_{critical} . Thus, if the mass distribution of the fine cut of AP is known, J can be determined as a function of d_{critical} .

Sturm used Equations 8 and 10, experimentally obtained burning rate data at three accelerations and a fixed pressure, and a calculated dependence of J on d_{critical} to obtain the dependence of \dot{r}/\dot{r}_0 on acceleration for a given propellant. Qualitative agreement existed between the model and experimental results.

Experimental

General Discussion

Recent experimental investigations into the effects of acceleration on the burning rates of solid propellants have been conducted primarily by four facilities; NASA-LRC, UTC, Atlantic Research Corp., and the NPS. Other related studies, such as the work of Mann, et. al. [19], have also been conducted. The review of experimental findings presented herein will be predominantly limited to the findings of the NASA-LRC, the UTC, and the NPS. In many cases different propellant formulations (AP size, binder type, etc.) have been used by the various investigators. Thus when opposite trends are reported for the effects of a given parameter, that parameter effect is in general quite dependent upon propellant formulation.

Metallized Propellants

Pressure

Northam and Lucy [1, 10] found that \dot{r}/\dot{r}_0 increased with increasing pressure. Anderson [4] found that augmentation increased with pressure to 1000 psia and then decreased. UTC [2, 8] and Sturm [5] found that average burning rate did not vary appreciably or consistently with pressure. Anderson and UTC both report an increase in post-fire slag weight with pressure at any given acceleration level.

Initial Propellant Temperature

Sturm [5] found that increasing the initial propellant temperature from 20C to 54C had no effect upon \dot{r}/\dot{r}_0 .

Burn Time (web thickness)

Anderson [4] found no appreciable change in average burning rate with strand length. Sturm [5] and UTC [2, 8] found that the average burning rate decreased with time. UTC actually observed a transient effect; \dot{r} at a given acceleration initially increased with time, reached a maximum, and then decreased with time.

Magnitude and Direction of Acceleration

Northam and Lucy [1, 10] have found that if the acceleration vector is directed into the burning surface at an angle greater than 15° from the normal then \dot{r} does not vary with acceleration. All investigators have found that \dot{r}/\dot{r}_0 increases with acceleration for the acceleration vector directed normal and into the burning surface. Anderson, Sturm, and UTC has found that a threshold acceleration exists below which \dot{r}/\dot{r}_0 does not change with acceleration. The magnitude of the threshold acceleration depends upon the particular propellant, pressure level, etc. Above the threshold acceleration, \dot{r}/\dot{r}_0 increased with increasing acceleration and generally approached a constant value at high accelerations.

Base Burning Rate

All investigators have found that \dot{r}/\dot{r}_0 decreases with increasing \dot{r}_0 . This result has normally been determined by adding catalysts and/or changing the oxidizer crystal size. Although the reported trend is obvious, the magnitude of the change of \dot{r}/\dot{r}_0 with \dot{r}_0 is in question because of the compound changes caused by either adding a catalyst and/or changing the oxidizer crystal size.

Metal Content

Northam and Lucy have found that the effect of percent by weight of aluminum depended upon the acceleration level. They report that above 150g, \dot{r}/\dot{r}_0 decreased with increasing weight percent of aluminum. UTC has found the opposite effect, \dot{r}/\dot{r}_0 increased with increased percent by weight of aluminum. Sturm and UTC both conducted tests with aluminum oxide replacing the aluminum. Sturm found that this increased \dot{r}/\dot{r}_0 and UTC found that it decreased. UTC also found a post-fire flood layer when using aluminum oxide which was not found when using aluminum. No explanation has yet been given for these differences in experimental findings. UTC has also reported an increased augmentation when aluminum was replaced with tungsten.

Metal Size

Sturm, UTC, and Northam and Lucy have all found that \dot{r}/\dot{r}_0 increases with increasing aluminum particle size. In addition, Sturm also found an increase in aluminum particle size decreased the post-fire residue weight.

AP Crystal Size

Anderson, Sturm, and UTC have found that reducing the AP size reduces \dot{r}/\dot{r}_0 . In photographic studies, UTC [8] has found that smaller AP crystals produce smaller metal agglomerates. Sturm also reports that increasing the AP size decreased the post-fire residue weight.

Binder Type

UTC, Northam and Lucy, and Sturm have all found that the binder type can effect \dot{r}/\dot{r}_0 . An explanation for this effect or how great it is has not been made.

Post-Fire Residue

Northam and Lucy have found that both post-fire residue weight and particle size increased with accelerations to 300g. Sturm also found that residue weight increased with acceleration. It should be noted that the residue found by Sturm in the bottom of the strand inhibitor case was usually in the form of a solid layer whereas that found in the slab motor by Northam and Lucy was in the form of particles. Sturm found that \dot{r}/\dot{r}_0 was greater for propellants with less residue weight. As discussed above, Sturm found that the initial metal particle size was the dominant factor effecting residue weight. Thus, he found that increasing the aluminum particle size decreased the residue weight and increased \dot{r}/\dot{r}_0 . Sturm found no consistent dependence of residue weight on pressure or base burning rate. He did find that the residue weight could be reduced by increasing the size of the large AP crystals and increasing the weight percent of fine AP crystals (in a bi-modal mix). Sturm has attributed the variation in burning rate with residue weight to two distinct modes of burning; 1) distinct metal agglomerates on the surface which cause a higher \dot{r}/\dot{r}_0 and lower residue weight and 2) a flood layer of metal which causes decreased burning rates and increased residue weight.

Nonmetallized Propellants

Temperature

Sturm found that increasing the initial propellant temperature from 20C to 54C increased the burning rate augmentation above 400g. These tests were conducted using bi-modal AP/PBAN propellants.

Magnitude and Direction of Acceleration Field

Using bi-modal AP/PBAN propellants, Sturm found three characteristic regions of augmentation when the acceleration was directed normal and into the burning surface. A "threshold" acceleration was observed, below which burning rate was not a function of acceleration. This "threshold" acceleration was normally less than 150g. Above the "threshold" acceleration, burning rate was increased with acceleration. At high acceleration, the burning rate reached a maximum value and remained constant with further increases in acceleration.

Anderson and Reichenbach [4] and Willoughby, et. al. [8] also observed the "threshold" acceleration noted by Sturm and found that above this value, burning rate increased with increasing acceleration directed normal and into the burning surface. Willoughby, et. al. utilized bi-modal AP/PBAN propellants and Anderson and Reichenbach used both uni-modal AP/polyurethane and bi-modal AP/PBAN propellants. The latter investigators also observed burning rate extinguishment of polyurethane propellants at high accelerations.

With the acceleration directed normal to and out of the burning surface Sturm found no change in augmentation. In contrast, King and McHale [11] found as much as a 30 percent decrease in burning rate for high accelerations directed normal to and out of the burning surface. However, a CTPB binder was used for the latter tests. This propellant was found to exhibit practically no augmentation when the acceleration was directed normal and into the burning surface.

Pressure

Sturm found that increasing pressure, a) decreased the threshold acceleration, b) decreased the acceleration level above which the burning rate remained constant, and c) increased the maximum obtainable value of augmentation. Anderson and Reichenbach also found that augmentation increased with increasing pressure.

Burn Time

Sturm found no time dependence of burning rate at any acceleration level.

Base Burning Rate

Sturm found that augmentation decreased with increasing base burning rate.

No significant findings have been reported with regard to the individual effects of AP crystal size and the binder type.

Concluding Remarks

UTC [8] concluded that the most important factors determining \dot{r}/\dot{r}_0 for metallized composite propellants are \dot{r}_0 and whether or not surface flooding occurs. Sturm [5] concluded that the most important parameter is residue weight.

For nonmetallized composite propellants Sturm [5] concluded that the primary factor effecting \dot{r}/\dot{r}_0 was the size of the fine AP crystals (in a bi-modal mix).

Northam and Lucy [1] found that the slab motor gave a fifty percent greater \dot{r}/\dot{r}_0 than the same propellant tested in strand form by Anderson [4]. The primary reason for this difference is probably the difference in the web thicknesses employed ; 0.5 in. for the slab motor and 2.0 in. for the strand.

Northam and Lucy [1] also report that burning rate data obtained with the slab motor differ significantly from data obtained with the UTC spinning motor at 100g and low pressures. At 100g and high pressure and at 0g the data agree quite favorably.

PURPOSE OF INVESTIGATION

The investigation had several related objectives which are discussed below. As a result of the differences in the acceleration induced burning rate augmentation data obtained by Northam and Lucy [1] and by Anderson [4] using the same propellant formulation, it was necessary to conduct an investigation into the effect of strand cross-sectional dimensions and length on the measured burning rate and on the residue formation of metallized solid propellants.

Sturm [5] has reported the effects of temperature on the acceleration sensitivity of both metallized and nonmetallized composite propellants. He studied the augmentation sensitivity at 20C and 54C. To better understand the effects of temperature on acceleration sensitivity, the temperature range was extended both above 54C and below 20C.

The data reported by the various investigators indicate that both metallized and nonmetallized composite propellants exhibit acceleration sensitivity. It is therefore doubtful that the acceleration sensitivity of aluminized composite propellants can be entirely attributed to the presence of the aluminum. A systematic experimental study was made to determine to what extent the AP crystals and the aluminum affect the total propellant acceleration sensitivity. Directly related to this study was an investigation which was conducted to determine the effects of acceleration on the burning rates of aluminized and nonaluminized double-base propellants.

Current analytical models for the acceleration sensitivity of solid propellants were evaluated.

EXPERIMENTAL EQUIPMENT AND PROCEDURES

The research discussed herein was conducted at the Naval Postgraduate School Rocket Test Facility. A centrifuge mounted combustion bomb was employed to study the influence of acceleration and pressure on the burning rates of solid propellants. Details of the test facility are presented in References 4, 5, 12, and 20 and will be only briefly discussed.

The combustion bomb mounted on the centrifuge is shown in Figure 1. The combustion bomb is mounted on the centrifuge arm at a radius of three feet and is connected to two surge tanks located near the centrifuge centerline. The centrifuge and bomb can be used to study the burning rates of propellant strands from atmospheric to 1500 psia and from zero to 2000g. A total bomb and surge tank volume of 1565 in.³ allowed experiments to be conducted with practically a constant pressure. The largest strands employed caused a pressure rise during firing of approximately 6 percent. The strand lengths employed varied from 1/2 inch to 2 inches. In all tests conducted in this investigation the acceleration force was directed normal and into the burning propellant surface. The large centrifuge radius allowed tests to be conducted at very nearly a constant acceleration. The largest variation in acceleration during a given test was less than 6 percent.

The propellant strands of various dimensions which were employed in this investigation were normally inhibited on all surfaces except the surface normal to the acceleration force. Selectron 5119 resin and "Garox" curing agent were employed as the inhibiting material for most tests. Selected test also used RTV as the inhibitor. Propellant strands enclosed in a rigid inhibitor were employed for several reasons [4, 5]. The inhibitor case provided support for the propellant in the high acceleration environment. The use of strand burners also allows the average burning rate to be determined quite accurately for a wide range of web thicknesses (strand lengths). In addition, the strands eliminate the major effects of erosive burning and the possible gaseous vortices which are generated in the grain port of an internally burning grain. Thus the effects of acceleration alone on burning rate can be studied.

Propellant strands were attached to a strand holder, inserted into the bomb and sealed. A schematic diagram of the strand holder in the combustion bomb is presented in Figure 2. The bomb and surge tanks were pressurized to the desired level and then the centrifuge was brought up to the desired speed. The propellant was then ignited and the pressure-time trace of the combustion bomb recorded. Average burning rate was determined by dividing the known strand length by the burn time measured from the pressure time trace. A typical pressure-time trace is shown in Figure 3. It has been estimated that the burning rate determinations were made with a maximum error of two percent.

Ignition was accomplished by a nichrome resistance wire placed adjacent to the propellant surface and a black powder-glue mixture placed across the propellant surface. Current through the ignition wire was adjusted so that the wire was not burned-out during a given test. The wire was located adjacent the propellant surface so that if the wire did burn, it would not fall on the burning propellant.

The desired initial bomb pressure (at 0g and before ignition) was determined by taking into account the change in bomb pressure due to centrifugal force [20] and propellant burning.

METHOD OF INVESTIGATION AND PROPELLANTS

General Discussion

A systematic variation in propellant properties and test conditions was used to determine the effects of the following parameters on burning rate acceleration sensitivity:

- a) strand cross-sectional area
- b) strand length (burn time)
- c) initial propellant temperature
- d) AP crystal size
- e) base burning rate (0g)
- f) aluminum
- g) double-base propellant additives
- h) residue formation

The majority of the tests were conducted at approximately 500 psia or 1000 psia. In most instances two data points were taken at each set of test conditions. Additional tests were conducted if inhibitor failure was apparent or if a particular propellant formulation yielded a typically wide variation in burning rate data.

Propellants

In order to accomplish the investigation of the above mentioned parameters fourteen propellant formulations were employed. Propellant designations and formulations are summarized in Tables I and II.

TABLE I COMPOSITE PROPELLANT FORMULATIONS

Propellant Designation	Weight %AP	AP Size, μ	Weight %PBAN	Weight %Aluminum	Aluminum Size, μ	Weight %Fe ₂ O ₃
N-1	79.00	unimodal 9	21.00	----	----	----
N-2	79.00	unimodal 90	21.00	----	----	----
N-3	79.00	unimodal 420	21.00	----	----	----
N-4	78.21	unimodal 90	20.70	----	----	1.00
N-5	77.42	unimodal 90	20.58	----	----	2.00
N-6	67.00	unimodal 9	18.00	15.00	44	----
N-7	67.00	unimodal 90	18.00	15.00	44	----
N-8	67.00	unimodal 420	18.00	15.00	44	----
N-9	66.33	unimodal 90	17.82	14.85	44	1.00
N-10	65.66	unimodal 90	17.64	14.70	44	2.00
UTX-3096A	68.0	65%-400 35%-8	16.0	16.0	46	----

NWC

Typical Aluminized Composite -- Unspecified Formulation

TABLE II DOUBLE-BASE PROPELLANT FORMULATIONS

Propellant Designation	Weight %Nitrocellulose	Weight %Nitroglycerin	Wt% Monobasic Cupric Salicylate	Wt% Monobasic Lead	Wt% Al
DBA	45.0	41.7	2.5	2.5	5.3
DBNA	48.0	44.5	2.5	2.5	---

Propellants N-1 through N-10 employed unimodal distributions of ammonium perchlorate. These propellants were fabricated by the Naval Weapons Center. All ammonium perchlorate was supplied by the American Potash & Chemical Corporation. The 9 μ AP had a measured average particle size of 8.2 to 9.4 μ . The 90 μ AP was used as supplied. A diameter distribution is shown in Figure 4. The large AP passed a Tyler #32 mesh (500 μ) and what held on a Tyler #35 mesh (420 μ) was used. The aluminum employed in propellants N-6 through N-10 was type H-30 and passed a Tyler #325 mesh (44 μ). The iron oxide employed had the following specifications:

Physical description - Yellow light lemon elongated particles

Chemical composition - Hydrated Fe₂O₃

Average particle diameter - 0.40 microns

Density - 3.401 gm/cc

A weight ratio of 79 parts AP to 21 parts PBAN was maintained in propellants N-1 through N-10.

Method of Investigation

General

The investigation was divided into several related parts and will be discussed separately.

Effect of Strand Cross-sectional Area

The initial investigation into the effect of strand cross-sectional area on the measured burning rate augmentation (\dot{r}/\dot{r}_0) was conducted with a typical aluminized composite propellant (NWC). These tests were made to determine the magnitude of the effect of strand cross-sectional area. Strand cross-sectional dimensions were varied from 1/4 in. x 1/4 in. to 1 in. x 1 in. In addition, propellants N-1 (non-metallized) and N-7 (aluminized) were burned in 1/4 in. x 1/4 in. and 1/2 in. x 1/2 in. configurations.

A comparison was necessary between the data obtained by the NASA-LRC, the UTC, and the NPS. The United Technology Center supplied a sample of their control propellant (UTX-3C961) and strands of various cross-sectional dimensions

(and lengths) were tested. Data were then available for comparison of the results obtained by the three facilities for the same propellant formulation.

Effect of Strand Length (Burn Time)

The effect of strand length on average burning rate augmentation (\dot{r}/\dot{r}_0) was determined for aluminized and nonmetallized composite propellants. Propellants N-1 and N-7 were tested at 500 psia with strand lengths of 1/2, 1, and 2 inches.

Effect of Temperature

Propellants N-1 and N-7 were tested at 4C, 21.5C, and 66C to determine the effects of temperature on burning rate augmentation of nonmetallized and aluminized propellants.

Effects of Base Burning Rate and

AP size on Nonmetallized Composite Propellants

Propellants N-1 through N-5 were employed to determine the effects of \dot{r}_0 and AP size on the burning rate augmentation of nonmetallized composite propellants. Because the AP size affects the base burning rate (\dot{r}_0), five propellants were required to separate the effects of \dot{r}_0 and AP size on burning rate augmentation. Propellants N-1, N-2, and N-3 were employed to determine the combined effects of \dot{r}_0 and AP size on burning rate augmentation. Propellants N-4 and N-5 were identical to N-2 except for a 1% and 2% addition respectively of yellow iron oxide catalyst. Thus, propellants N-2, N-4, and N-5 were employed to determine the effects of base burning rate. The effects of AP size and \dot{r}_0 could then be separated.

Effects of \dot{r}_0 and AP Size on

Aluminized Composite Propellants

Propellants N-6 through N-10 were identical to propellants N-1 through N-5 respectively except that approximately 15% aluminum was added. The procedure to separate the effects of \dot{r}_0 and AP size were identical to those discussed above for the nonaluminized propellants.

Effects of Aluminum and AP

By comparing the results obtained for the nonmetallized propellants (N-1 through N-5) with the results obtained for the corresponding aluminized propellants (N-6 through N-10) the separate effects of the aluminum and the ammonium perchlorate on burning rate augmentation could be determined.

Effects of Double Base Propellant Additives

In order to determine the effects of double-base propellant additives on burning rate augmentation, propellants DBA and DBNA were tested at 250, 500, and 1000 psia and at various acceleration levels.

Effects of Propellant Residue

The study of the effects of propellant residue on burning rate augmentation was actually a study of the form of the molten metallic substance which lies on or slightly above the burning propellant surface. There are three methods which can be employed to study these effects; 1) photographic studies, 2) extinguishment studies, and 3) post-fire residue studies. It was the latter method which was employed throughout this investigation.

EXPERIMENTAL RESULTS AND DISCUSSION

General Discussion

The discussion of experimental results is divided into the following interrelated sections:

1. Effects of strand cross section and web thickness on measured burning rate augmentation.
2. Nonmetallized composite propellants.
3. Aluminized composite propellants
4. Double-Base propellants.

The data are presented in two forms; burning rate augmentation vs acceleration and post-fire residue weight per unit of original strand volume vs. acceleration. Burning rate augmentation is defined as \dot{r}/\dot{r}_0 where \dot{r} is the burning rate at acceleration (a) and pressure (p) and \dot{r}_0 is the burning rate at zero acceleration and pressure (p).

The primary objectives of the experimental investigation were to experimentally determine the effects of a) base burning rate, b) AP crystal size, c) aluminum content, and d) temperature on the burning rate acceleration

sensitivity of composite propellants. In addition the acceleration sensitivity of double-base propellants was investigated. The experimental results were compared with current analytical models.

Before the investigation of these effects was begun a study was made to determine the effects of propellant strand cross-sectional area and length (web thickness) on the experimentally measured burning rate sensitivity. This study was prompted by the contrast in results obtained for identical propellants by Northam and Lucy [1] at the LRC and by Anderson [4] at the NPS. As was discussed above, the LRC uses a centrifuge mounted slab motor whereas the NPS uses a centrifuge mounted strand burner.

Effects of Strand Cross-Section and Length

General Discussion

The acceleration induced burning rate augmentation data obtained from the various facilities (LRC, UTC, NPS) generally agree qualitatively but to date quantitative agreement has not been found except as noted in Reference 8. As Northam and Lucy [1] have indicated, in order to compare the data obtained by the different techniques, it is necessary to conduct experiments in each of the facilities using the same propellant and the same base parameters (pressure, average acceleration, etc.).

Northam and Lucy have made an initial attempt to compare results for the various facilities. The data from experiments conducted at UTC and LRC using the same propellant formulation have been found to agree quite favorably [8].

Northam also conducted tests with a metallized propellant designated E-107 which had the same formulation as propellant X-104 used by Anderson [4]. The slab motor burning rate augmentation was found to be approximately 50 percent higher than that reported by Anderson. Possible causes for the differences in the results obtained from the two techniques have been attributed to [1] differences in a) burning surface area, b) web thickness, c) retention of Al_2O_3 on the surface, d) methods of determining burning rate, e) gas flow effects, or f) igniter effects.

The possibility of aluminum or aluminum oxide retention in the strand case affecting the burning rate has been noted by the various investigators. This

possibility has been noted because the results reported by Anderson [4] and Sturm [5] indicate that considerably more post-fire metallic residue exists for the strand than for the slab or spin-motors.

The noted good agreement between UTC and LRC data [8] was obtained with similar web thicknesses (0.6 inches and 0.5 inches respectively) whereas the comparison between NPS and LRC data [1] was made with considerably different web thicknesses (2-1/4 inches and 0.5 inches respectively). All of the above investigators have observed that web thickness has a significant effect upon the average burning rate (surface flooding effects, etc.). In general, average burning rate decreases with increasing strand length. It is not unusual then that there exists a significant difference between the burning rates determined by Anderson and by Northam and Lucy.

An initial investigation at the NPS [12] indicated that strand length had a significant effect upon the average burning rate whereas strand cross-sectional area had much lesser effects.

Data Comparison Using Propellant UTX-3096A

In order to better determine the agreements and differences between data obtained from strand burners, slab motors, and spin motors, propellant UTX-3096A, supplied by the United Technology Center, was tested in the NPS centrifuge. This propellant was identical to that which had been used by both Northam [1] and the UTC [8]. Propellant strands of 0.6 inches length and various cross-sections were burned at various pressures and acceleration levels. Results of these tests are shown in Table III and also in Figure 5, where the data are compared with the data obtained by UTC and LRC.

TABLE III: UTX-PROPELLANT DATA WITH 0.6 INCH STRAND LENGTH

<u>Strand Cross-section (in. x in.)</u>	<u>Average Bomb Pressure (psia)</u>	<u>Burning Rate (in/sec)</u>	<u>Acceleration (g)</u>
1/4 x 1/4	189	.166	0
1/2 x 1/2	198	.164	0
3/4 x 3/4	214	.155	0
1/2 x 1/2	307	.173	0
1/4 x 1/4	448	.181	0
1/4 x 1/4	645	.237	0

TABLE III (Cont.)

<u>Strand Cross-section (in. x in.)</u>	<u>Average Bomb Pressure (psia)</u>	<u>Burning Rate (in/sec)</u>	<u>Acceleration (g)</u>
1/2 x 1/2	662	.264	0
3/4 x 3/4	698	.258	0
1/4 x 1/4	940	.243	0
1/4 x 1/4	942	.272	0
1/4 x 1/4	1480	.288	0
1/4 x 1/4	190	.232	100
1/2 x 1/2	197	.230	100
3/4 x 3/4	236	.262	100
1/2 x 1/2	309	.275	100
1/2 x 1/2	460	.317	100
1/2 x 1/2	462	.342	100
1/4 x 1/4	638	.374	110
1/2 x 1/2	665	.406	110
1/4 x 1/4	949	.403	100
1/2 x 1/2	1509	.475	100

Good agreement is noted between the data obtained by all three methods. The effect of strand cross-section does not appear to significantly effect the measured burning rate at low acceleration levels.

In addition to the UTX-propellant tests conducted with a 0.6 inch strand length, several tests were also conducted utilizing a two inch strand length. The data obtained are shown in Table IV and also in Figure 5.

TABLE IV: UTX-PROPELLANT DATA WITH 2.0 INCH STRAND LENGTH

<u>Strand Cross-section (in. x in.)</u>	<u>Average Bomb Pressure (psia)</u>	<u>Burning Rate (in/sec)</u>	<u>Acceleration (g)</u>
1/4 x 1/4	703	.192	0
1/4 x 1/4	703	.189	0
1/4 x 1/4	704	.317	101
1/4 x 1/4	703	.333	101

Figure 5 indicates that the burning rate decreased with strand length at both 0g and 100g.

These results indicate that the primary reason for the difference in the burning rate (at low acceleration levels) measured by Anderson and by Northam and Lucy was due to the strand length or web thickness employed.

Propellants N-1 and N-7

General Discussion

In order to better understand the effects of strand length (burn time) and strand cross-sectional area on the average propellant burning rate, additional tests were conducted with both nonmetallized and aluminized composite propellants. Propellants N-1 and N-7 were tested at 500 psia and at accelerations from 0 to 1000g. Three strand lengths (1/2, 1, 2 in.) and two strand cross-sections (1/4 in. x 1/4 in. and 1/2 in. x 1/2 in.) were investigated.

Effects of Strand Cross-Sectional Area

Figure 6 presents the results obtained for the nonmetallized propellant (N-1). The 1/2 in. x 1/2 in. strand had a base burning rate approximately 3 percent greater than the 1/4 in. x 1/4 in. strand. The lines in Figure 6, as well as in all subsequent figures presenting experimental data, are drawn only to help visualize the location of data points. Although the 1/4 in. x 1/4 in. strand appears to augment slightly more than the 1/2 in. x 1/2 in. strand above 250g, the data scatter does not allow any definite conclusions to be made. It appears that strand cross-sectional area has only minor effects on the measured average burning rate of nonmetallized composite propellants.

Comparison of data for an aluminized composite propellant (N-7) is made in Figures 7 and 8. Figure 7 presents burning rate augmentation data and Figure 8 presents post-fire residue data for 1/4 in. x 1/4 in. and 1/2 in. x 1/2 in. strands. Figure 7 indicates that strand cross-sectional area has very little effect on augmentation of aluminized composite propellants. The greatest difference in measured augmentation occurred at 500g and this difference was only approximately 4 percent.

The base burning rates were also within 4 percent. Figure 3 presents the post-fire residue data taken from the inhibitor cases. The figure presents the residue weight per unit of original strand volume and the general appearance of the residue. Residue appearance has been divided into five categories: 1) a solid layer of metallic residue covering the entire cross-section of the strand, designated L, 2) a solid layer of metallic residue covering less than the entire cross-section of the strand, designated PL, 3) numerous pieces of metallic residue of various shapes and sizes designated P, 4) a metallic powder, designated PW, and 5) metallic discs and/or spheres, designated S. In addition, most propellants produced an appreciable amount of "fluffy" carbon material at low accelerations. At higher accelerations this material almost completely disappeared.

The 1/4 in. x 1/4 in. strand had a solid layer of residue, L, at all accelerations less than 1000g whereas the 1/2 in. x 1/2 in. strand residue varied with acceleration. At low g (< 100g) a solid layer was found. As the acceleration increased above 100g the residue appearance changed from a solid layer to a partial solid layer, and at high accelerations to a partial layer plus spheres. The residue weight per unit volume for both strand sizes increased to a maximum and then decreased as the acceleration increased. This characteristic of the residue weight will be evident in much of the data presented below. It should be noted that the largest difference in the augmentation between the two strands occurred at approximately 500g - the same location as the maximum difference in residue weight per unit volume and the same location where the residue form became different. The 1/4 in. x 1/4 in. strand had more residue per unit volume, a solid layer of residue and less augmentation at 500g. Thus the residue weight and/or physical appearance appears to affect the augmentation.

Although the augmentation for both strand cross-sections are nearly the same for propellant N-7, the variation in residue appearance with acceleration of the 1/2 in. x 1/2 in. strand is in better agreement with motor extinction test data [1, 10]. It is conceivable that for other

propellants and test conditions (pressures, accelerations, etc.) that the difference in the physical appearance of the residue could have a more pronounced effect on the augmentation. For these reasons strands with 1/2 in. x 1/2 in. cross-sections were employed throughout this investigation.

Effects of Strand Length (web thickness/burn time)

The initial tests conducted to study the effects of strand length [12] and the tests conducted with propellant UTX-3096A discussed above indicated that strand length effected the average burning rate. For this reason additional tests were conducted utilizing propellants N-1 (nonmetallized) and N-7 (aluminized).

Figure 9 presents the results obtained with the nonmetallized propellant, N-1, for 0.5 in. and 1.0 in. strand lengths. The base burning rates are essentially unchanged with length. Again the data scatter for propellant N-1 prevented any definite conclusions from being made. It does appear that in general the strand length had only small effects (< 10 percent for a 100 percent increase in length) upon the augmentation and/or burning rate of nonmetallized composite propellants. This conclusion is in agreement with the experimental findings of Sturm [5].

Figures 10 and 11 present the data obtained for the aluminized composite propellant N-7. Figure 10 presents the augmentation and Figure 11 presents the residue data. The base burning rate decreased as the strand length increased. This result is in agreement with the UTX-3096A propellant data presented in Figure 5. At 100g, the 1/2 in. and 1 in. strands had practically the same augmentation but the 2 in. strand augmented to a much lesser extent. This is also in agreement with the data presented in Figure 5 for propellant UTX-3096A. Figure 11 indicates that at 100g the residue weight (gm/cc) increased with strand length. The 1/2 in. and 1 in. strands had practically the same residue weight and the 2 in. strand had considerably more residue. Thus, it is again noted that at low acceleration levels burning rate and/or augmentation decreases with increasing residue weight. Another important feature of the residue data at 100g should be noted. As the strand

length was decreased, the residue appearance changed from a solid layer to a partial solid layer to spheres and discs. Thus, the residue type as well as weight has a significant effect upon the augmentation. At low accelerations (100g) augmentation decreases with increasing residue weight and decreases as the residue becomes more of a solid layer.

At 250g, increasing strand length decreased augmentation. In this case, however, the residue weights per unit volume were practically the same for all lengths. Although the trend is not as dominant as at 100g, the residue form changed with length. The trend is from particles to a solid layer as the length is increased. The 1/2 in. strand was the only one with distinct spheres and discs and it had a significantly greater augmentation at 250g. This same effect of residue type appears at 500g. Although the residue weights are significantly different at 500g, the residue type and augmentation are practically the same. Again at 1000g the residue weights are different but the residue forms are similar. The 1/2 in. strand had a slightly higher augmentation and more distinct spheres and discs in the residue. Several conclusions can be made from these observations. The amount (weight) and form of the molten metal(s) on the surface of a burning composite propellant both have a dominant effect upon the burning rate augmentation at low acceleration levels. At high acceleration levels the form of the molten metal becomes dominant rather than the quantity although the two are somewhat related. Since the strand length (or burn time) significantly effects the residue weight and form it is a very important parameter in the design of motors which will be subjected to acceleration environments. For accelerations less than 500g the average burning rate decreases with time. This result is in agreement with the experimental findings of Sturm [5] and UTC [2, 8]. For accelerations greater than 500g the burning rate was not strongly dependent on time.

Nonmetallized Composite Propellants

General Discussion

Five nonmetallized composite propellants were employed in this investigation (propellants N-1 through N-5). The objectives of this study were to

determine the effects of a) initial propellant temperature, b) pressure, c) base burning rate, \dot{r}_0 , and d) AP crystal size on the acceleration induced burning rate augmentation. In addition, Sturm's model [5] for acceleration effects on the burning rates of nonmetallized composite propellants was evaluated. All tests were conducted utilizing 1/2 in. x 1/2 in. x 2 in. propellant strands

Temperature Effects

The effect of temperature on augmentation, \dot{r}/\dot{r}_0 , was determined for propellant N-1. This propellant had small AP crystals (9 μ) and a correspondingly high base burning rate. Figure 12 presents the data obtained for propellant N-1 at 4C and 66C. The base burning rate (\dot{r}_0) increased with temperature as expected. It is observed that there was no appreciable effect of temperature on augmentation below 250g. Even at 1000g there was less than an 8 percent increase in augmentation when the temperature was raised from 4C to 66C. Sturm [5] found that increasing the initial temperature from 20C to 54C increased the augmentation for nonmetallized composite propellants at high accelerations.

As noted above, propellant N-1 had very small (9 μ) AP crystals. If the physical model of Sturm [5] is in fact valid (discussed above) the increase in augmentation with temperature is probably directly related to the AP crystals that normally leave the surface at low accelerations but are held on the surface at high accelerations. At the higher temperature these crystals have an increased initial energy content and are closer to the decomposition temperature. Thus, one would expect that if they contributed to the surface combustion process (at high accelerations) the burning rate should increase.

Pressure Effects

The effect of pressure on propellant burning rate augmentation was determined for propellants N-1 and N-3. Figures 13 and 14 present the data obtained for these propellants at approximately 500 psia and 1000 psia.

At a pressure of 480 psia, propellant N-1 exhibited a gradual and continuous increase in augmentation with increasing acceleration. At a pressure of 985 psia this propellant was insensitive to accelerations below approximately 100g. Above 100g the augmentation increased more rapidly with acceleration than was observed at 480 psia. At 1000g the augmentation at 480 psia was only 14 percent whereas at 985 psia it was 40 percent. Thus, except at low accelerations, increasing pressure increased the acceleration sensitivity. This observation is in agreement with the predictions obtained using Sturm's model.

At a pressure of 490 psia, propellant N-3 exhibited a gradual and continuous increase in augmentation with acceleration to 150g. The augmentation then decreased slightly with acceleration to 250g. Above 250g the propellant did not exhibit reproducible ignition characteristics (delay times). Therefore, there was a considerable variation in the measured average burning rate above 250g. Above approximately 600g the propellant could not be ignited. At 995 psia propellant N-3 was insensitive to accelerations below approximately 50g. Above 50g the augmentation increased with increasing acceleration to 250g. Above 250g the ignition characteristics (delay times) again were not reproducible. In contrast to the 490 psia tests, however, propellant N-3 could be ignited at 995 psia at all acceleration levels to 1000g.

An explanation of the observed behavior of propellants N-1 and N-3 can be made utilizing Sturm's physical model [5] for nonmetallized propellants. Fenn [18] has indicated that the "phalanx" flame penetration rate between the oxidizer crystal and binder should increase with increasing pressure. This would "free" more AP crystals at 0g and one would then expect more augmentation with increasing acceleration at the higher pressures. In Equation 9, the effect of pressure is through the parameter f . Increasing pressure increases f and therefore, increases the augmentation. Sturm attributes the insensitivity of burning rate at low accelerations to a "threshold acceleration" concept. Below the "threshold acceleration" the acceleration force is not great enough to hold any of the AP crystals on the surface that would have been forced from the surface at 0g.

The data presented in Figures 13 and 14 permit certain conclusions to be made. Thus, increasing the pressure level resulted in: 1) apparent commencement of burning rate augmentation at higher acceleration although possible error and data scatter preclude a definite conclusion; 2) achievement of the maximum burning rate augmentation at a higher acceleration level; and 3) a higher value of burning rate augmentation except at low accelerations. The first two results are opposite to the experimental findings of Sturm in which bi-modal AP propellants were employed. Thus, these particular results appear to depend upon the physical characteristics of the oxidizer crystals.

One possible explanation is presented for the failure of propellant N-3 to ignite above 600g and 490 psia and for the successful ignition at all accelerations to 1000g at 995 psia. The AP crystals were more dense than the binder. At 490 psia and high accelerations the large AP crystals are forced into the somewhat compressible binder. This provided a fuel rich surface which either ignited erratically or not at all. As the pressure was increased to 995 psia the binder was compressed. The acceleration force could not then force the AP crystals as far into the binder before ignition. Propellants N-1 and N-2 had smaller AP crystals than propellant N-3. Thus, enough oxidizer was always present on the surface to permit ignition.

Combined Base Burning Rate and AP Size Effects

When the AP crystal size is increased the O_g burning rate decreases. Thus, burning rate augmentation may be affected by both parameters as the AP size is changed. Propellants N-1, N-2, and N-3 were identical except for the unimodal AP crystal size distribution employed. They were 9μ , 90μ , and 420μ respectively. Figure 15 presents the data obtained for these three propellants. As expected, the base burning rate decreased as the AP size increased. Propellant N-2 had the greatest augmentation and propellant N-3 exhibited the unusual ignition characteristics discussed above.

Propellant N-1 had small AP crystals (9μ) and a high base burning rate. Thus, according to Sturm's model, at O_g many of the crystals are forced from the surface. As the acceleration is increased, an increasing number of these particles are prevented from leaving the surface. A gradual increase in augmentation with acceleration is therefore obtained. It would require very

high accelerations to hold all of the crystals on the surface and effect a maximum augmentation.

The smallest AP crystals in propellant N-3 were 420 μ . These AP crystals are so large that practically none leave the surface at 0g. Thus, very little augmentation at higher accelerations should be expected and the augmentation should reach a maximum value at low acceleration. The data confirm this behavior. The ignition difficulties at high accelerations for propellant N-3 were discussed above.

In addition to these combined effects of base burning rate and AP crystal size on burning rate augmentation it is possible that the mode of combustion may change from propellant to propellant. Bastress [21] has discussed the effects of oxidizer crystal size and pressure on the mode (or controlling mechanism) of combustion of polysulfide propellants.

Base Burning Rate Effects

In order to isolate the effects of base burning rate (\dot{r}_0) on acceleration sensitivity propellants N-2, N-4, and N-5 were employed. All three propellants had 90 μ AP and were identical except for the yellow iron oxide catalyst which was added to propellants N-4 (1%Fe₂O₃) and N-5 (2%Fe₂O₃). Figure 16 presents the data obtained for these three propellants. As expected, increasing the percent by weight of catalyst increased the base burning rate and decreased the acceleration sensitivity.

Propellants N-4 and N-5 exhibited erratic augmentation below 250g with only 4 percent augmentation at 1000g. Propellant N-2 exhibited little augmentation below 50g but at 1000g had a 36 percent augmentation. This behavior is also explainable with the physical model proposed by Sturm [5]. The higher burning rate propellants eject the AP crystals at 0g at a much higher velocity and therefore require considerably higher accelerations to effect augmentation.

AP Crystal Size Effects

In order to isolate the effects of AP crystal size on acceleration sensitivity, the data from propellants N-1, N-2, and N-4 were compared. Propellant N-1 had 9 μ AP crystals and propellants N-2 and N-4 had 90 μ AP crystals. The iron oxide catalyst in propellant N-4 increased its base burning rate to approximately 16% above that of propellant N-1. Increasing or decreasing the AP size changes the base burning rate. Thus, the effect of AP size on burning rate augmentation is not readily apparent. Ideally, the effect could have been isolated if the burning rate catalyst had increased the base burning rate of propellant N-2 (90 μ AP) to exactly that of propellant N-1 (9 μ AP). Unfortunately, both of the catalyzed propellants, N-4 and N-5, had base burning rates greater than that of propellant N-1. In order to isolate the effect of AP size on augmentation, the percent increases in augmentation per percent decreases in corresponding base burning rates were compared for three cases; 1) no change in AP size, 2) an increase in AP size by 900%, and 3) a decrease in AP size by 90%. The fixed AP results obtained from propellants N-2 and N-4 served as the norm, i.e., the effect of only base burning rate on augmentation. The results are presented in Figure 17.

From 500g to 1000g, increasing or decreasing the AP crystal size decreased the augmentation only slightly. Decreasing the AP size had possibly a little greater effect. As the acceleration level was decreased, the combined effects of AP size and base burning rate began to differ more appreciably from the effects of base burning rate alone. The lines in Figure 17 were drawn as smooth curves to the 100g point to approximate the trend in the data. The oscillations in the data at low accelerations in Figure 17 result from the unusual behavior of propellant N-4 at 150g and 250g (see Figure 16). At low accelerations it appears that increasing the AP size increases the augmentation and decreasing the AP size decreases the augmentation.

Comparison With Sturm's Model

It was found in this investigation that augmentation increased with a) increasing temperature at high accelerations, b) decreasing base burning rate, c) increasing pressure except at low accelerations. These experimental findings are in basic agreement with Sturm's analytical model. Threshold accelerations were observed which also agrees with the model.

The assumption of Stokes' flow around the separated AP crystals lead to Equation 8 for dependence of d_{critical} on burning rate, pressure, and acceleration. Stokes' flow is applicable for inert spheres in flows where the Reynolds number is less than one. Representative values for the parameters ρ_p , \dot{r} , d , and μ_g for a nonmetallized composite propellant yield Reynolds numbers much greater than one. The AP crystals are not spheres and the surface is undergoing decomposition. The latter condition may significantly reduce the drag force. However, the dependence of the drag force on particle diameter and gas velocity, as given by Equation 3 for Stokes' flow assumption, may be incorrect. The standard drag equation for Reynolds numbers greater than one is given by

$$F_D = \frac{\pi}{8} C_D \rho_g d^2 v_g^2 \quad (11)$$

where C_D = drag coefficient

In this case

$$F_D \propto \left(\frac{\dot{r}^2 d^2}{P} \right) \quad (12)$$

and

$$d_c = \frac{3C_D \rho_p^{2.2} \dot{r}^2 R T}{4 P a \rho_d} \quad (13)$$

Thus, for a given propellant formulation

$$d_c \propto \left(\frac{\dot{r}^2}{P a} \right) \quad (14)$$

Using representative values for the parameters in Equation 7, Sturm determined the critical particle diameter as a function of acceleration at 500 psia. The result is shown in Figure 18. Using the same values for the parameters but with $C_d = 1$ ($R_e = 100$ for inert spheres) Equation 13 was also plotted in Figure 18. It can be seen that the Stokes' and standard drag equations result in similar variations in the critical particle diameter with acceleration for these particular conditions. Also plotted in Figure 18 are the corresponding Stokes' and standard drag results with the burning rate doubled. The standard drag assumption is seen to yield a much greater change in the critical particle diameter with burning rate at low accelerations.

Utilizing the same procedures and parameter values as Sturm for two nonmetallized composite propellants, but replacing Equation 8 with Equation 14, new theoretical curves for \dot{r}/\dot{r}_0 as a function of acceleration were obtained. The results are shown in Figures 19 and 20 and are compared with the results obtained by Sturm in which the Stokes' flow assumption was employed. It is seen in Figures 19 and 20 that a dependence of the critical particle diameter on \dot{r}^2/Pa results in a somewhat better agreement with experimental data at low accelerations.

As noted above, J is the fraction of the small AP oxidizer particle mass released by decomposition on the propellant surface. In order to calculate J as a function of the critical particle diameter, Sturm assumed that all of the AP in the smaller cut decomposed on the surface until the drag forces became greater than the acceleration forces. The theoretical dependence of augmentation on acceleration presented in Equation 10 is strongly dependent upon how large a crystal is able to leave the surface at any given acceleration. This particle size is a function of the "phalanx" flame penetration rate, the crystal consumption rate, the binder type, and the actual critical particle diameter. King and McHale [11] have suggested that ten to twenty percent (or more) of a given AP crystal may be consumed

between the time that the crystal is first exposed at the burning surface and the time that the crystal is freed from the surface by the planar flame. In this way they were able to reasonably explain the experimentally observed decrease in augmentation which occurred when the acceleration was directed normal to and outward from the burning surface. They postulated that the outward directed acceleration physically pulled the oxidizer crystals from their pits prematurely. This decreased the heat release at the surface below that of the O_g condition and decreased the burning rate (this corresponds to $J < 1$ in Equation 10 when referred to the O_g condition). However, King and McHale have also noted that the exposed pits increase the surface area which would increase the burning rate. Thus, either an increased or decreased burning rate is possible.

As noted above, the parameters η , f , and J in Equation 10 are unknown functions of acceleration, pressure, and propellant composition. A quantitative prediction of burning rate augmentation using Sturm's analytical expression does not appear likely.

In conclusion, the physical model proposed by Sturm can explain most of the phenomena associated with the acceleration sensitivity of nonmetallized composite propellants. In addition, Sturm's analytical expression (Equation 10) was found to qualitatively agree with the experimental results although a standard drag force expression better correlates the experimental data at low acceleration than the Stokes' drag force expression.

Aluminized Composite Propellants

General Discussion

In addition to propellant UTX-3096A discussed above, five aluminized composite propellants were tested (propellants N-6 through N-10). The objectives of this study were to study the effects of a) initial propellant temperature, b) pressure, c) base burning rate, and d) AP crystal size on the burning rate augmentation of aluminized composite propellants. As discussed in "Method of Investigation and Propellants,"

the aluminized and nonmetallized composite propellants were formulated such that the relative effects of the AP crystals and the aluminum on burning rate augmentation could be separated. The effects were separated by comparing the results of this section with the results presented above in "Nonmetallized Propellants." In addition, the Crowe, et. al. model [8] for acceleration effects on the burning rates of metallized composite propellants was evaluated. All tests were conducted utilizing 1/2 in. x 1/2 in. x 2 in. propellant strands.

Temperature Effects

The data obtained for propellant N-7 burned at 4C, 21.5C and 66C are shown in Figure 21. The base burning rate increased with temperature as expected. Post-fire residue data was not plotted because the weight and form of the residue did not change appreciably with temperature. Increasing the temperature from 4C to 21.5C had virtually no effect upon the augmentation. Increasing the temperature to 66C decreased the augmentation by approximately 4 percent at all acceleration levels. This decrease in augmentation of an aluminized propellant at elevated temperatures is difficult to explain except for the possible change in thermal gradient through the metal agglomerates. Sturm [5] found no change in augmentation with temperature for an aluminized composite propellant.

Pressure Effects

Propellant N-7. The data obtained for propellant N-7 at 510 psia and 1024 psia are presented in Figures 22 and 23. The base burning rate increased significantly with pressure as expected. The augmentation decreased with increasing pressure and the effect was greater at higher accelerations. Figure 23 indicates that pressure did not have a significant effect on the form of the residue. Higher pressures did produce more residue at accelerations between 100g and 500g. The same trend in residue weight with acceleration, increasing to a maximum and then decreasing, was obtained at both pressures.

Propellant N-6. The data obtained for propellant N-6 are presented in Figures 24 and 25. Propellant N-6 had a smaller AP crystal size (9 μ) than propellant N-7 (90 μ). Again the base burning rate increased with pressure as expected. In contrast to propellant N-7 however, the augmentation increased slightly with pressure. Again, pressure did not have a significant effect upon the form of the residue. The residue weight increased with pressure at all acceleration levels. At 1000g the residue weight increased rapidly with pressure. However, the augmentation did not change, indicating again that at high accelerations residue form (not weight) has the dominant effect on augmentation.

The differences in the results for propellants N-6 and N-7 can be due to several mechanisms. The smaller AP crystal size for propellant N-6 prevents larger metal agglomerate pits from forming and more readily allows surface flooding. This is demonstrated by the data presented in Figures 23 and 25. Propellant N-6 (9 μ AP) in most instances had a solid layer of post-fire residue whereas propellant N-7 (90 μ AP) in most instances had only a partial solid layer and discs and spheres of residue. Anderson [4] and Sturm [5] also did not find a consistent variation in augmentation with pressure for various aluminized composite propellants. Anderson and UTC both report increased residue weight with pressure at any given acceleration level which is in agreement with the data presented in Figures 23 and 25.

The variation in the results obtained from these two propellants at 500 psia and 1000 psia indicates the complicated effects that pressure introduces into the augmentation mechanism. The higher pressure increases the base burning rate which decreases augmentation (discussed below). In addition the propellant burning mechanism may change with pressure as discussed by Bastress [21] for nonmetalized propellants. The heat transfer through the gas layer between the burning propellant surface and the metal agglomerates and the quantity and shape of the molten metal are also affected by pressure.

Northam [10] has found that n , in the expression $\dot{r} = bP^n$, varies with acceleration below approximately 120g. Between 120g and 300g he found that n did not change appreciably with acceleration. Values of b and n were calculated for propellants N-6 and N-7. The results are presented in Table V. The values of n do appear to remain approximately constant for intermediate acceleration levels. At high accelerations, however, n decreased with increasing acceleration.

TABLE V: EFFECT OF ACCELERATION ON b AND n IN THE EQUATION $\dot{r} = bP^n$
(PRESSURE RANGE: 500 - 1000 PSIA)

<u>Propellant</u>	<u>Acceleration (G)</u>	<u>b</u>	<u>n</u>
N-6	0	.057	.30
	100	.050	.34
	250	.053	.34
	500	.054	.35
	1000	.092	.27
N-7	0	.013	.45
	100	.024	.40
	250	.025	.40
	500	.050	.32
	1000	.071	.29

Another interesting observation is the difference in the pressure dependence of augmentation for nonmetallized and aluminumized propellants. Propellants N-1 and N-6 were identical except for the aluminum content in the latter. Comparing Figures 24 and 13 it is observed that the augmentation of the nonmetallized propellant (N-1) was significantly pressure dependent. Adding aluminum to this propellant practically eliminated the sensitivity of augmentation to pressure variations.

Combined Base Burning Rate and AP Size Effects

The same problems exist when attempting to separate the effects of base burning rate and AP crystal size on burning rate augmentation of aluminized composite propellants as exist for nonmetallized propellants. When changing the AP crystal size the base burning rate also changes. Three propellants were employed in this study (propellants N-6, N-7 and N-8).

Propellants N-6, N-7, and N-8 had a fixed weight ratio of AP to PBAN and a fixed percent of aluminum. Each had a unimodal AP crystal size distribution (N-6, 9 μ ; N-7, 90 μ ; N-8, 420 μ).

The combined effects of changing AP size and base burning rate are shown in Figures 26 and 27. As expected, the base burning rate decreased and the augmentation increased as the AP crystal size was increased. These effects increase with acceleration. The augmentation may be due to both the AP crystals (as for nonmetallized propellants N-1 through N-5) and the molten metal agglomerates on the burning surface.

Post-fire residue data are presented in Figure 27. It is observed again that the AP crystal size had a significant affect upon the form of the molten metal agglomerates. Propellant N-8, which had 420 μ AP crystals, had post-fire residue even at 0g. The residue weight decreased continuously with increasing acceleration. The residue was in the form of particles, discs, etc. except at 100g. This indicates that the metal agglomerates were usually in separate and distinct "pits" between the large AP crystals. At high accelerations, the large AP crystals may tend to "flood" the surface and thus decrease the allowable metal pit size.

The smaller AP propellants (N-6 and N-7) characteristically had no post-fire residue at 0g. At low accelerations propellants N-6 and N-7 had heavy solid layers of metallic residue. At higher accelerations the residue changed in form . more distinct particles and decreased in weight. These smaller AP propellants present smaller areas between crystals for "pit" formation by the metal agglomerates. Thus, at low accelerations when the metal agglomerates do not penetrate deeply into the surface, surface

flooding readily occurs. At very higher accelerations the metal agglomerates are flattened out but penetrate more deeply into the surface and remain as distinct agglomerates.

Figure 28 presents several photographs of the post-fire residue typically found during this investigation. Figure 28a shows typical residue from a low acceleration test with propellant N-7 at 500 psia. Small particles and spheres are seen on top of the solid metallic layer. Figure 28b is a photograph of the inhibitor case after removing the residue for propellant N-7 at high accelerations. Each pit mark in the plastic case had a small metallic spheroid imbedded in it with a diameter of approximately .050 inches.

It should be noted that at 1000g the residue form and weight for all three propellants were practically identical yet the greatest difference in augmentations occurred at this acceleration. This points to the possibility of different augmentation mechanisms for different propellant physical characteristics and will be discussed below.

Base Burning Rate Effects

In order to separate the effects of base burning rate from the combined effect of \dot{r}_0 and AP size discussed above, propellants N-7, N-9, and N-10 were tested. Propellants N-9 and N-10 were identical to propellant N-7 except that one-percent and two-percent by weight of yellow iron oxide catalyst were added respectively. Figure 29 indicates the increase in base burning rate obtained by adding the catalyst. The two fast burning propellants (N-9, N-10) exhibited practically the same augmentation. The slower burning propellant (N-7) augmented considerably more than either propellants N-9 or N-10.

Evidently, the high burning rate propellants forced the metal agglomerates and/or smaller AP crystals away from the surface at significantly higher velocity than occurred for propellant N-7. Thus, higher accelerations are required to obtain significant augmentation for fast burning rate propellants.

One assumption has been made in the above discussion which is not necessarily valid. The iron oxide catalyst was assumed to increase the base burning rate without causing a significant change in the physical behavior of the metal agglomerates. This was assumed because the iron oxide catalyst was not considered to have any effects on the metal combustion. Figure 30 indicates that the form of the residue changed when a catalyst was added. The catalyzed propellants had residue with a powdered texture in contrast to the solid layer and/or particles found for non-catalyzed propellants. Preliminary X-ray diffraction analysis of the residues indicated that the iron-oxide possible had a retarding effect on the metal oxidation process.

AP Crystal Size Effects

The effect of AP crystal size on the burning rate augmentation of aluminized composite propellants was determined by using propellants N-6 and N-9. Propellant N-6 had 9 μ AP crystals and propellant N-9 had 90 μ AP crystals. In addition, propellant N-9 contained 1 percent by weight of yellow iron oxide burning rate catalyst. Figure 31 presents the augmentation data obtained for these propellants. Note that there is less than a 2 percent difference in base burning rate. There appears to be no significant effect of AP crystal size on the augmentation for these two propellants. Propellant N-9 exhibited slightly less augmentation above 100g. Comparison of Figures 27 and 30 indicates that propellant N-9 produced more post-fire residue except at 1000g. In addition, the residue appearances were considerably different. As noted above, the AP crystal size influences the metal agglomerate size and in this manner may effect augmentation for propellants containing larger AP crystals. The possible chemical effects of the iron oxide have not been considered.

Aluminum Effects

Ten propellants (N-1 through N-10) were used to determine how much of the observed burning rate augmentation of aluminized composite propellants was due to the AP crystals and how much was due to the metal agglomerates on the burning propellant surface. Propellants N-1 through N-5 were identical to propellants N-6 through N-10 respectively except that the latter had 15 percent by weight of 44 μ aluminum added. Figures 32 through 36 present the augmentation data for corresponding aluminized and nonaluminized composite propellants. The lines in these figures are made only to indicate the trend in the data presented previously. It is somewhat difficult to separate the effects of the AP crystals and the aluminum in these Figures because the base burning rates for corresponding aluminized and nonmetallized propellants were different in most cases. The following general observations can be made for the noncatalyzed propellants [Figures 32, 33, and 34]: a) for small AP crystals, the AP crystals and metal agglomerates have an approximately equal influence on burning rate augmentation, and b) for very large AP crystals, the metal agglomerates are responsible for practically all of the burning rate augmentation.

A possible explanation for this observed behavior is presented below. The physical models of Sturm and Crowe, et. al. are utilized together. For small AP crystals there are probably many very small metal agglomerates on the surface and they may actually flood the surface. The smallest AP crystals and metal agglomerates are forced from the surface in the Og condition. As the oxidizer size increases, the agglomerate "pits" in the surface increase in size, the agglomerates are more distinct, and their effect is greater. At the same time, less AP is forced from the surface at Og. This process continues as the AP size is increased until practically all of the AP remains on the surface at Og and the metal agglomerates remain in distinct pits at all acceleration levels. In this limiting condition, the AP has practically no effect on the burning rate augmentation.

Figures 35 and 36 present the burning rate augmentation comparisons for the aluminized and nonmetallized propellants which contained a burning rate catalyst. Except at low accelerations, the augmentation of a fast burning rate propellants appears to be largely due to the metal agglomerates.

The above physical interpretation of the effect of AP size and the molten metal agglomerates has been oversimplified. The AP crystals and metal agglomerates interact and this interaction also may effect the augmentation.

Applicability of Crowe, et. al. Model

The analytical model developed by Crowe, et. al. [9] for burning rate augmentation of metallized composite propellants was discussed above. With certain simplifications, Equation 1 was developed.

$$\frac{\dot{r}_a}{\dot{r}_o} = 2 \left[\frac{r_s}{a} \left[\frac{\rho_p P_c^a}{r_s} \right]^{1/4} \frac{k^1}{\rho_s \dot{r}_o (1-W)} - 0.2 \right] + 1 \quad (1)$$

For a given propellant, Equation 1 may be written

$$\frac{\dot{r}_a}{\dot{r}_o} = 2 \left[k'' \frac{(P_c G)^{1/4}}{\dot{r}_o} - 0.2 \right] + 1 \quad (15)$$

In Equation 15, k'' is considered to be a constant. k'' is a function of r_s and a which provide a physical description of the metal agglomerates. The parameters r_s and a are functions of the acceleration, pressure, burning rate, AP size, etc., and therefore k'' is not actually a constant. Practical application of the model, however, requires that k'' be an experimentally determined constant. The value of k'' will thus depend upon the pressure and acceleration employed in the experiment.

In order to determine whether or not Equation 1 predicts the correct dependence of augmentation on acceleration, pressure, and base burning rate, Equation 15 was used in an attempt to correlate the experimental data. All of the aluminized composite propellants employed in this investigation (propellants N-6 through N-10) had essentially the same metal content (W).

An acceleration level of 250g was arbitrarily selected for determination of k'' in Equation 15. Using the experimentally known values of \dot{r}/\dot{r}_0 and \dot{r}_0 for each propellant at 500 psia and 250g, values of k'' were determined. Equation 15 was then employed to generate theoretical curves of augmentation as a function acceleration at 500 psia. Figures 37 and 38 show the comparison between the theoretical predictions and the experimental results for propellants N-6 through N-10. A curve representing experimental data was obtained by fitting a smooth curve through the experimental data.

Selection of another acceleration for determining k'' merely changes the cross-over point of the theoretical and experimental curves.

By determining k'' from an experimental datum point, the magnitude of the augmentation predicted by Equation 15 is forced to be nearly that of the experimental data for a wide range in values of acceleration. Nevertheless, Figures 37 and 38 indicate that the model does give the correct qualitative dependence of augmentation on acceleration. The slope of the experimental and theoretical curves are somewhat different. However, the variation of k'' with acceleration has been neglected. In addition, it does appear that the model breaks down at very low acceleration ($\dot{r}/\dot{r}_0 < 1.06$ as noted in reference 8).

In order, to evaluate the dependence of augmentation on base burning rate that is predicted by Equation 15, the experimental data from propellants N-7 and N-9 were employed. Although some evidence existed to indicate that the catalyst in propellant N-9 affected the metal agglomerates, it was assumed in this case that k'' for propellant N-9 was the same as

k'' for propellant N-7. A theoretical curve was generated for propellant N-9 using k'' for propellant N-7 and \dot{r}_0 for propellant N-9 in Equation 15. The results are shown in Figure 39. Figure 39 indicates that the model predictions agreed quite favorably with the experimental dependence of augmentation on base burning rate **except at low accelerations.**

Using the values of k'' determined at 500 psia for propellants N-6 and N-7, theoretical augmentation curves were determined for a pressure of 1000 psia by using 1000 psia and the experimentally determined values of \dot{r}_0 at 1000 psia in Equation 15. The results are shown in Figures 40 and 41. Comparison of Figures 37 and 40 indicates that the model provided a good estimate for the experimentally determined decrease in augmentation with increasing pressure for propellant N-7. Comparison of Figures 37 and 41 indicates that the model predicted the opposite effect of pressure on augmentation as determined by experiment for propellant N-6. However, the weak dependence on pressure predicted for propellant N-6 agrees with the experimental data.

In conclusion, the Crowe Model can be employed to predict the dependence of augmentation on pressure, base burning rate, and acceleration when one experimental datum point is used to determine the unknown constant in Equation 15 and the base burning rate dependence on pressure is known. The failure of the model to correctly predict the dependence of augmentation on pressure for propellant N-6 probably resulted from the assumption in this case that k'' in Equation 15 was constant. As noted above, k'' is a function of \dot{r} , a , etc. which are in turn functions of pressure, AP size, and etc.

The significant augmentation obtained for nonmetallized propellants (discussed above) indicates that the model neglects an important part of the augmentation mechanism for aluminized composite propellants. As noted by Crowe et. al. [8], the model also does not consider the effects of **burn time or acceleration** on particle size and shape. Thus, the analytically unknown constant k'' (or k') prevents quantitative predictions with the model. The model also appears to break down at very low accelerations.

slightly with acceleration and then decreased to less than one at 1000g. At 1000 psia the augmentation remained practically constant at all accelerations.

The post-fire residue form and weight are practically the same to 600g for both pressures. Above 600g the residue weight varied considerably from run to run at fixed acceleration and pressure. A general trend was observable. At high accelerations, increasing pressure decreased residue weight and increased augmentation. The post-fire residue consisted of lead and/or copper in addition to the aluminum and/or aluminum oxide.

Comparison of Figures 42 and 44 indicates that the presence of aluminum enhanced the augmentation at high accelerations.

The following conclusions can be made:

- (a) Lead and/or copper additives tend to flood the propellant surface and decrease augmentation at high accelerations.
- (b) Lead and/or copper flooding may cause unstable burning at high accelerations.
- (c) Addition of aluminum increases the augmentation but the lead and/or copper additives prevent significant acceleration induced burning rate augmentation.

Double-Base Propellants

General Discussion

The effects of acceleration on the burning rates of aluminized and nonaluminized double-base propellants were investigated in hopes of obtaining a better understanding of the effects of aluminum on augmentation. The propellant composition for the two propellants employed in this investigation were presented in Table II. The propellants were practically identical except that propellant DBNA was nonaluminized and propellant DBA had 5.3 percent aluminum. Both propellants had lead and copper additives.

Nonaluminized Double-Base Propellants

The data obtained for propellant DBNA are presented in Figures 42 and 43. The burning rate augmentation is observed to decrease with decreasing pressure and increasing acceleration. Post-fire residue data were taken for the 265 psia runs. A typical post-fire residue obtained for accelerations greater than 250g is shown in Figure 28c. Comparing Figures 42 and 43 it can be seen that the augmentation began to decrease at approximately the same acceleration level that post-fire residue began to appear.

The residue was in the form of pieces and/or partial layers of lead and/or copper. The characteristic carbon "fluf" found in the inhibitor cases of the composite propellants burned at low accelerations was not present. The lead and/or copper have low melting points and probably form a partial "flood layer" of molten metal on the surface of the burning propellant - thereby decreasing the burning rate. Several 500 psia tests and one 265 psia test exhibited unstable burning. The pressure trace would oscillate in a low frequency sinusoidal motion. The instability could be the result of periodic flooding and unflooding of the propellant surface.

Aluminized Double-Base Propellants

The data obtained for the aluminized double-base propellant DBA are presented in Figures 44 and 45. The burning rate augmentation increased with pressure at high accelerations. At 503 psia, augmentation increased

CONCLUSIONS

Nonmetalized Composite Propellants

1. In general, burning rate augmentation increases with increasing acceleration.
2. Strand cross-sectional area has no appreciable effect on burning rate augmentation.
3. Strand length (burn time) has only small effects on burning rate augmentation and/or burning rate.
4. Burning rate augmentation increases slightly with temperature at high accelerations.
5. Burning rate augmentation increases with increasing pressure except at low accelerations.
6. Burning rate augmentation increases with decreasing base burning rate.
7. AP crystal size has no appreciable effect on augmentation at high accelerations.
8. Sturm's physical model [5] can be used to explain most of the phenomena associated with the acceleration sensitivity of nonmetalized composite propellants.
9. Sturm's analytical expression(s) for burning rate augmentation was found to qualitatively agree with experimental results. However, use of a standard drag force expression in place of the Stokes' drag force expression improved the agreement between experimental results and the analytical model at low accelerations. The dependence of the model parameters on "phalanx" flame penetration rate, crystal consumption rate, and binder type are not known.

Aluminized Composite Propellants

1. Burning rate augmentation increases with increasing acceleration and decreasing base burning rate.
2. Burning rate augmentation is not a consistent function of pressure.
3. Increasing pressure increases post-fire residue weight but does not appreciable change the residue appearance.

4. For a fixed base burning rate, AP crystal size has no appreciable effect on burning rate augmentation (for small AP crystal sizes).
5. Burning rate augmentation decreases slightly with increasing temperature above 20C.
6. Iron oxide catalysts may effect metal combustion.
7. Strand cross-sectional area does not affect burning rate augmentation at low accelerations but may affect augmentation at high accelerations.
8. Strand cross-sectional area affects the post-fire residue appearance.
9. Average base burning rate and burning rate augmentation decrease with increasing strand length (burn time) for accelerations less than 500g. Augmentation was not a function of strand length for accelerations greater than 500g.
10. The weight and appearance of the molten metallic material on the surface of a burning propellant have a strong effect on augmentation. Weight and form have a strong effect at low accelerations and form has a dominant effect at high accelerations. Both the form and weight change with burn time (strand length).
11. Post-fire residue weight characteristically increases to a maximum with increasing acceleration and then decreases with further increases in acceleration. Maximum residue weight was found to occur at accelerations less than 300g.
12. Burning rate augmentation increases as the metal agglomerates become more distinct.
13. For a fixed size and weight percentage of aluminum, the following conclusions can be made with respect to the percentages of the total augmentation that are caused by the metal agglomerates and the AP crystals in an aluminized composite propellant:
 - a) For small AP crystals, the AP augmentation effect and the metal agglomerate augmentation effect are approximately equal in their contribution to the total burning rate augmentation.
 - b) For very large AP crystals, practically all burning rate augmentation is due to the metal agglomerate effect.

14. The Crowe, et. al. model can be employed to predict the dependence of augmentation on pressure, base burning rate, and acceleration when experimental data are available at one non-zero acceleration and the base burning rate dependence on pressure is known. The primary weaknesses in the model are that it does not account for the AP crystal induced augmentation and that there is no method for predicting the quantity or form of the molten metal.
15. Base burning rate and burn time have the greatest effect upon augmentation.

Nonaluminized Double-Base Propellants

(with copper and lead additives)

1. Burning rate augmentation decreases with decreasing pressure and increasing acceleration.
2. Burning rate augmentation decreases as the molten metal on the surface increases in weight (flood layer).
3. Burning rate instability may exist at high accelerations as a result of periodic surface "flooding" and "unflooding".

Aluminized Double-Base Propellants

(with copper and lead additives)

1. Burning rate augmentation increases with increasing pressure at high accelerations.
2. Burning rate augmentation is not a strong function of acceleration. The aluminum increases the augmentation but the effect is practically cancelled by the opposite effect of the copper and lead additives.

FUTURE INVESTIGATIONS

The following is a list of the investigations which are planned for the next year:

1. Detailed study of the effects of acceleration and burn time on residue weight and form of aluminized composite propellants.
2. Photographic study of the effects of AP size, aluminum, and catalysts on burning rate augmentation.
3. Continued study of the acceleration sensitivity of nonmetallized composite propellants.

REFERENCES

1. Northam, W. B. and Lucy, A. H., "On the Effects of Acceleration Upon Solid Rocket Performance," presented at the 1968 ICRPG/AIAA 3rd Solid Propulsion Conference, Atlantic City, New Jersey, 4-6 June, 1968, AIAA Paper No. 68-530.
2. "Investigation of Performance Losses and Ballistics Effects in Solid Propellant Rockets," UTC2197-FR (Naval Ordnance Systems Command Contract No. N0w-0444C), United Technology Center, Sunnyvale, California, April, 1967.
3. "Investigation of Internal Ballistics Effects in Spinning Solid Propellant Motors," UTC 2281-QTR 1 (Naval Ordnance Systems Command Contract No. N00017-67-C-2429), United Technology Center, Sunnyvale, California, August, 1967.
4. Anderson, J. B. and Reichenbach, R. E., "An Investigation of the Effect of Acceleration on the Burning Rate of Composite Propellants," Naval Postgraduate School Report Number NPS-57RV7071A, July, 1967.
5. Sturm, E. J., "A Study of the Burning Rates of Composite Solid Propellants in Acceleration Fields," Ph.D. Thesis, Naval Postgraduate School, March, 1969.
6. Glick, R., "An Analytical Study of the Effects of Radial Acceleration Upon the Combustion Mechanism of Solid Propellant," Thiokol Report No. 42-66, NASA Report No. 66218, Thiokol Chemical Corporation, Huntsville, Alabama, December, 1966.
7. Glick, R., "The Effect of Acceleration on the Burning Rate of Nonmetallized Composite Propellants", 3rd ICRPG Combustion Conference, CPIA Publication No. 138, Vol. 1, February, 1967.
8. Willoughby, P. G., Crowe, C. T., Dunlap, R., and Baker, K. L., "Investigation of Internal Ballistic Effects in Spinning Solid Propellant Motors," UTC Report No. UTC 2281-FR, October, 1968, Final Report on NOSC Contract No. N00017-67-C-2429.

9. Northam, G., "An Experimental Investigation of the Effects of Acceleration on the Combustion Characteristics of an Aluminized Composite Solid Propellant," proceedings of the ICRPG/AIAA Solid Propulsion Conference, CPIA Publication No. 111, Vol. II, Washington, D. C., July, 1966, p. 129.
10. Northam, G. B., "Effects of Steady-State Acceleration on Combustion Characteristics of an Aluminized Composite Solid Propellant," NASA TN D-4914, December, 1968.
11. "An Optical Bomb Study of the Combustion of Solid Propellants in High Acceleration Fields," Atlantic Research Corporation, Second Annual Technical Report, July, 1969.
12. Bringhurst, W., "The Effect of Strand Size on Experimental Measurement of Solid Propellant Burning Rate Augmentation," unpublished MS Thesis, Naval Postgraduate School, December, 1968.
13. Anderson, J. B. and Reichenbach, R. E., "An Investigation of the Effect of Acceleration on the Burning Rate of Composite Propellants," AIAA Journal, 6, pp 271-277, 1968.
14. Sturm, E. J. and Reichenbach, R. E., "An Experimental Study of the Burning Rates of Aluminized Composite Solid Propellants in Acceleration Fields," presented at the 1968 ICRPG/AIAA 3rd Solid Propulsion Conference, Atlantic City, New Jersey, 4-6 June, 1968, AIAA Paper No. 68-529.
15. Sturm, E. J. and Reichenbach, R. E., "A Study of the Burning Rates of Composite Solid Propellants In Acceleration Fields," Naval Postgraduate School Report No. NPS-57RV8121A, December, 1968.
16. Bulman, M. J., "The Effect of Acceleration on the Burning Rate of Double Base Solid Propellant With and Without Aluminum," MSAE Thesis, Naval Postgraduate School, June, 1969.
17. Summerfield, M. et. al., "Burning Mechanism of Ammonium Perchlorate Propellants," Progress in Astronautics and Rocketry, Vol. 1, New York: Academic Press, 1960, p. 142.

18. Fenn, J. B., "A Phalanx Flame Model for the Combustion of Composite Solid Propellants," Project Squid Technical Report PR-114-P, April, 1967.
19. Mann, R., et. al., Control of Solid Propellant Combustion," Journal of Spacecraft and Rockets, 3, 1966.
20. Anderson, J. B., and Reichenbach, R. E., "76-Inch Diameter Centrifuge Facility," Naval Postgraduate School Technical Note No. TN 66T-4, September, 1966.
21. Bastress, E. K., Ph.D. Thesis, Princeton, 1961.
22. Schlichting, H., Boundary Layer Theory, McGraw-Hill Book Co., Inc., 1960, pp. 95-98.

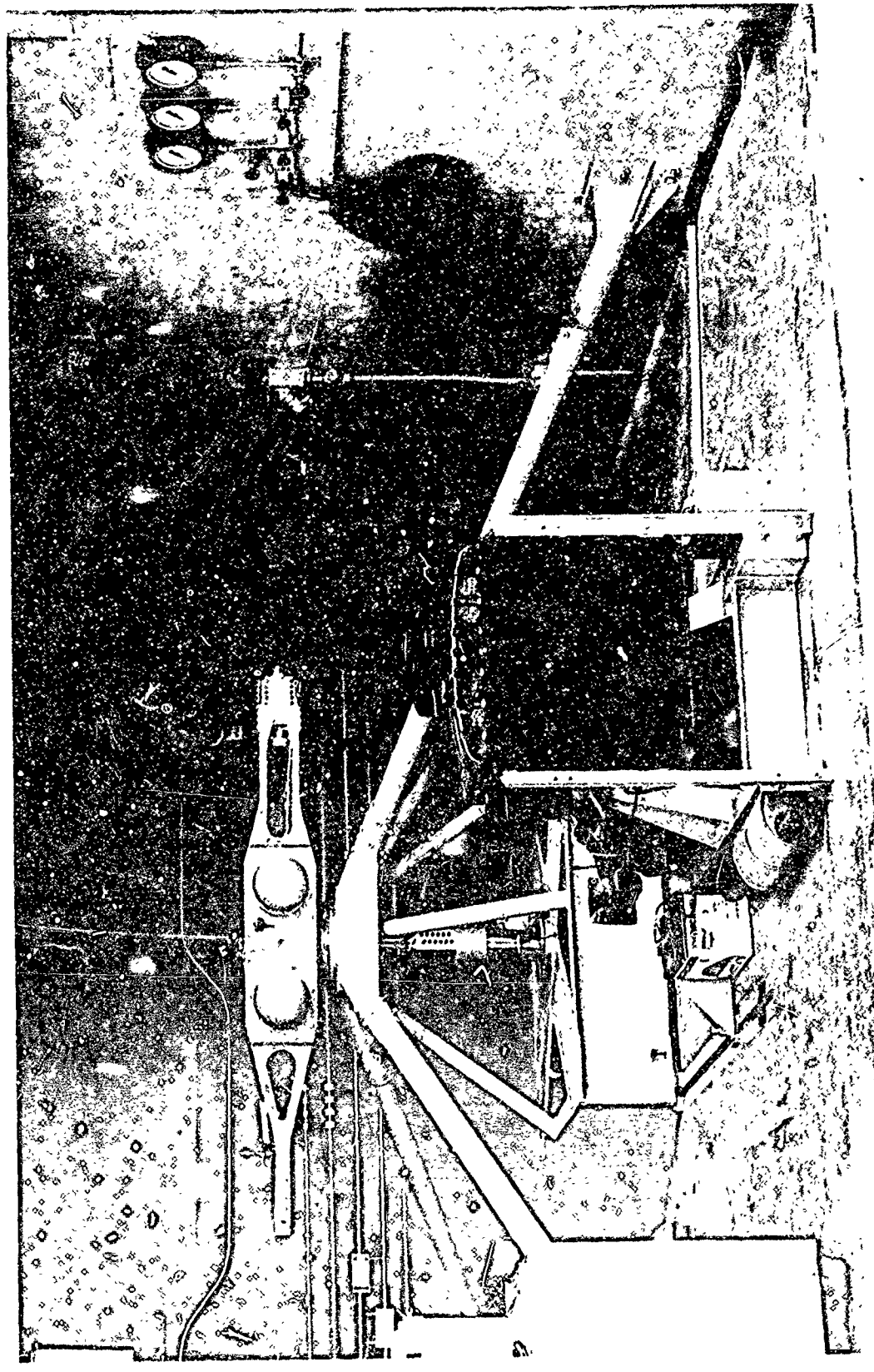


FIGURE 1. N.P.S. CENTRIFUGE

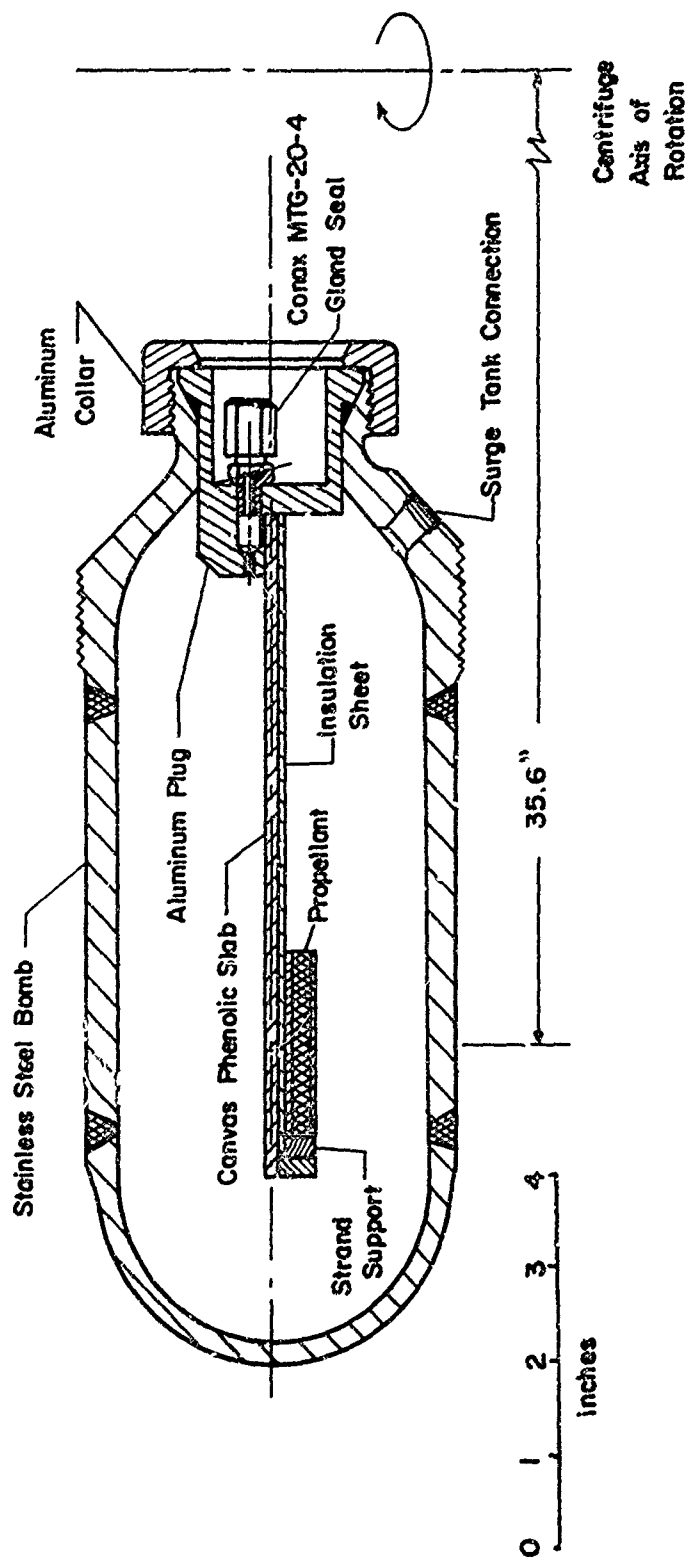


FIGURE 2 . COMBUSTION BOMB AND STRAND HOLDER

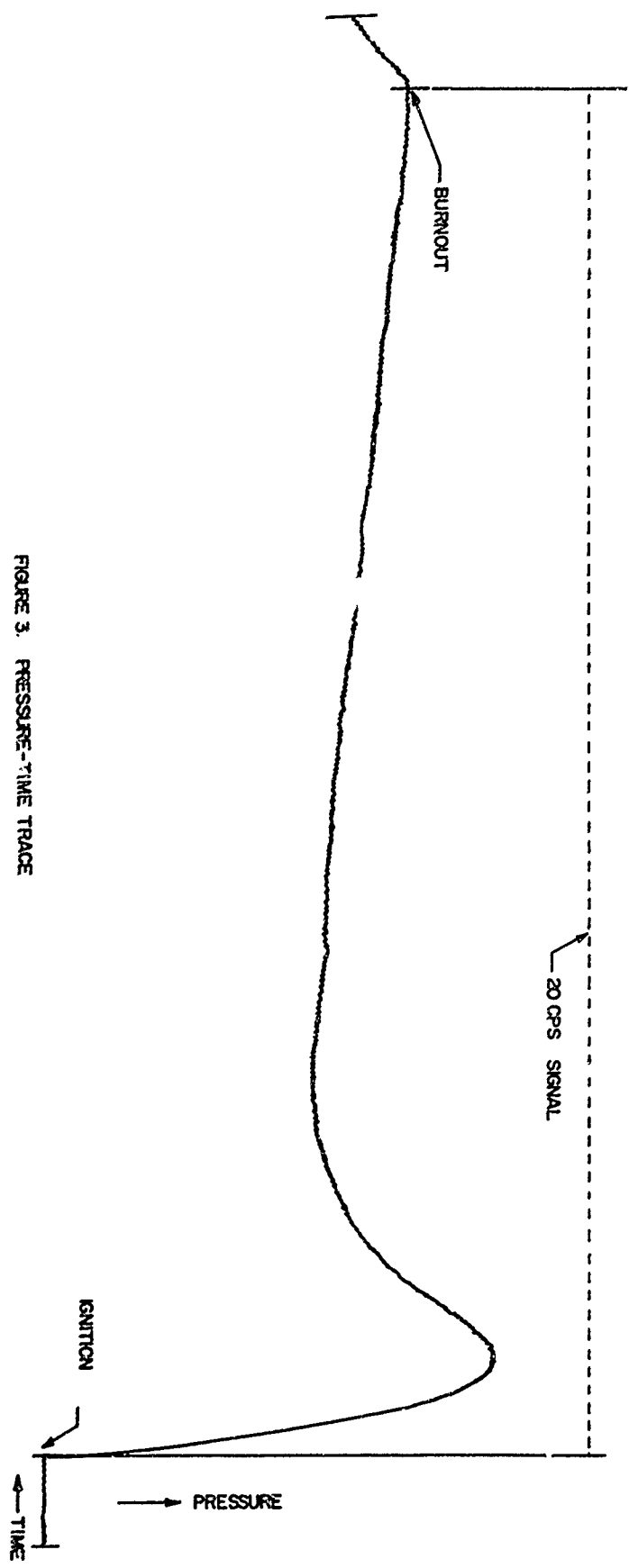


FIGURE 3. PRESSURE-TIME TRACE

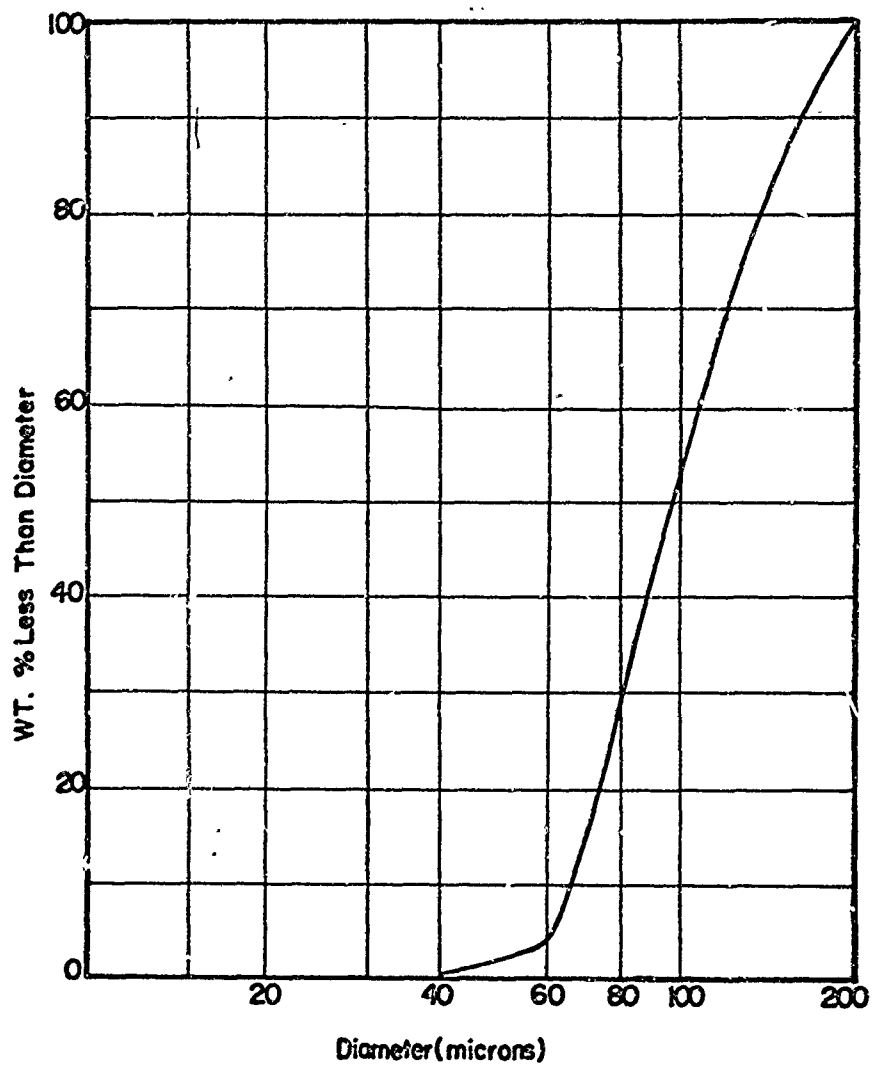


FIGURE 4 . AMMONIUM PERCHLORATE SIZE DISTRIBUTION.

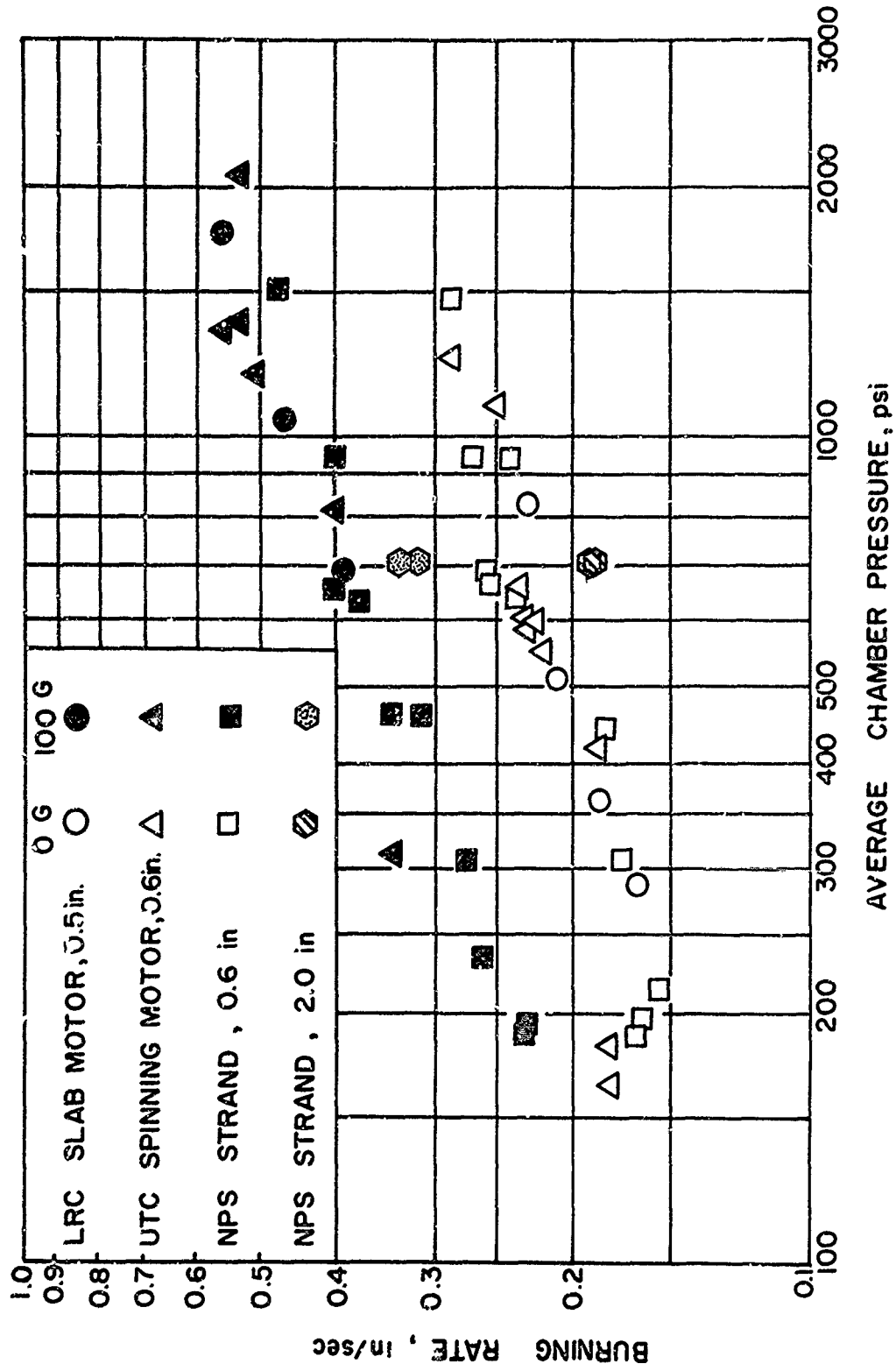


FIGURE 5 . COMPARISON OF BURNING RATE DATA FOR UTC CONTROL PROPELLANT (ADAPTED FROM REF 8)

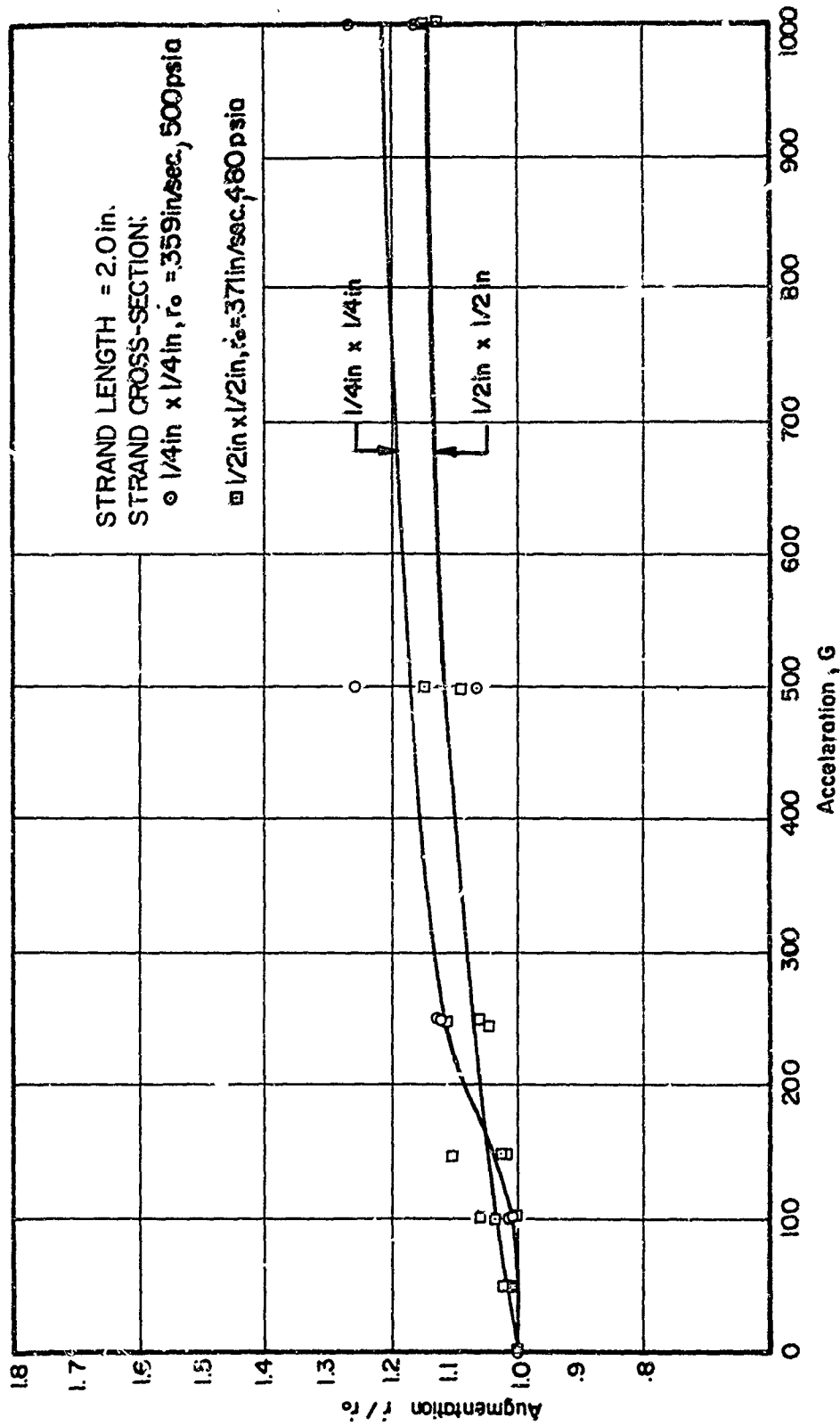


FIGURE 6. EFFECT OF STRAND CROSS-SECTION ON BURNING RATE AUGMENTATION OF NON-ALUMINIZED COMPOSITE PROPELLANT (N-1) AT 500 PSIA

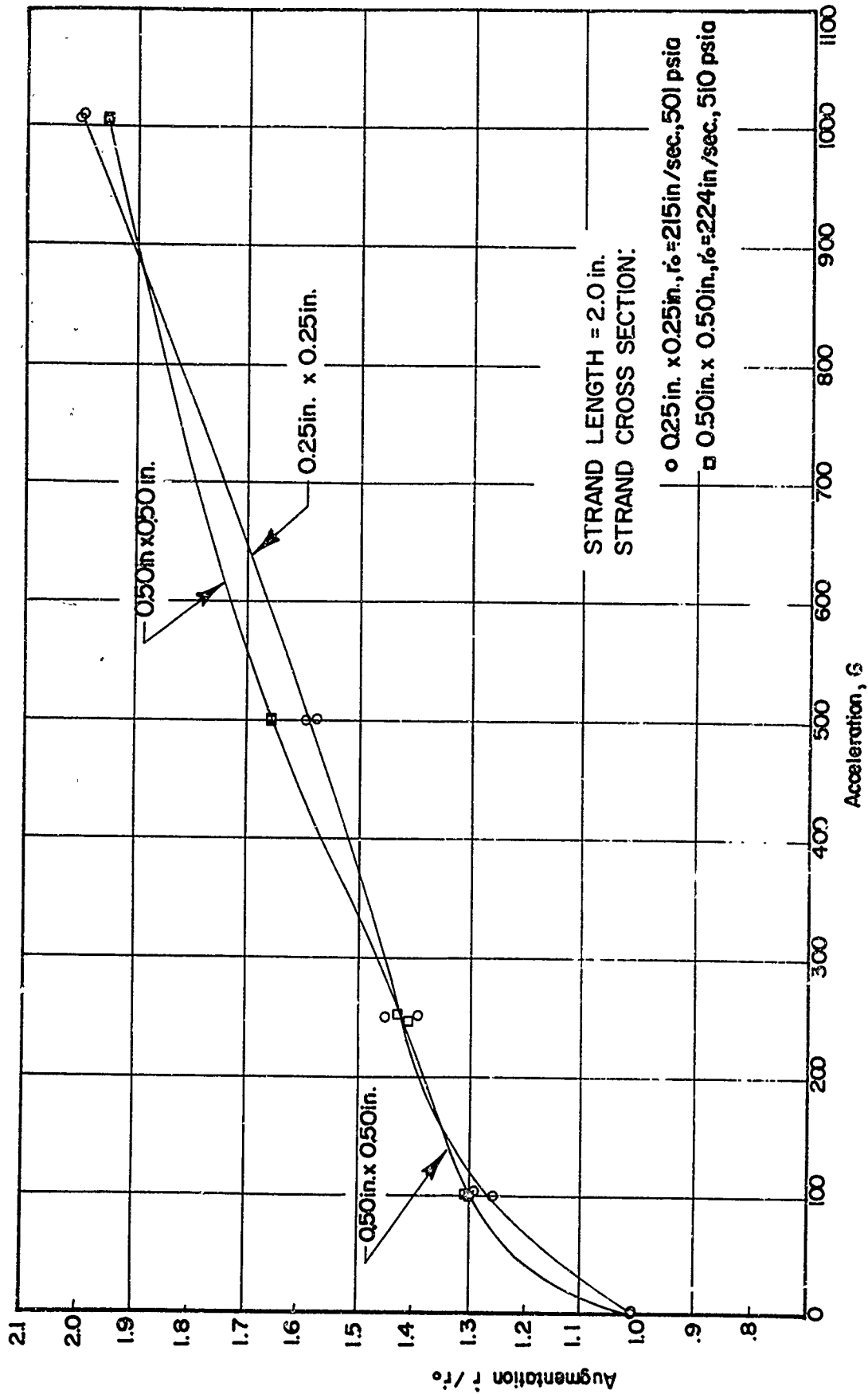


FIGURE 7. EFFECT OF STRAND CROSS-SECTION ON BURNING RATE AUGMENTATION OF ALUMINIZED COMPOSITE PROPELLANT (N-7) AT 500PSIA

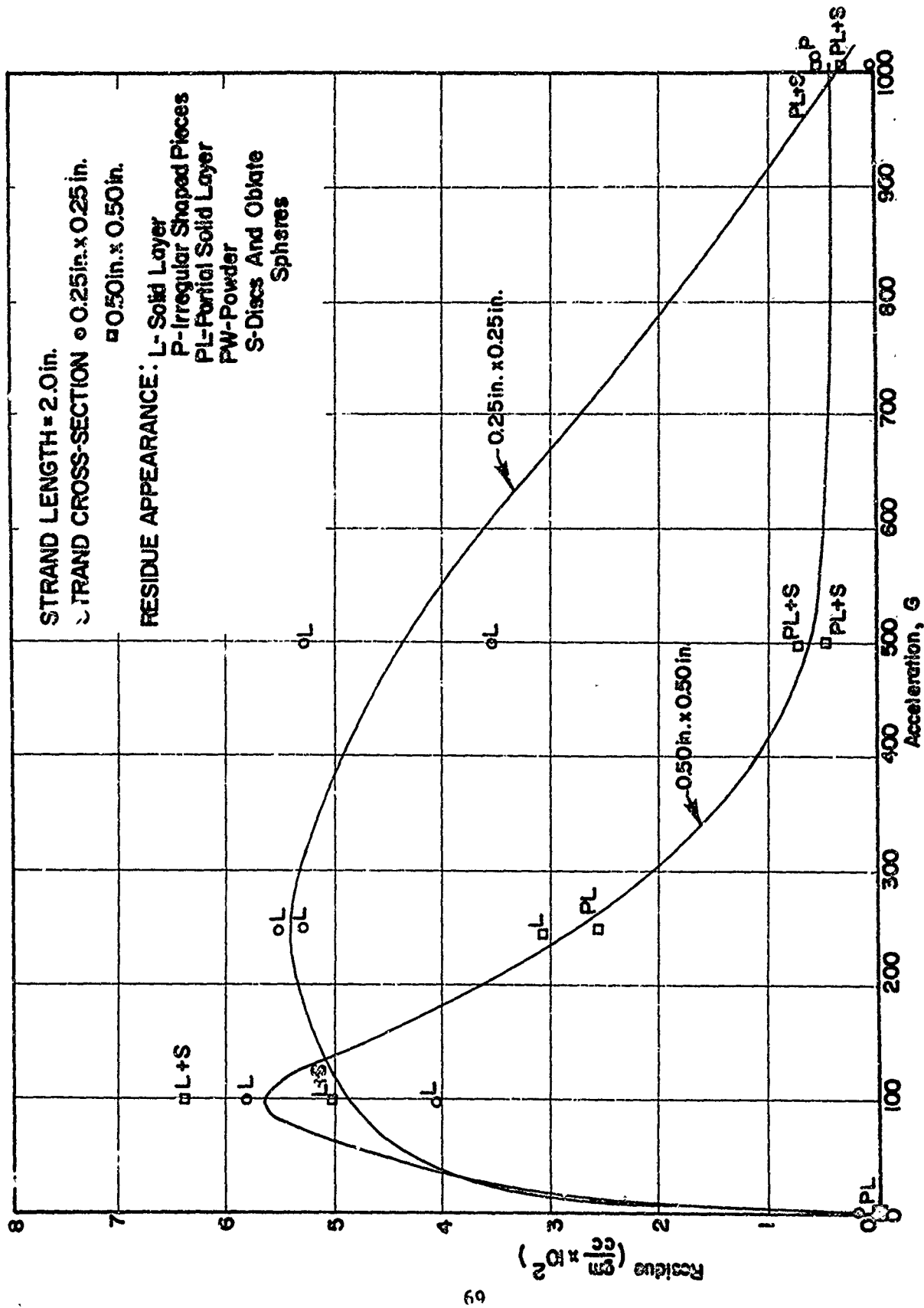


FIGURE 8. EFFECT OF STRAND CROSS-SECTION ON RESIDUE FORMATION OF ALUMINIZED COMPOSITE PROPELLANT(N-7) AT 500PSIA

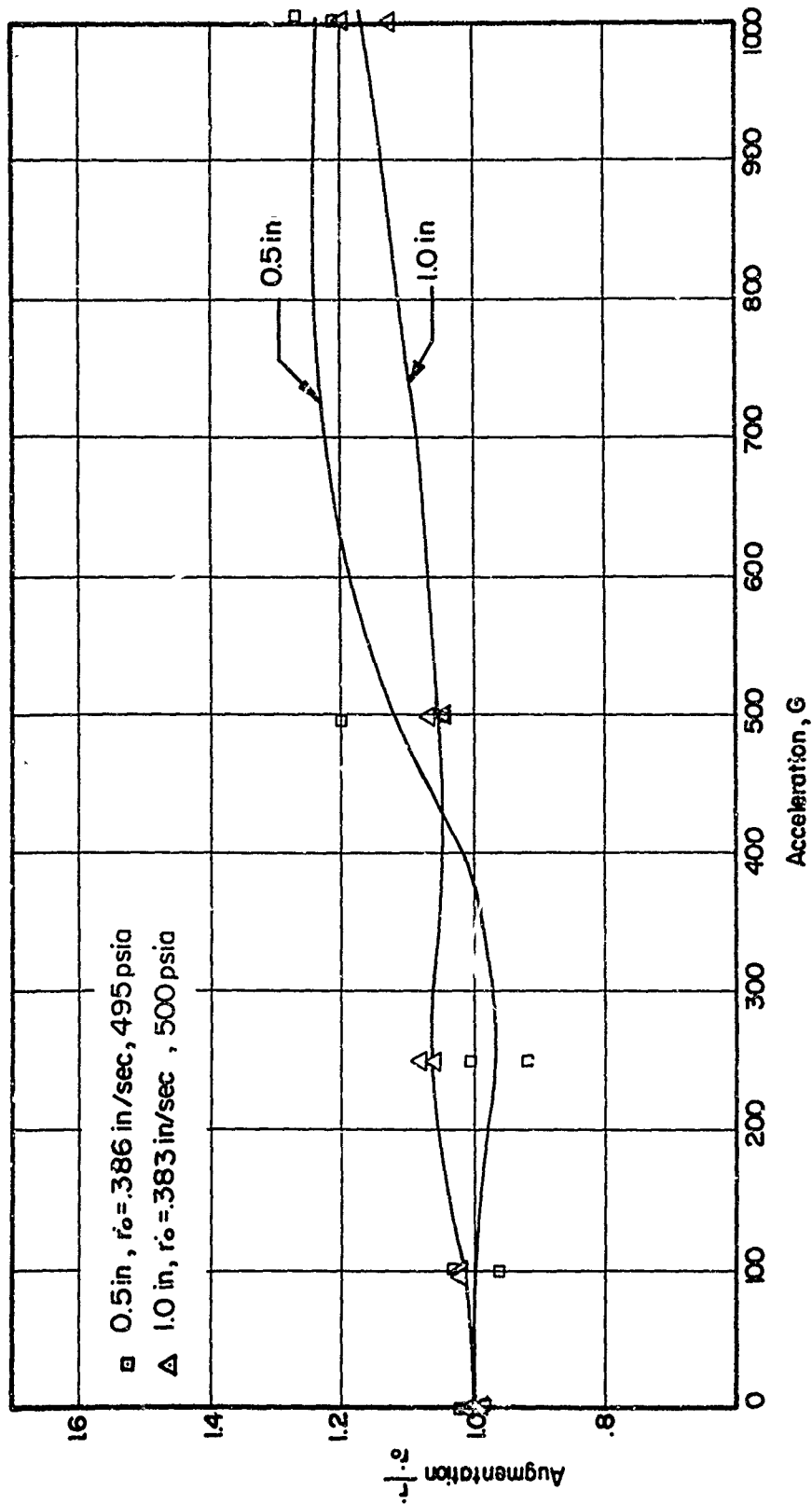


FIGURE 9. EFFECT OF STRAND LENGTH ON BURNING RATE AUGMENTATION OF NON-ALUMINIZED COMPOSITE PROPELLANT(N-I) AT 500 PSIA

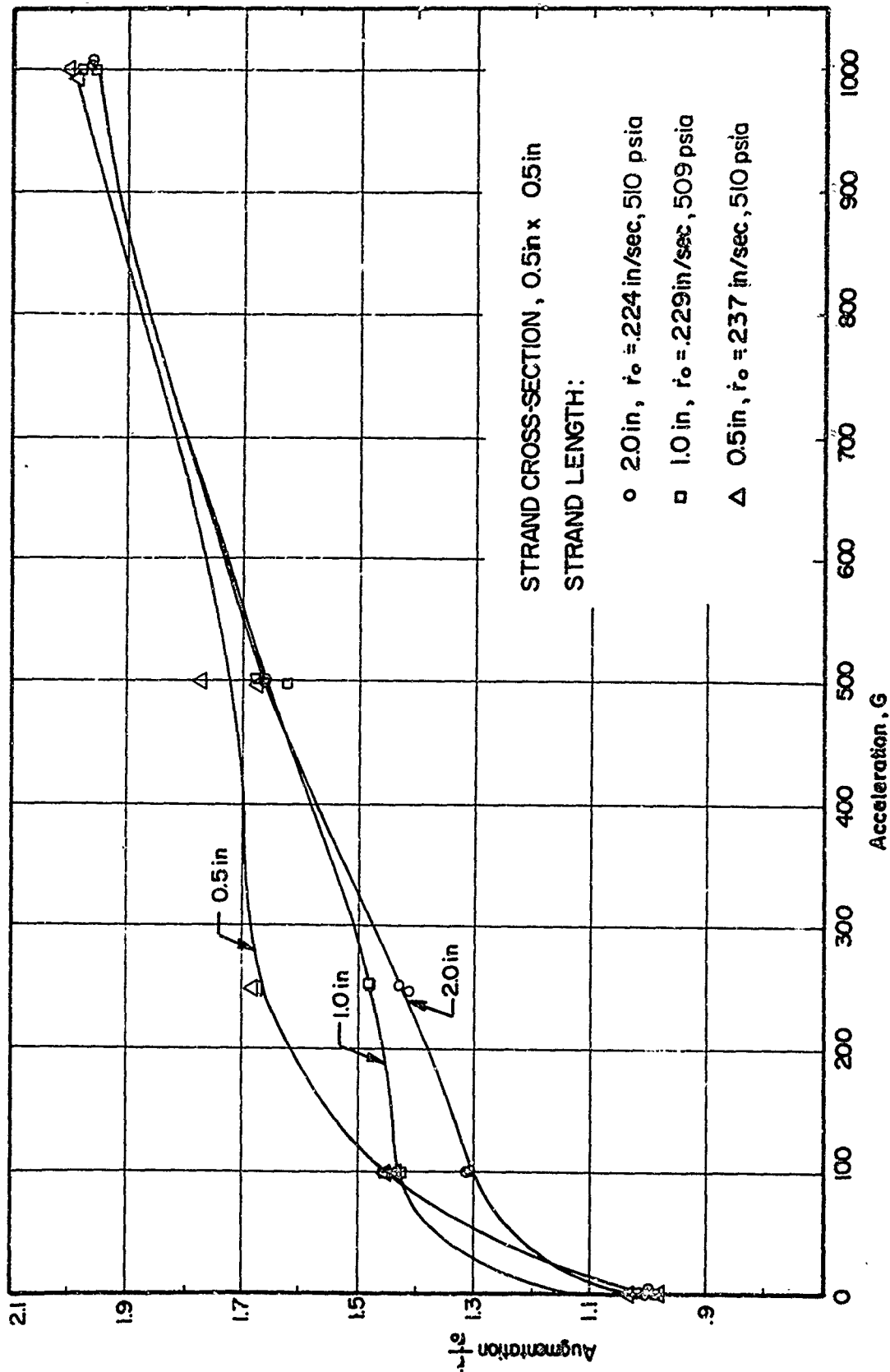


FIGURE 10. EFFECT OF STRAND LENGTH ON BURNING RATE AUGMENTATION OF ALUMINIZED COMPOSITE PROPELLANT (N-7) AT 500 PSIA

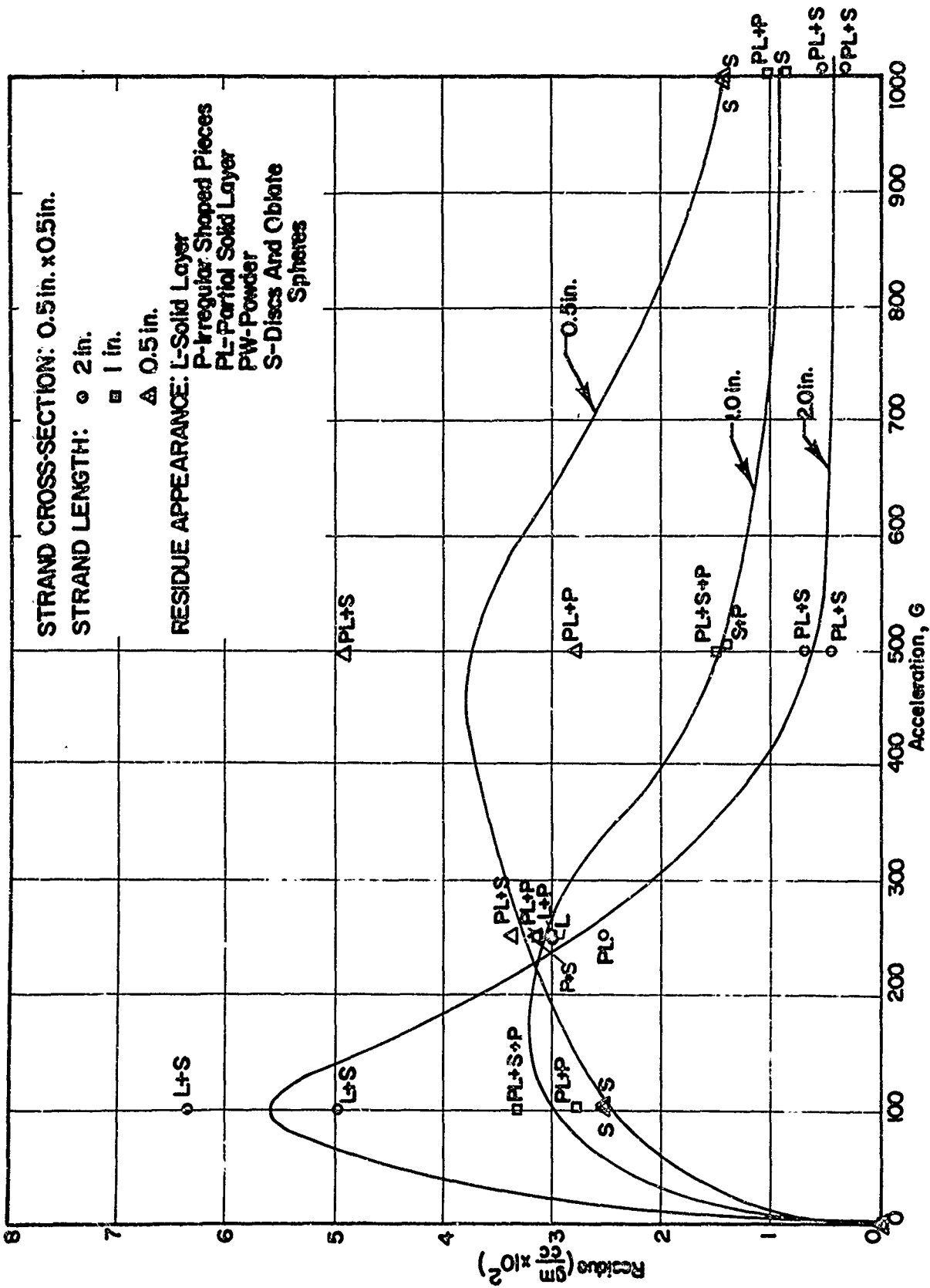


FIGURE 11. EFFECT OF STRAND LENGTH ON RESIDUE FORMATION OF ALUMINIZED COMPOSITE PROPELLANT (N-7) AT 500 PSIA

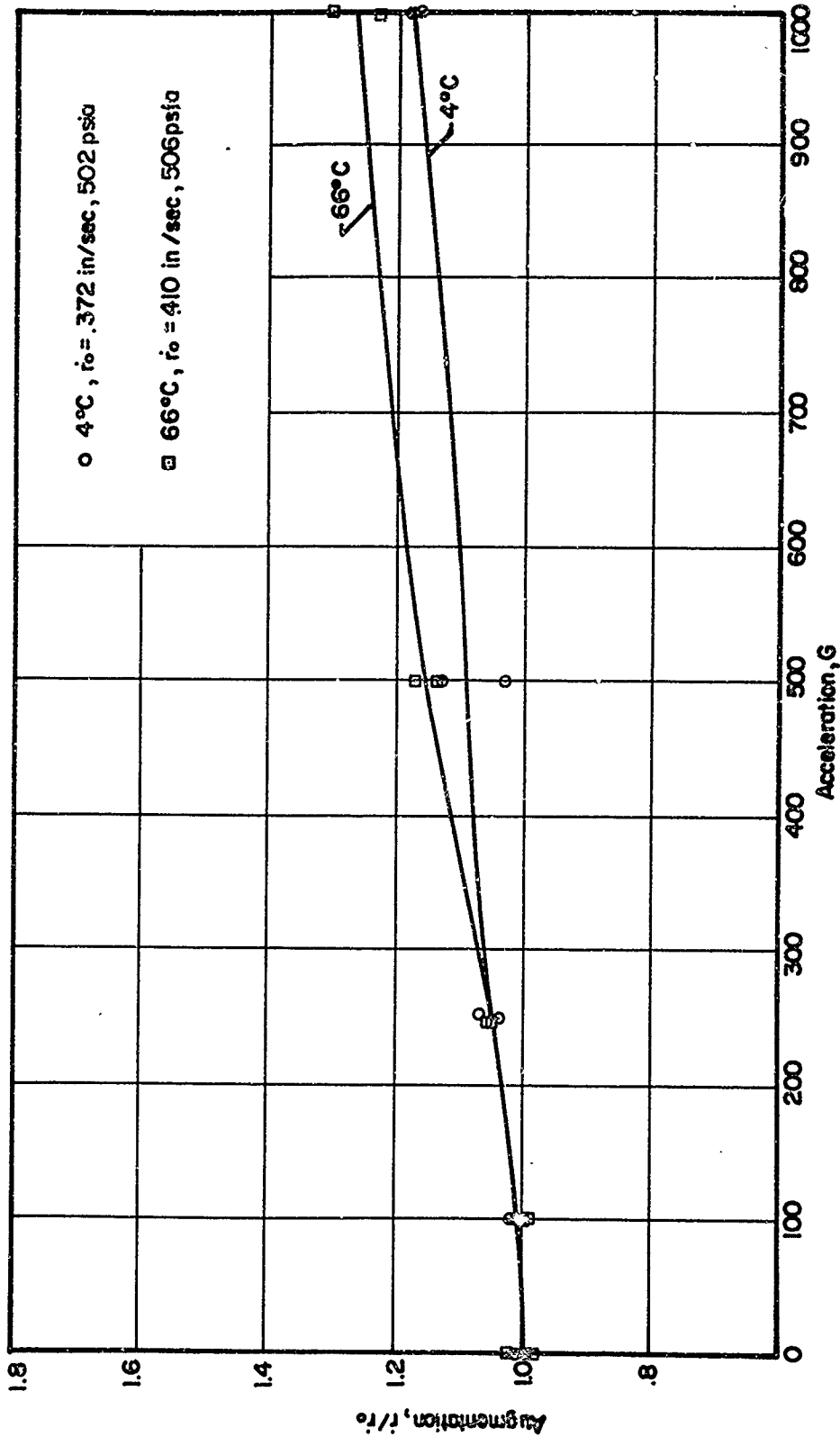


FIGURE 12. EFFECT OF TEMPERATURE ON BURNING RATE AUGMENTATION OF NON-ALUMINIZED COMPOSITE PROPELLANT(N-I) AT 500 PSIA.

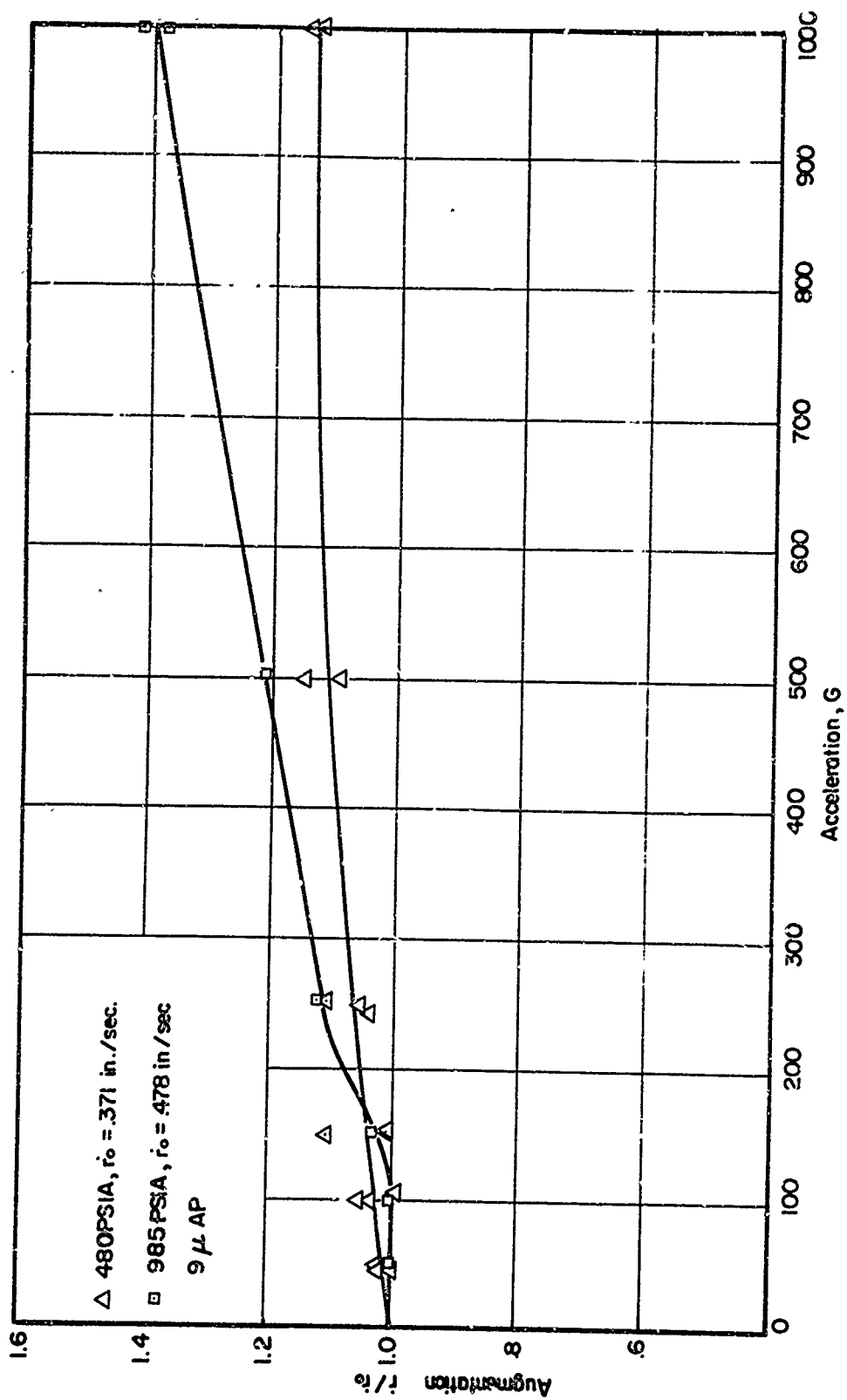


FIGURE 13. EFFECT OF PRESSURE ON BURNING RATE AUGMENTATION OF NON-METALLIZED COMPOSITE PROPELLANT(N-1)

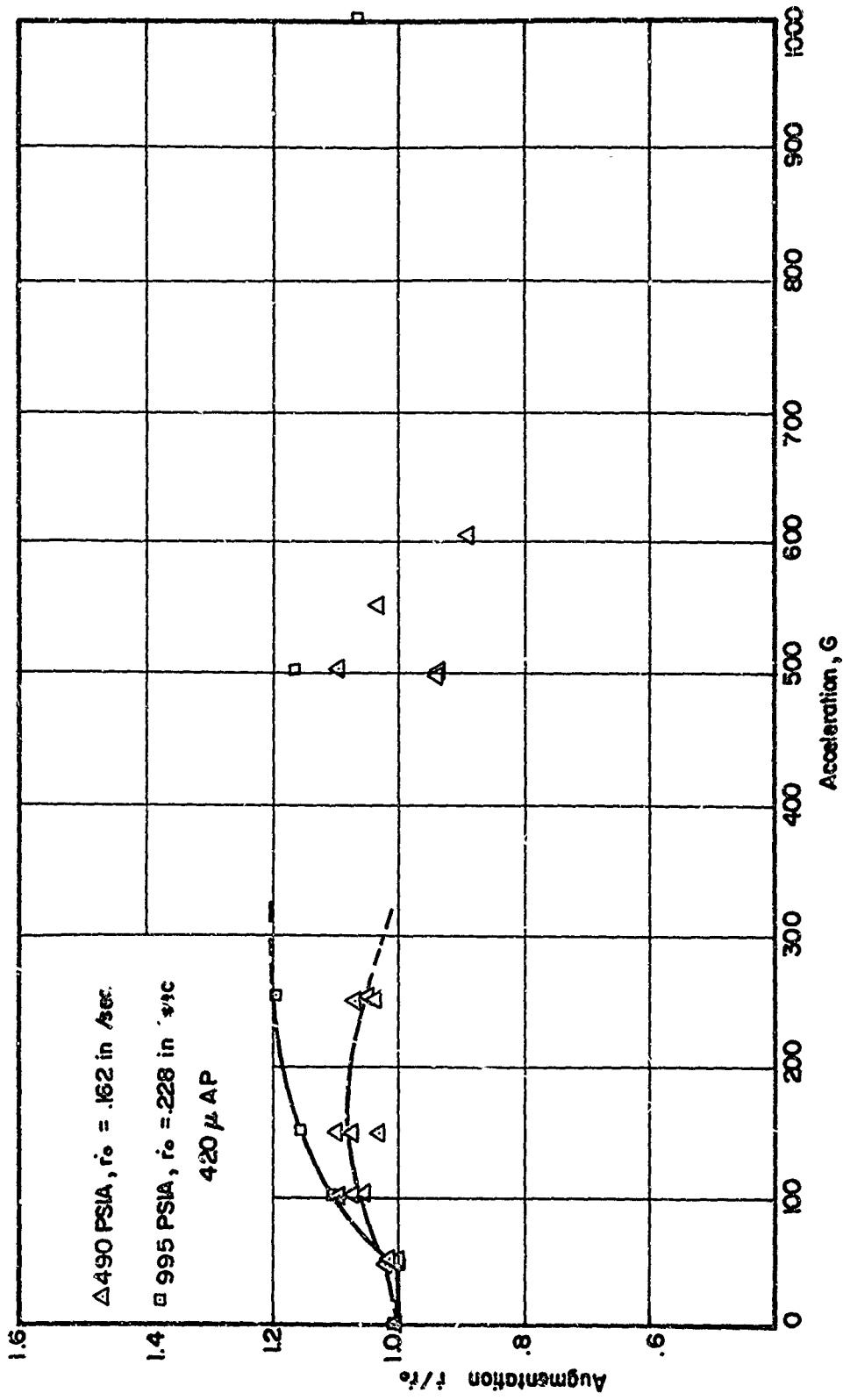


FIGURE 14. EFFECT OF PRESSURE ON BURNING RATE AUGMENTATION OF NON-METALLIZED COMPOSITE PROPELLANT (N-3)

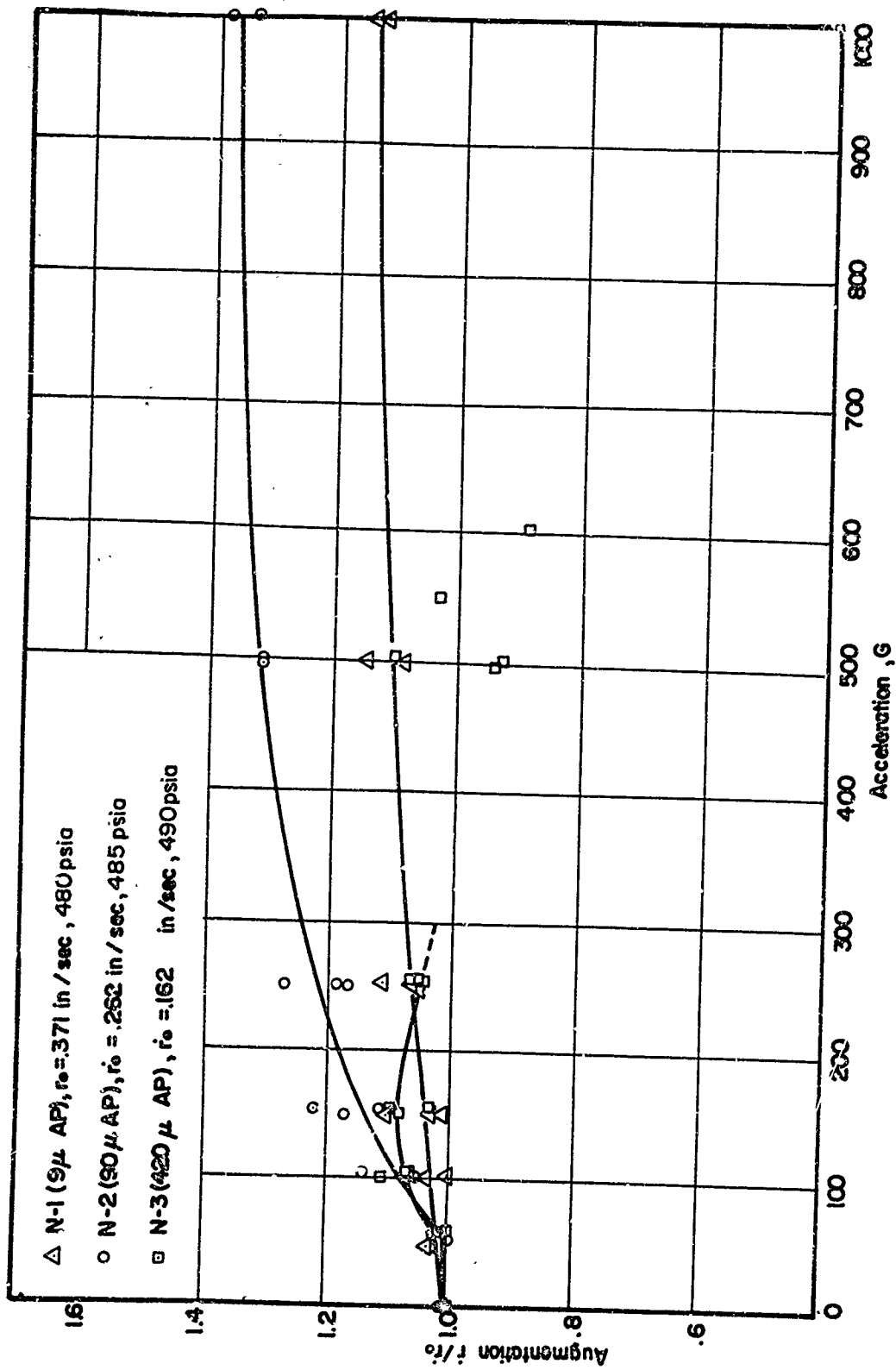


FIGURE 15. EFFECT OF AP SIZE AND r_0 ON BURNING RATE AUGMENTATION OF NON-METALLIZED COMPOSITE PROPELLANTS AT 500 PSIA.

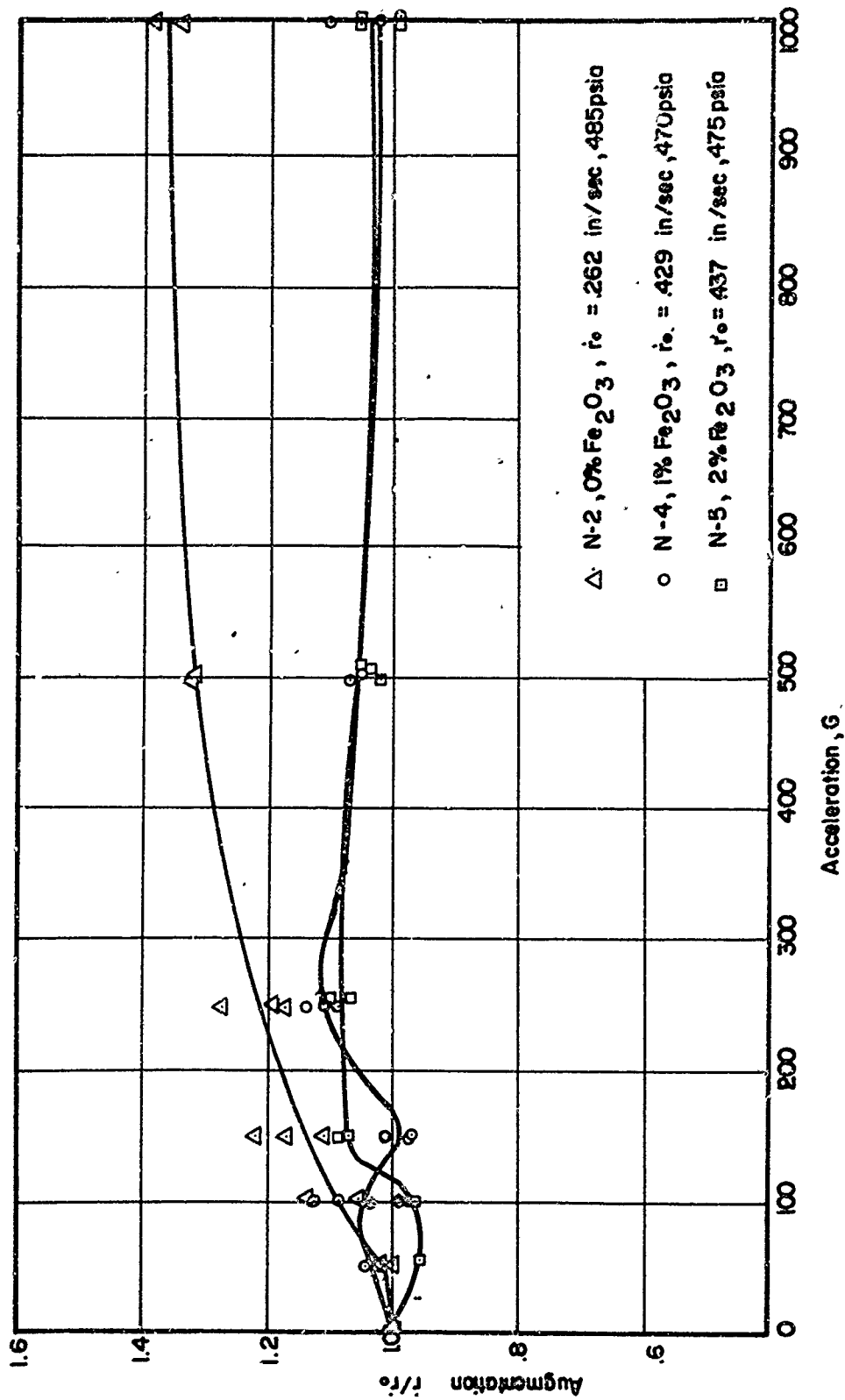


FIGURE 16. EFFECT OF r_0 ON BURNING RATE AUGMENTATION OF NON-METALLIZED COMPOSITE PROPELLANTS AT 500PSIA. (90 μ AP)

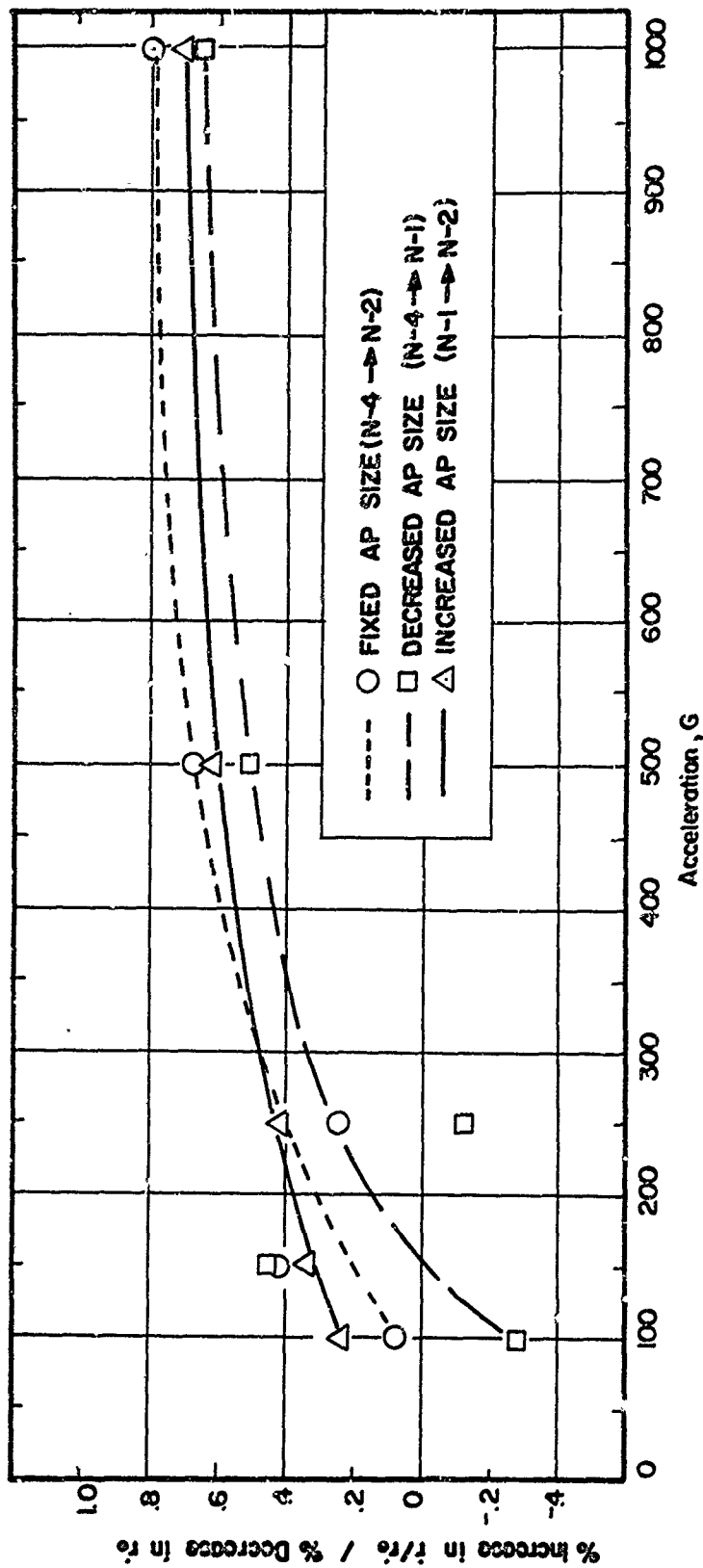


FIGURE 17. EFFECT AP SIZE ON BURNING RATE AUGMENTATION OF NON-METALLIZED COMPOSITE PROPELLANTS AT 500 PSIA.

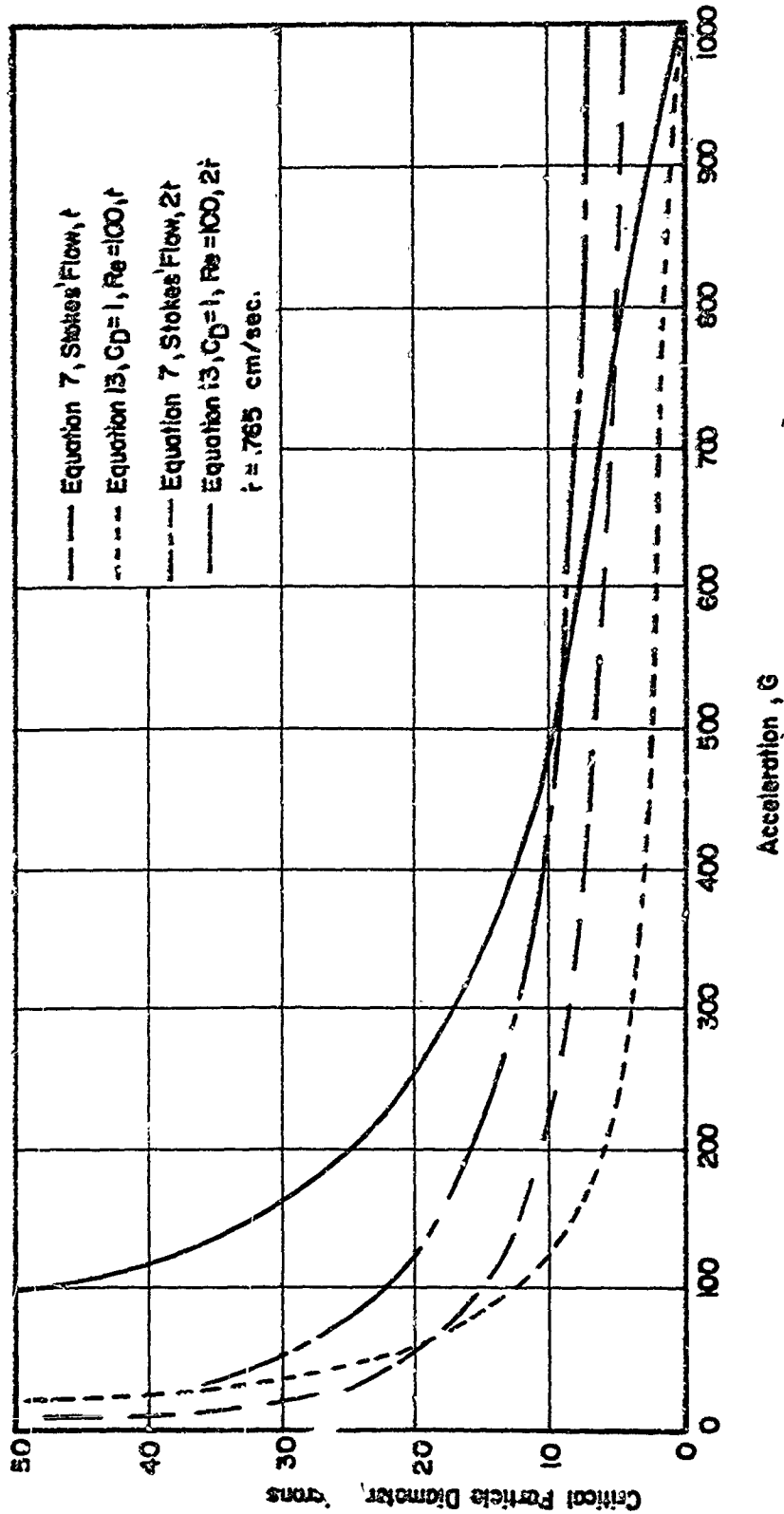


FIGURE 18. CRITICAL PARTICLE DIAMETER VERSUS ACCELERATION AT 500 PSIA.

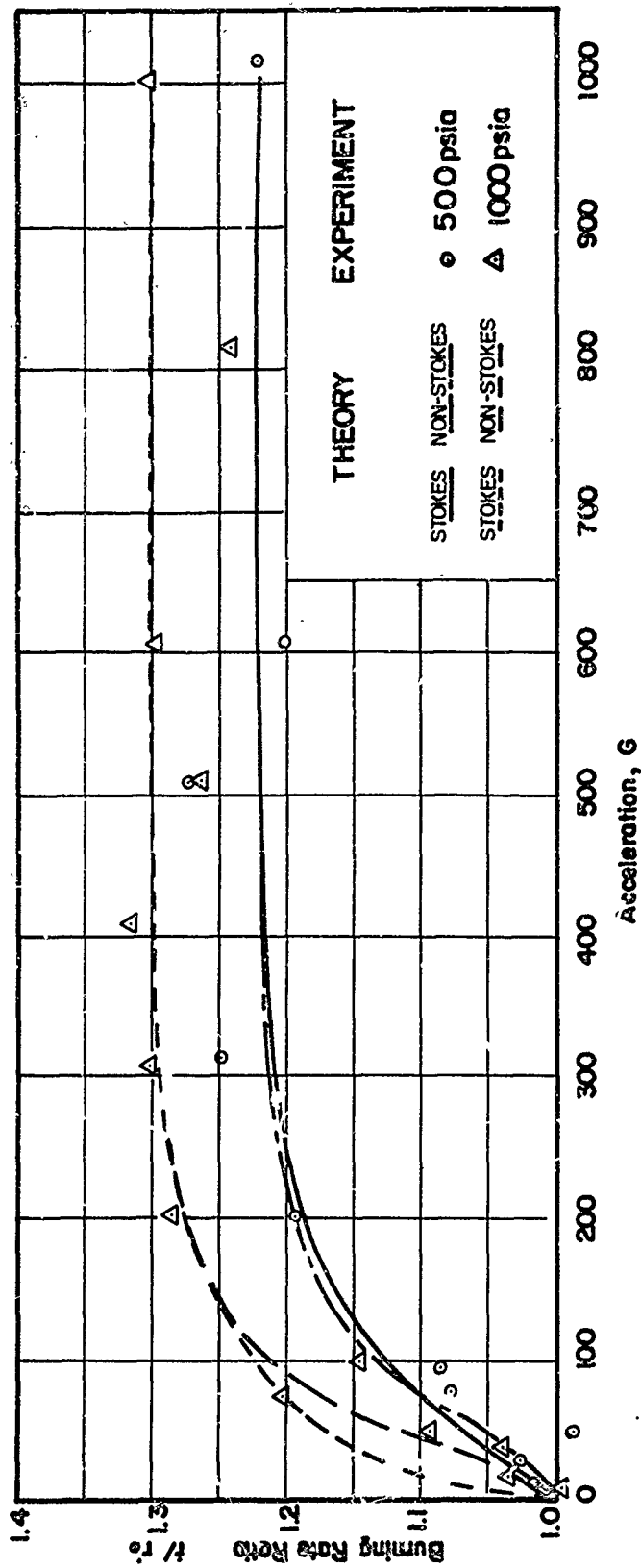


FIGURE 19 COMPARISON OF STOKES VS. NON-STOKES THEORY WITH EXPERIMENT FOR P410 PROPELLANT (adapted from ref. 5)

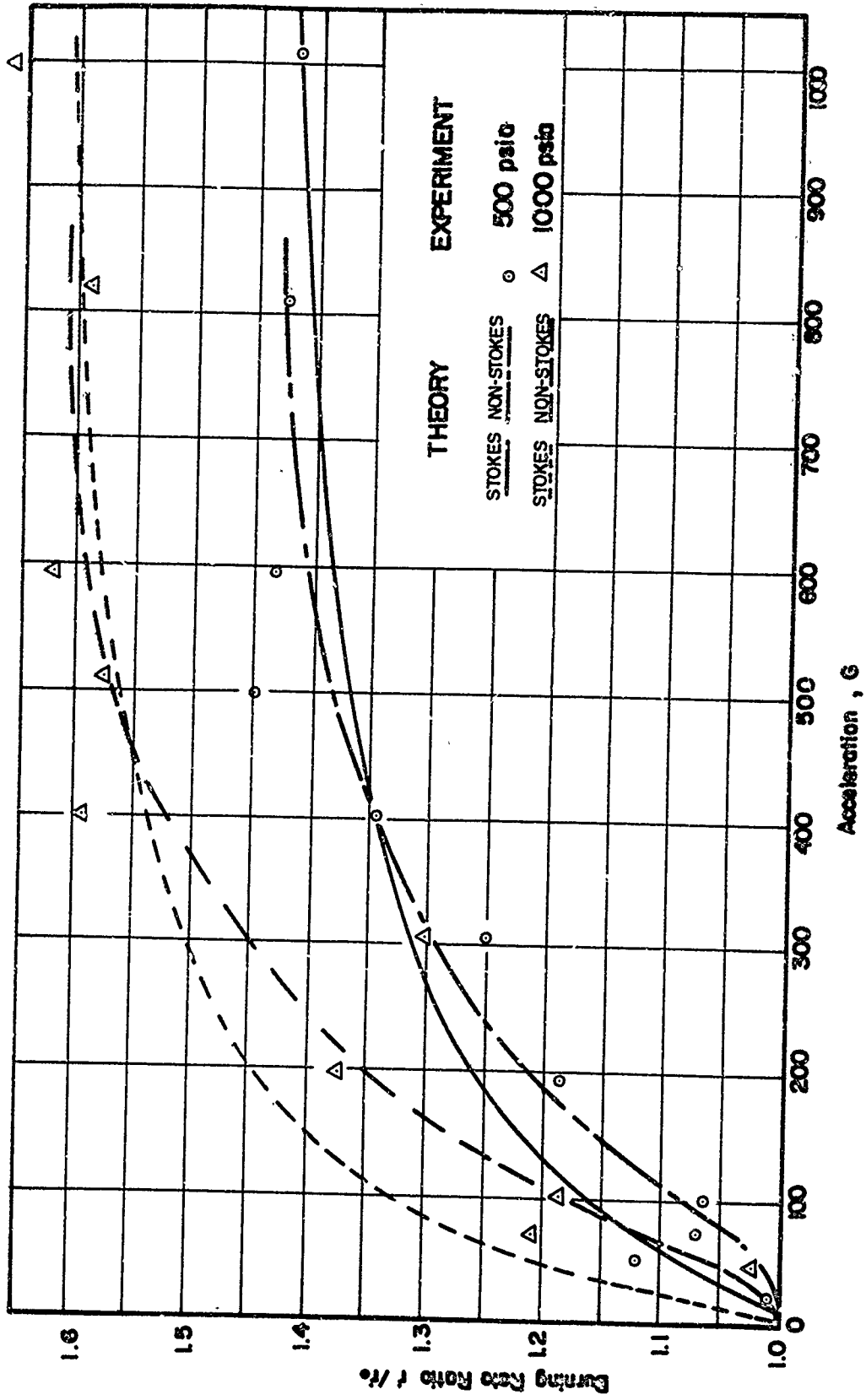


FIGURE 20 COMPARISON OF STOKES VS. NON-STOKES THEORY WITH EXPERIMENT FOR P 411 PROPELLANT (adapted from ref. 5)

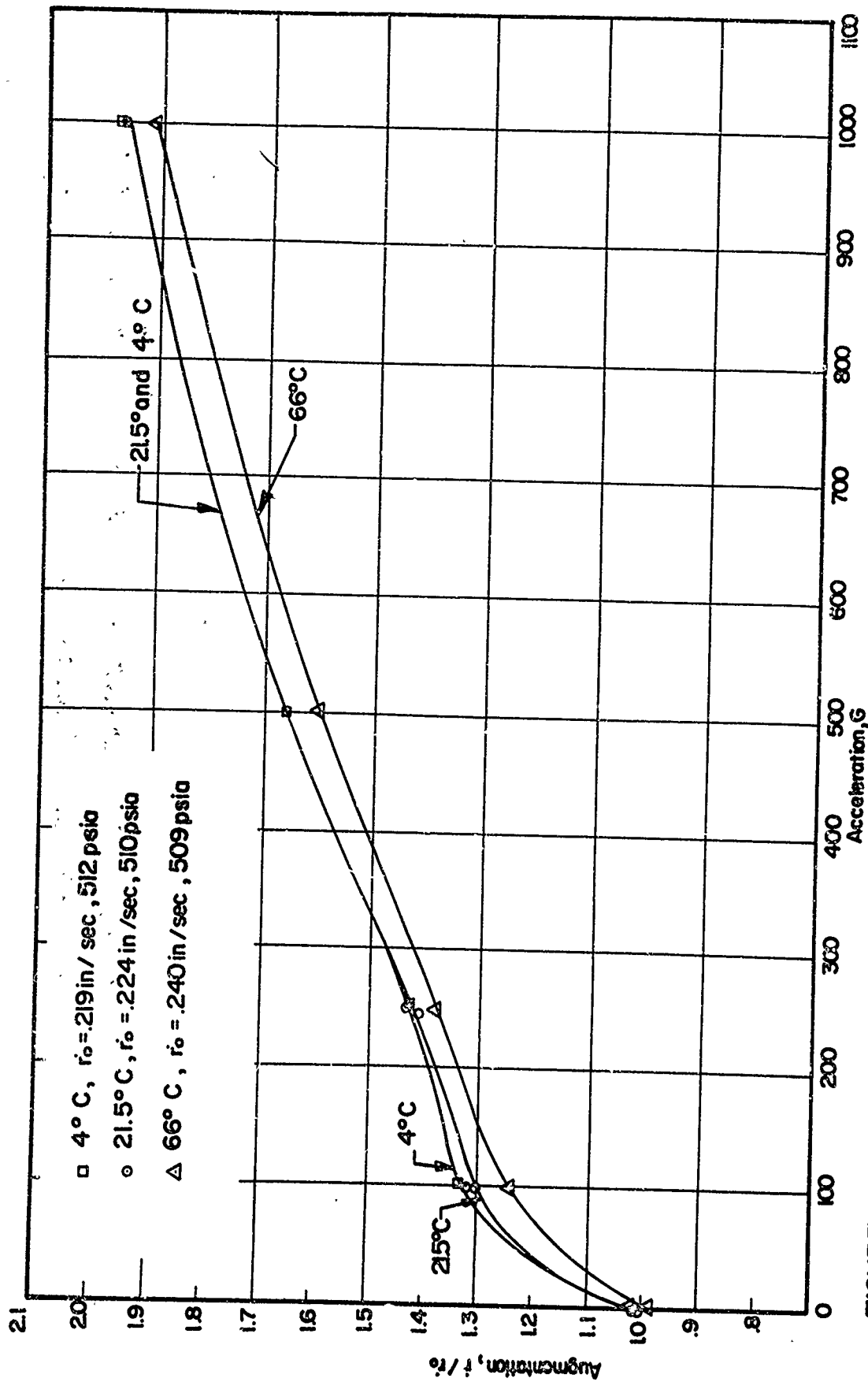


FIGURE 21 . EFFECT OF TEMPERATURE ON BURNING RATE AUGMENTATION OF ALUMINIZED
 COMPOSITE PROPELLANT (N-7) AT 500 PSIA

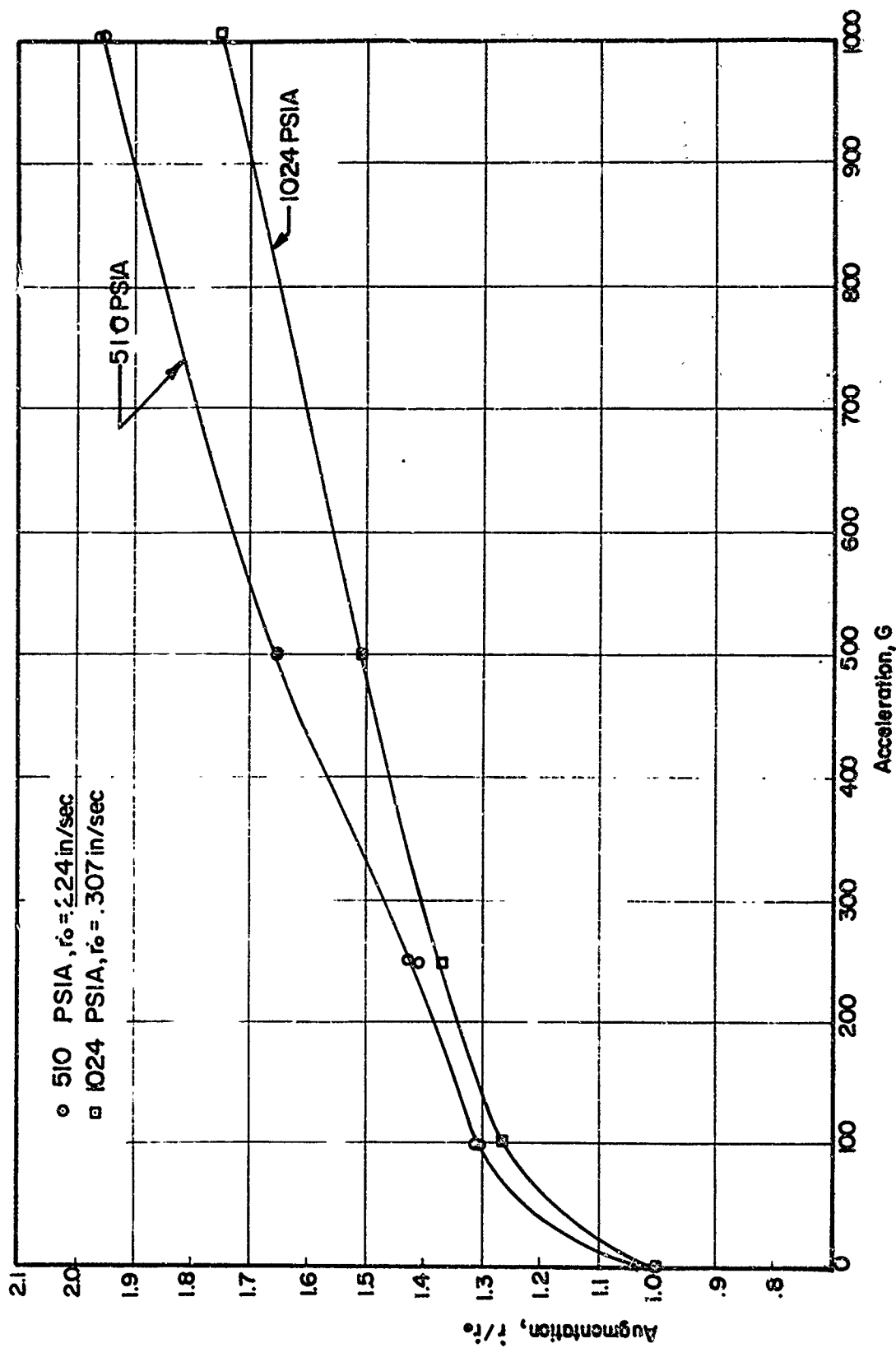


FIGURE 22. EFFECT OF PRESSURE ON BURNING RATE AUGMENTATION OF ALUMINIZED COMPOSITE PROPELLANT (N-7)

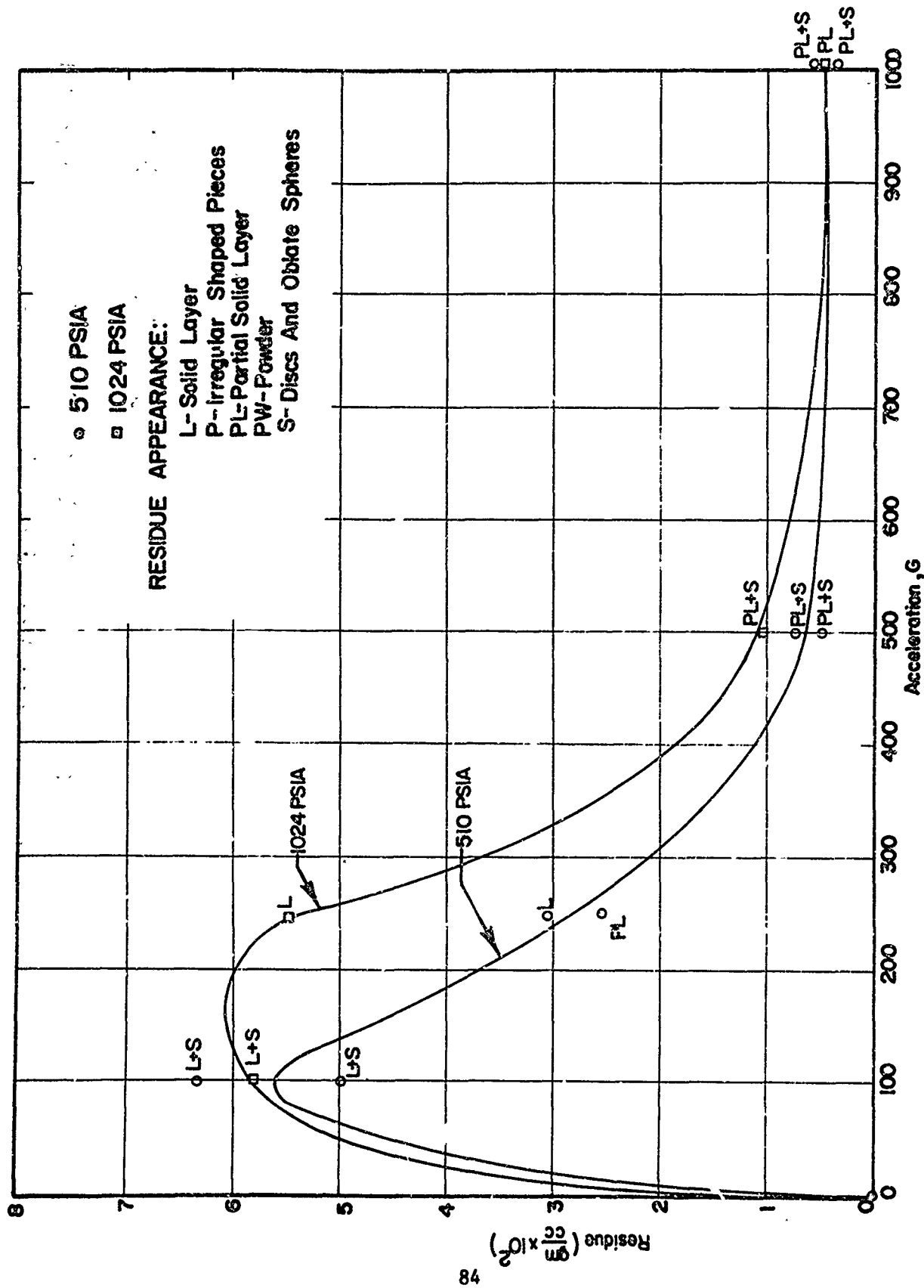


FIGURE 23. EFFECT OF PRESSURE ON RESIDUE FORMATION OF ALUMINIZED COMPOSITE PROPELLANT (N-7)

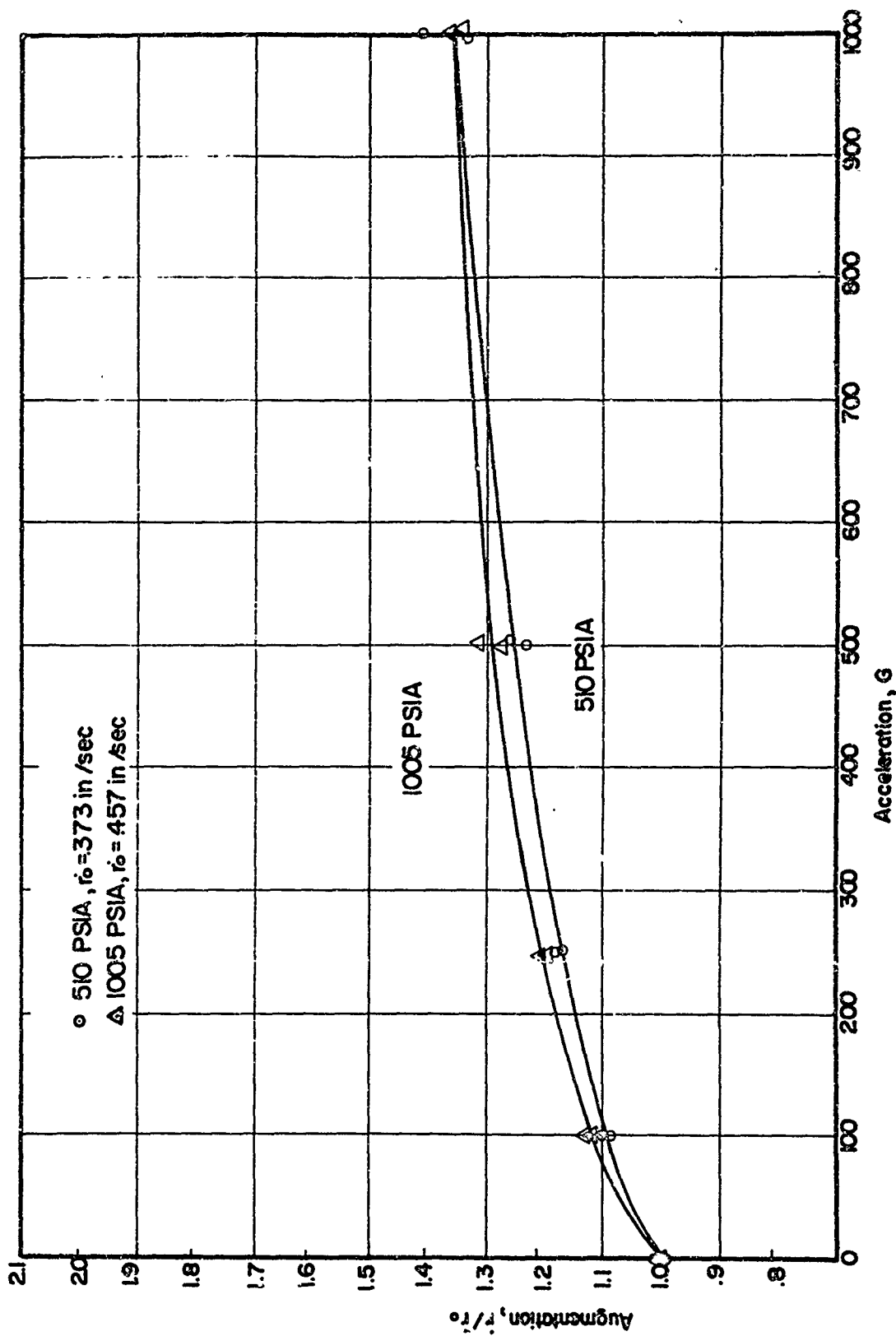


FIGURE 24 EFFECT OF PRESSURE ON BURNING RATE AUGMENTATION OF ALUMINIZED COMPOSITE PROPELLANT (N-6)

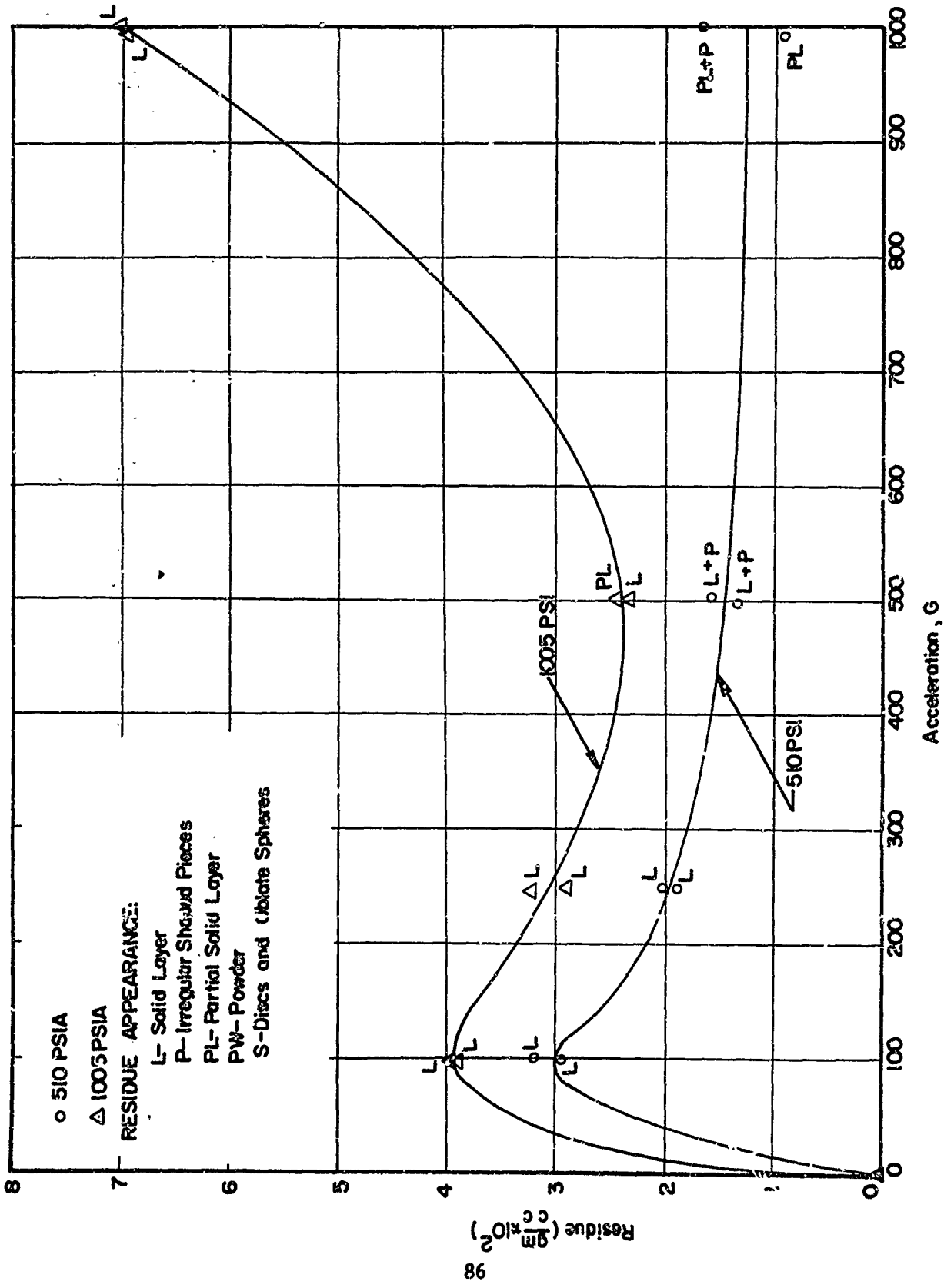


FIGURE 25. EFFECT OF PRESSURE ON RESIDUE FORMATION OF ALUMINIZED COMPOSITE PROPELLANT (N-6)

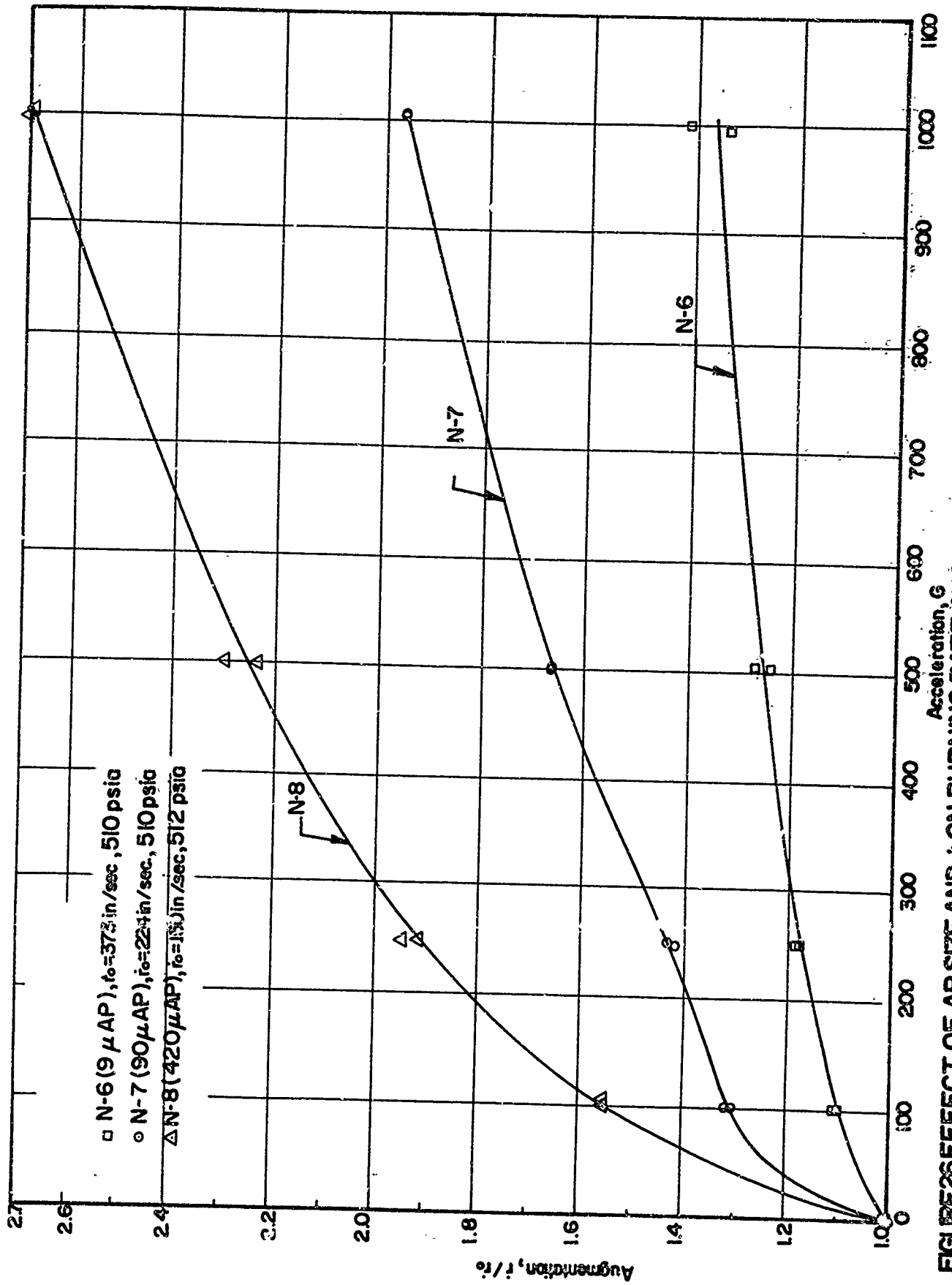


FIGURE 26 EFFECT OF AP SIZE AND t_0 ON BURNING RATE AUGMENTATION OF ALUMINIZED COMPOSITE PROPELLANTS AT 500 PSIA.

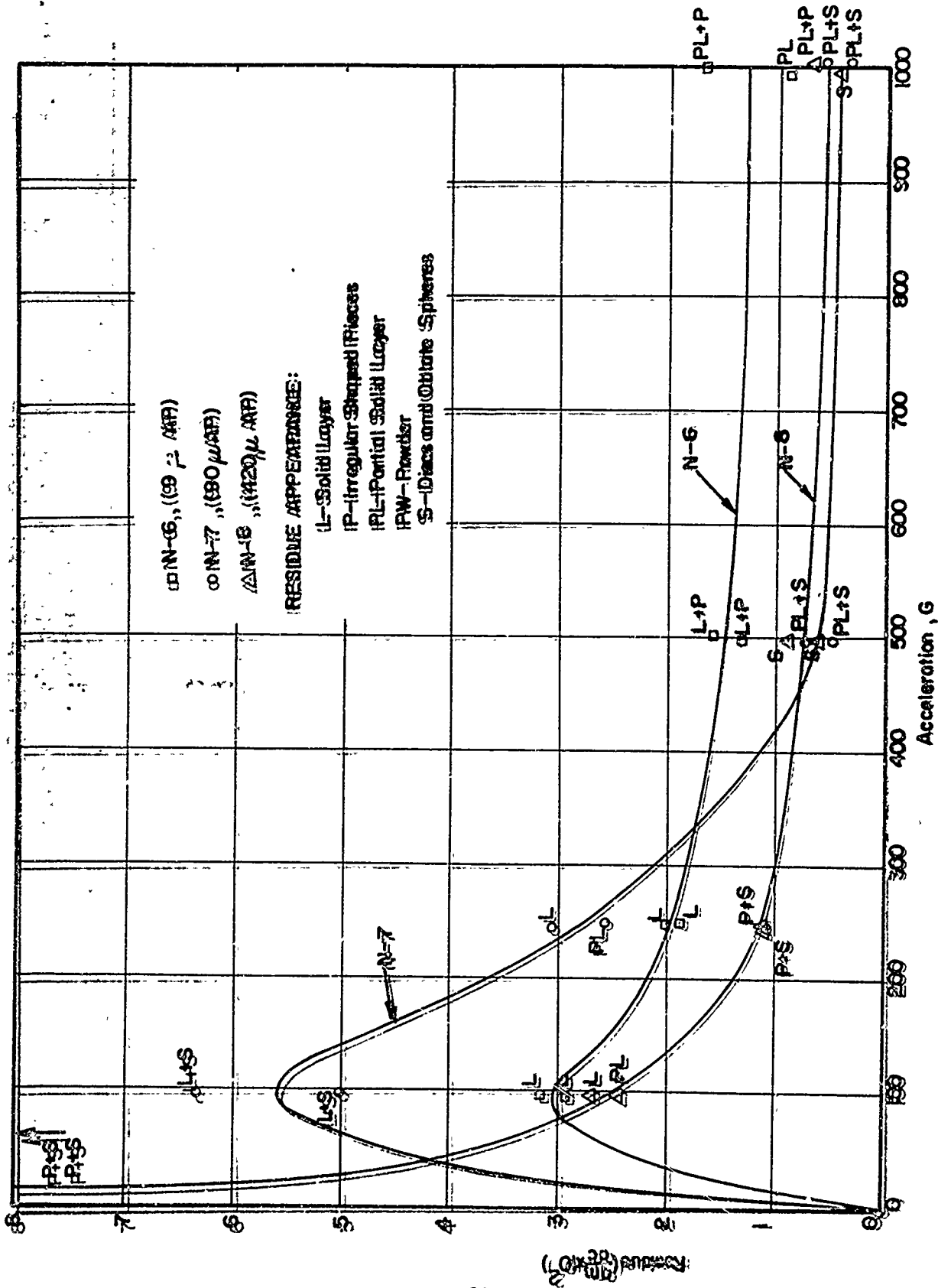
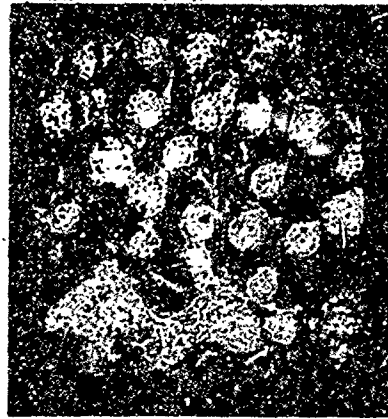


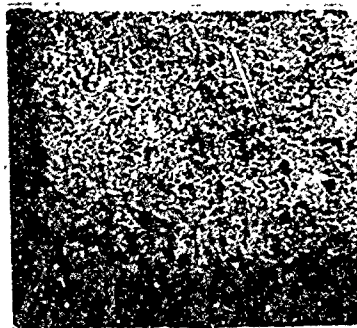
FIGURE 27. EFFECT OF AP SIZE AND r_s ON RESIDUE FORMATION OF ALUMINIZED COMPOSITE PROPELLANTS AT 500PSIA



a) Propellant N-7, 100g, 500PSIA



b) Propellant N-7, 1000g, 500PSIA



c) Propellant DBNA, 500-1000g, 265PSIA

FIGURE 28. POST-FIRE RESIDUE

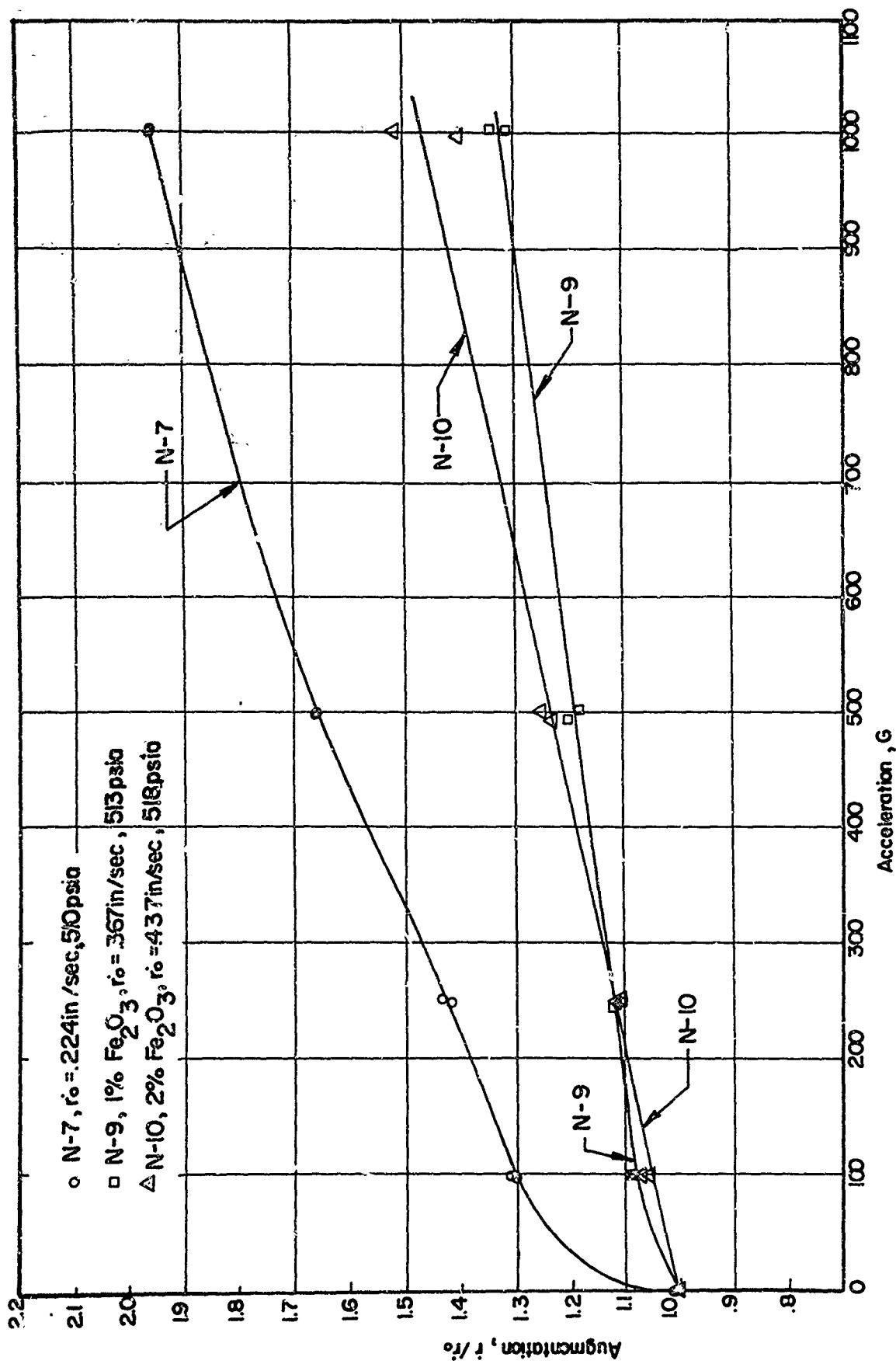


FIGURE 29. EFFECT OF \dot{r}_0 ON BURNING RATE AUGMENTATION OF ALUMINIZED COMPOSITE PROPELLANTS AT 500 PSIA

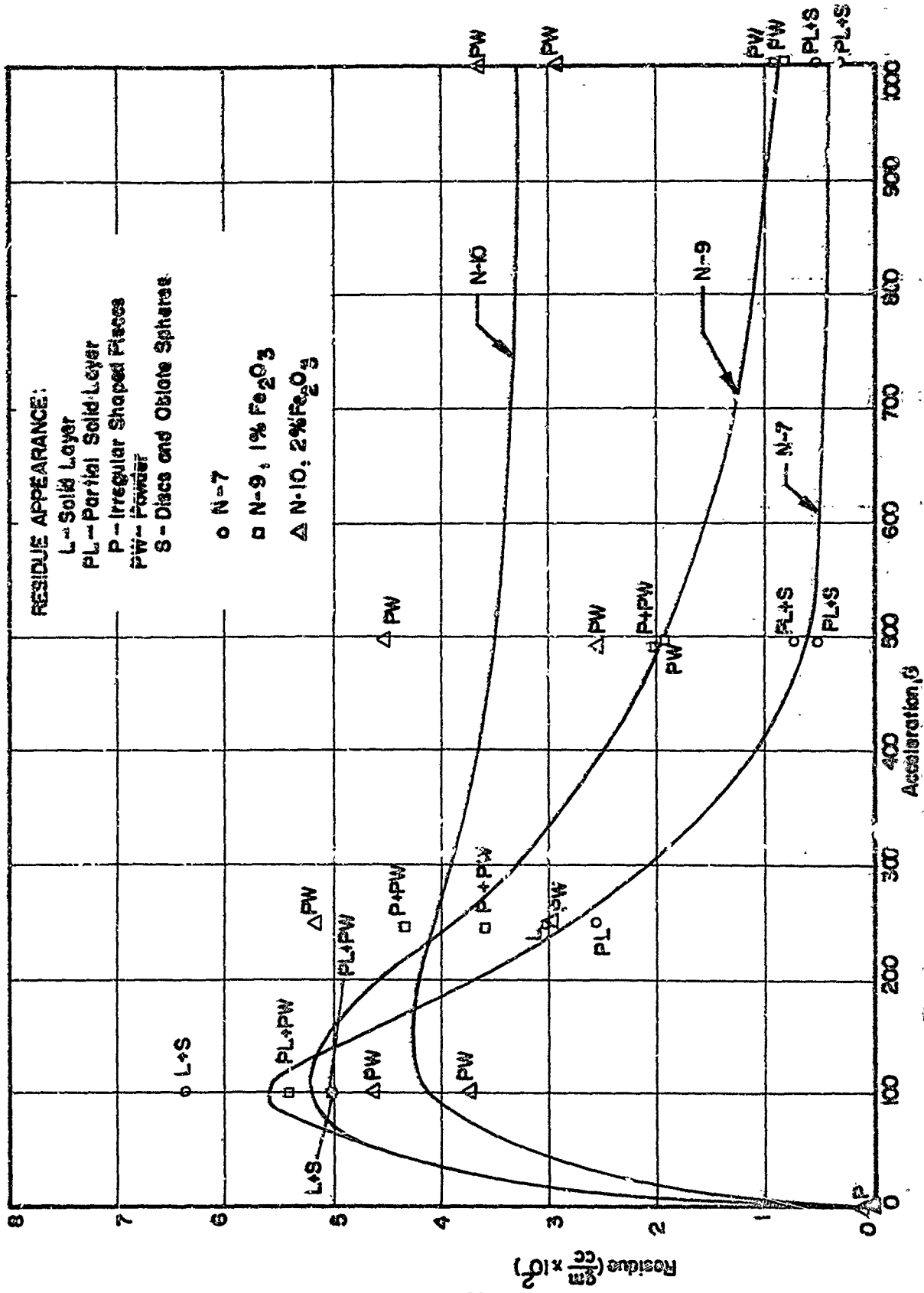


FIGURE 30 EFFECT OF r_0 ON RESIDUE FORMATION OF ALUMINIZED COMPOSITE PROPELLANTS AT 500 PSIA

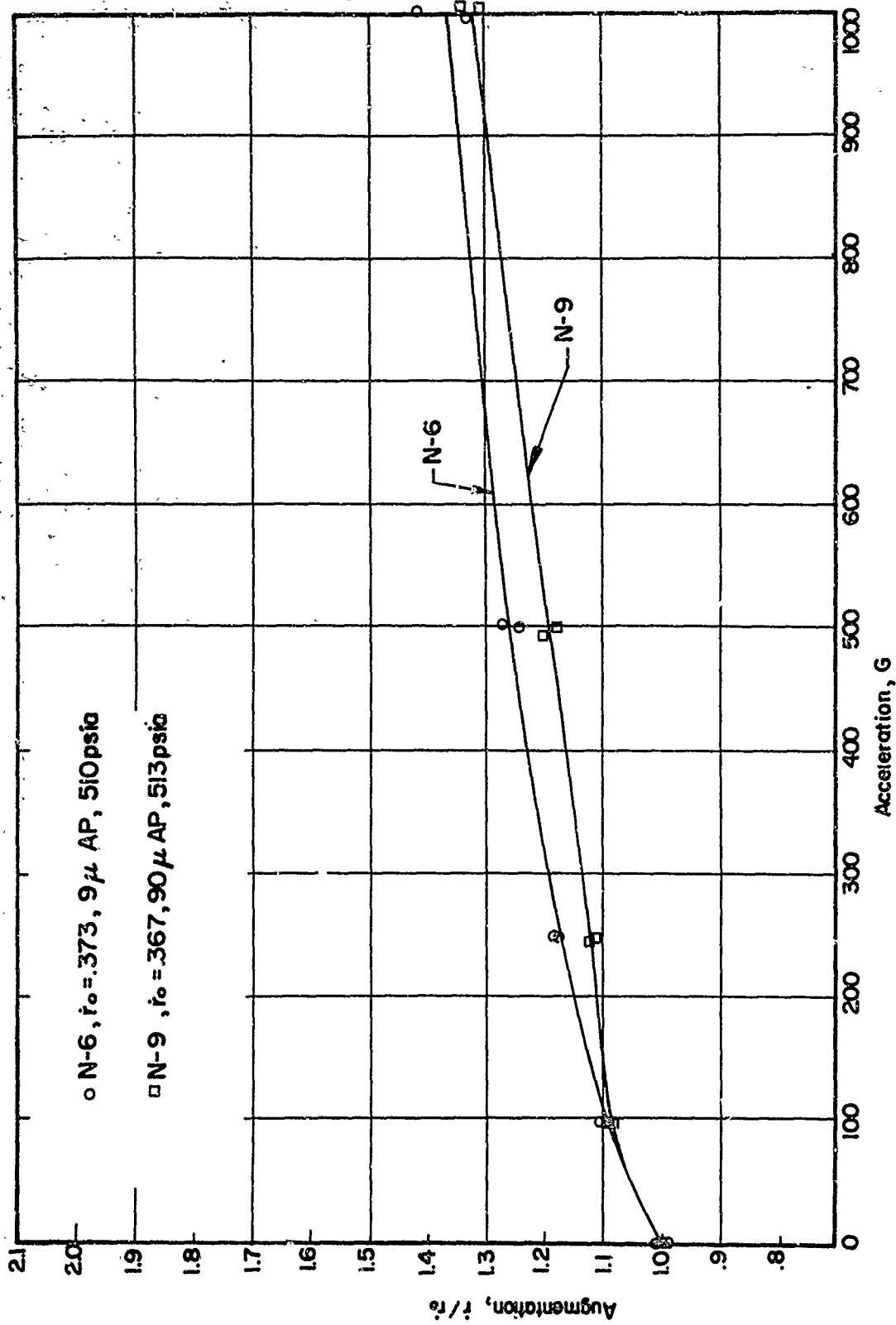
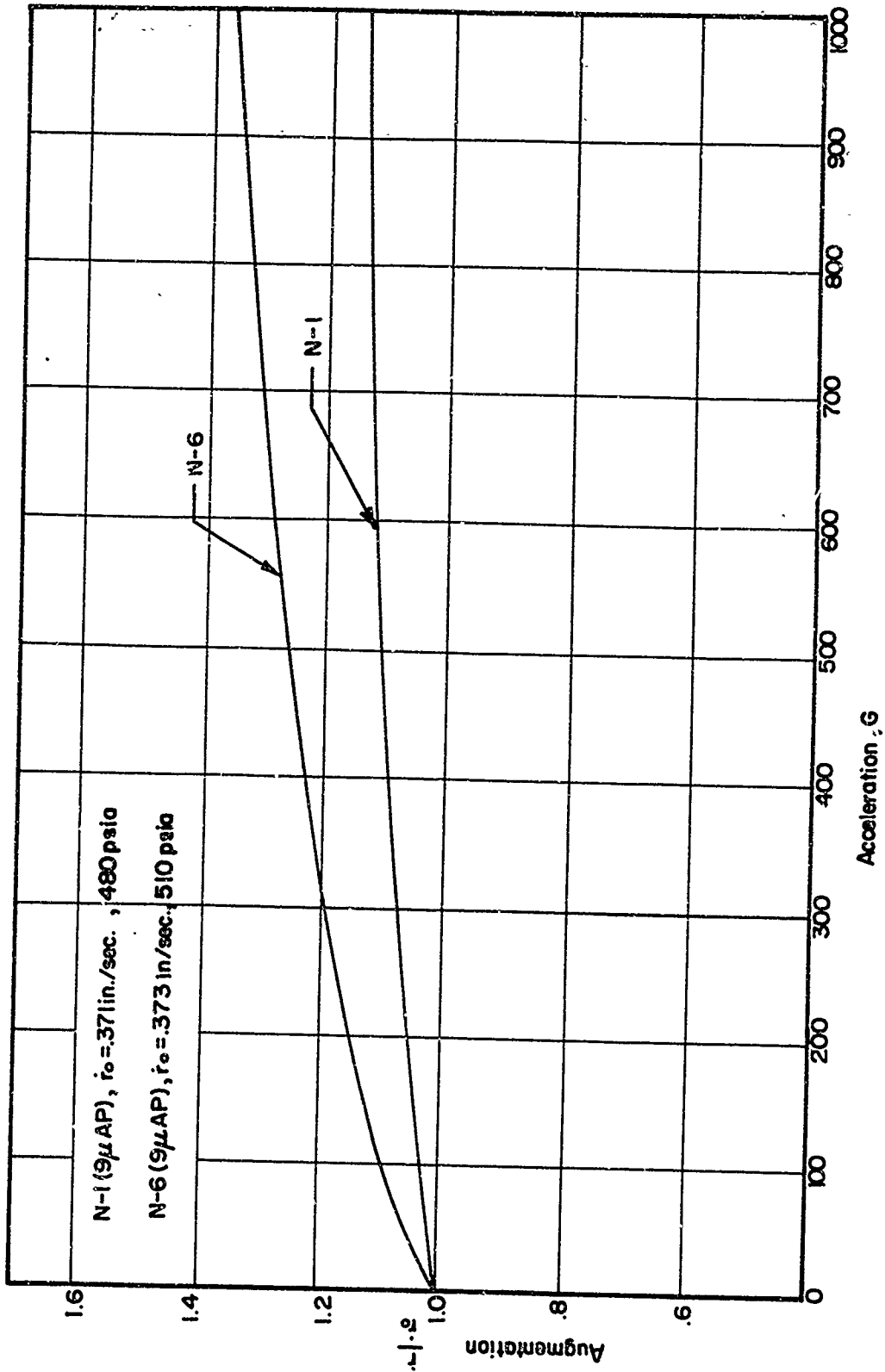


FIGURE 31. EFFECT OF AP SIZE ON BURNING RATE AUGMENTATION OF ALUMINIZED COMPOSITE PROPELLANTS AT 500 PSIA



N-1 (9μAP), $\dot{r}_0 = .37$ in./sec., 480 psia
 N-6 (9μAP), $\dot{r}_0 = .373$ in./sec., 510 psia

FIGURE 32 EFFECT OF ALUMINUM, N-1 VS. N-6

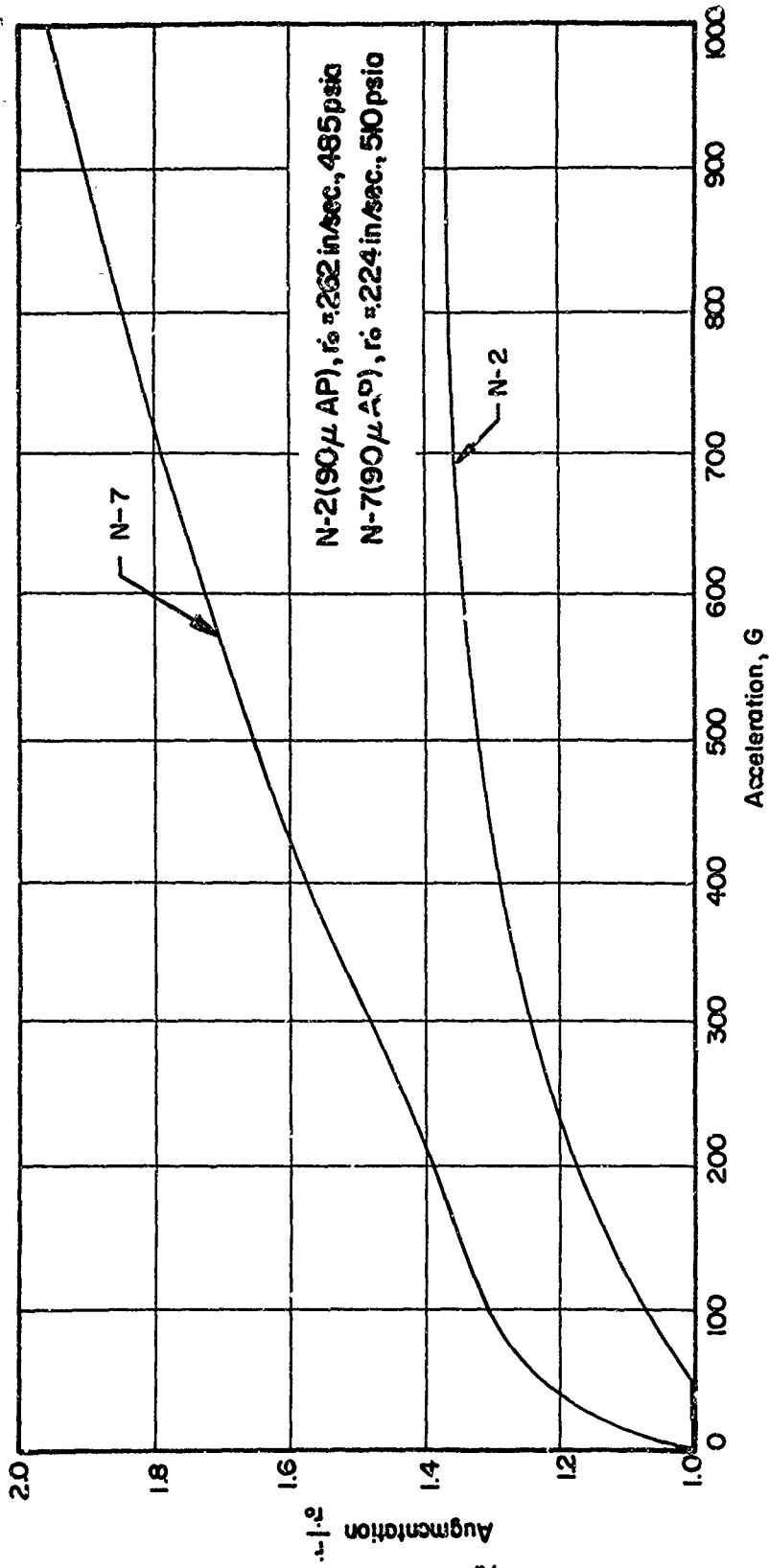


FIGURE 33. EFFECT OF ALUMINUM, N-2 VS N-7

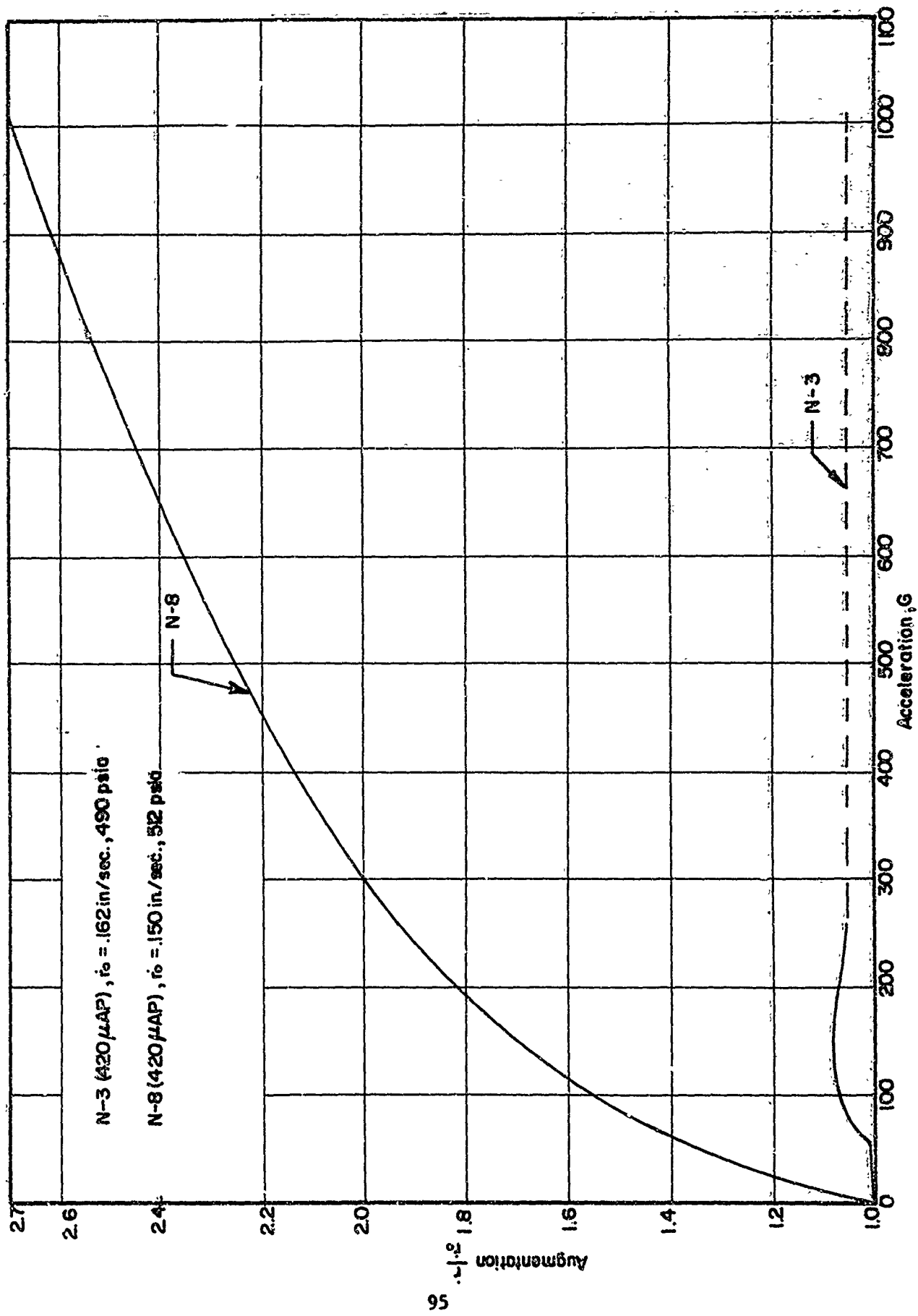


FIGURE 34 EFFECT OF ALUMINUM, N-3 VS. N-8

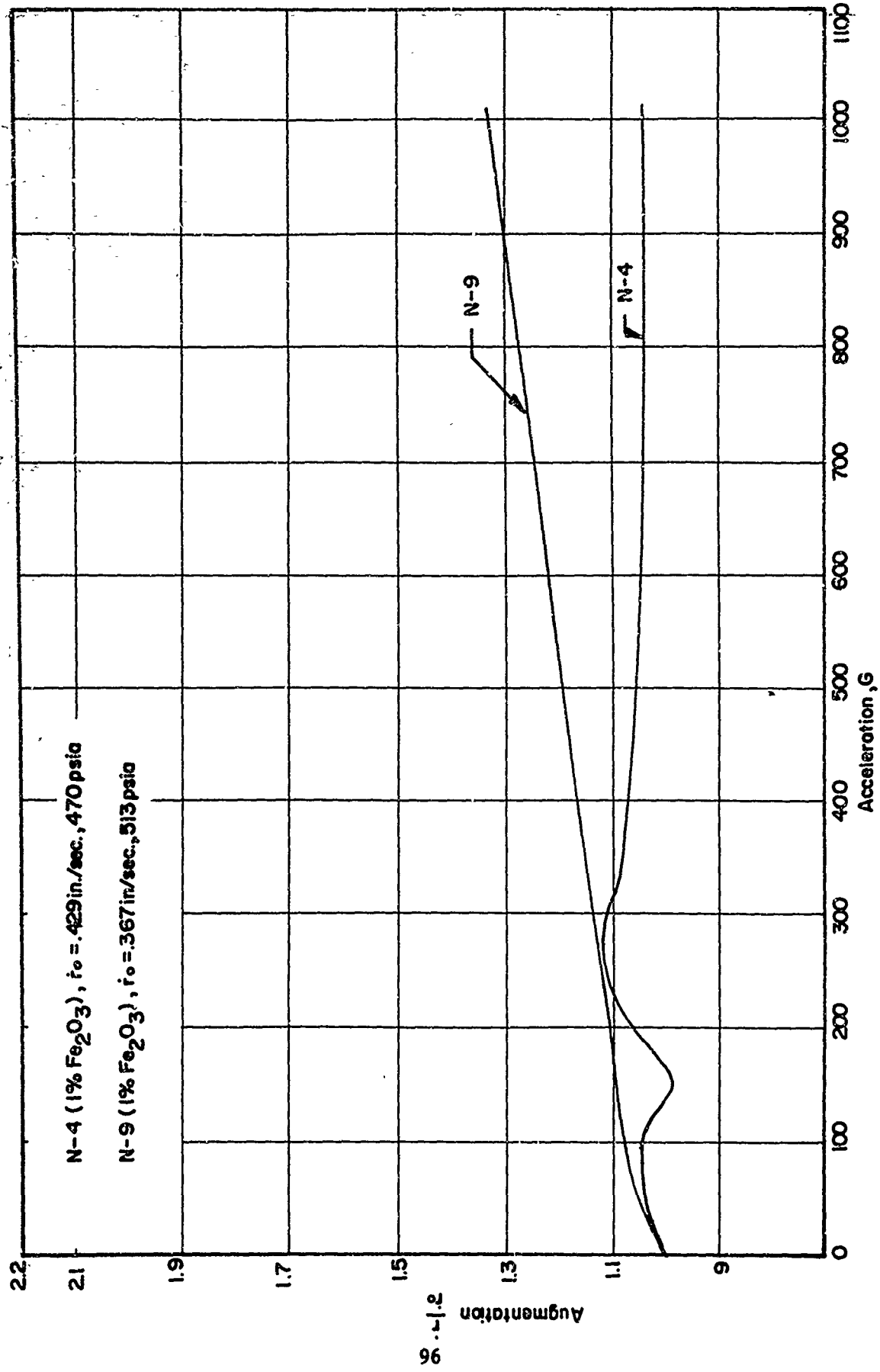


FIGURE 35. EFFECT OF ALUMINUM, N-4 VS. N-9

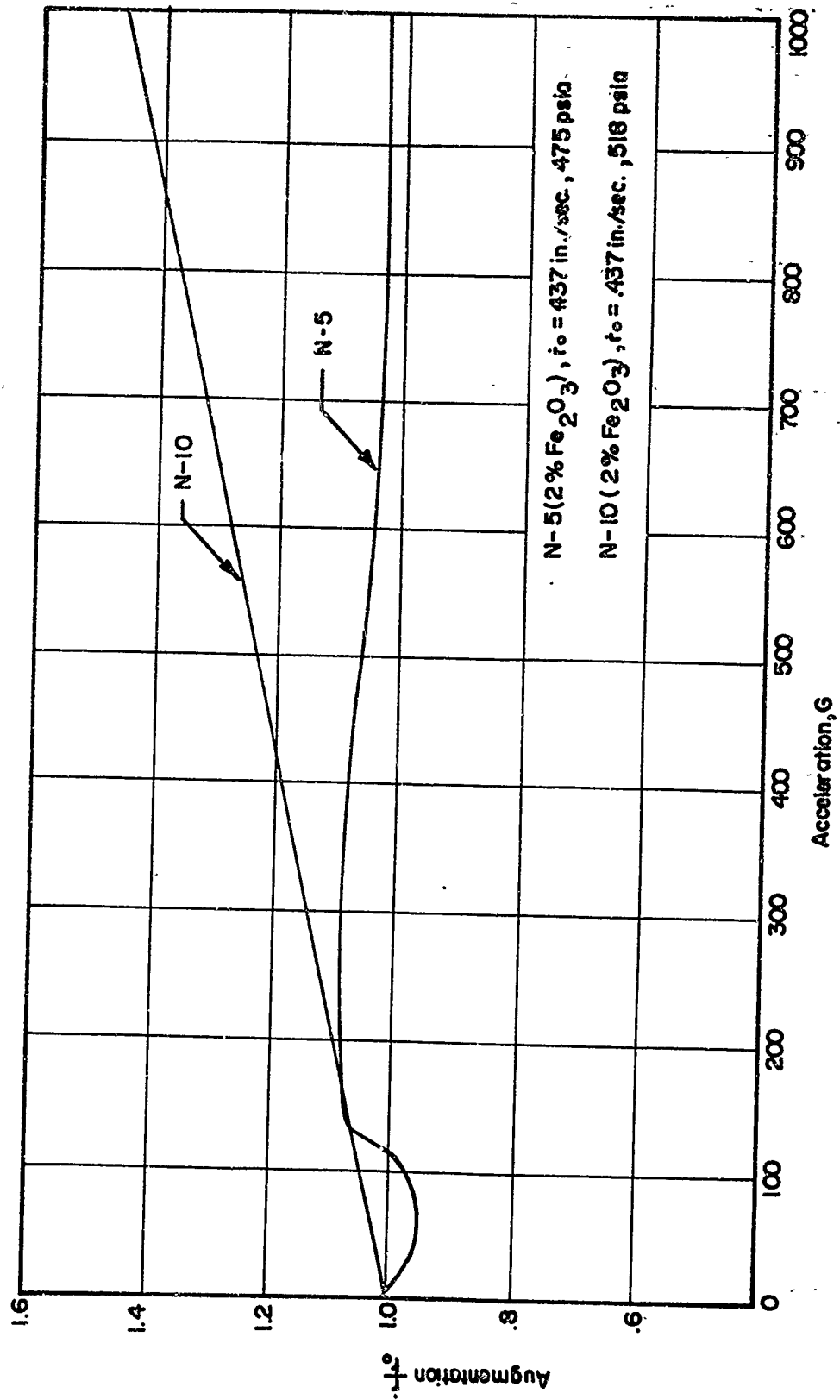


FIGURE 36. EFFECT OF ALUMINUM, N-5 VS. N-10

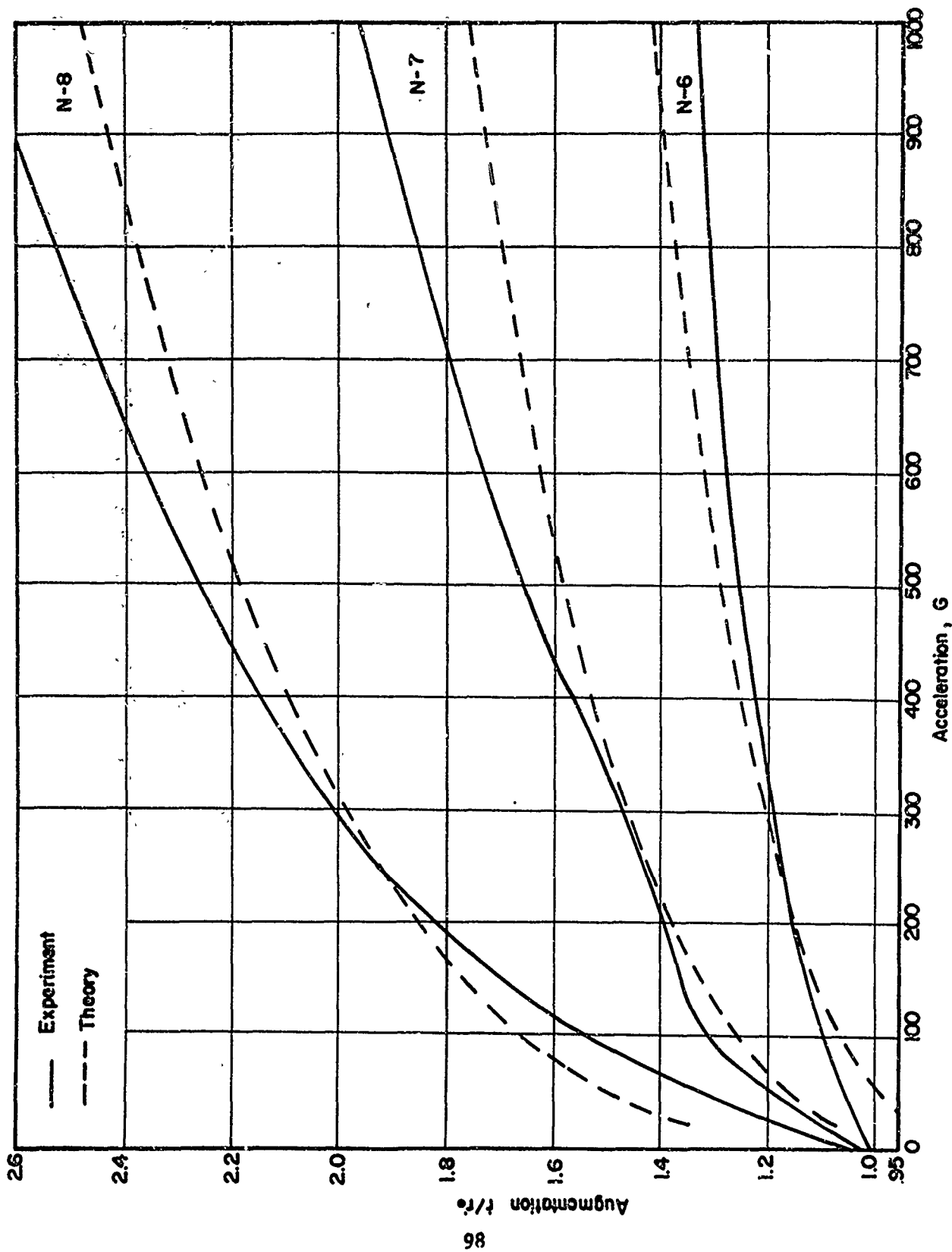


FIGURE 37. COMPARISON OF CROWE MODEL WITH EXPERIMENTAL DATA AT 500 PSIA

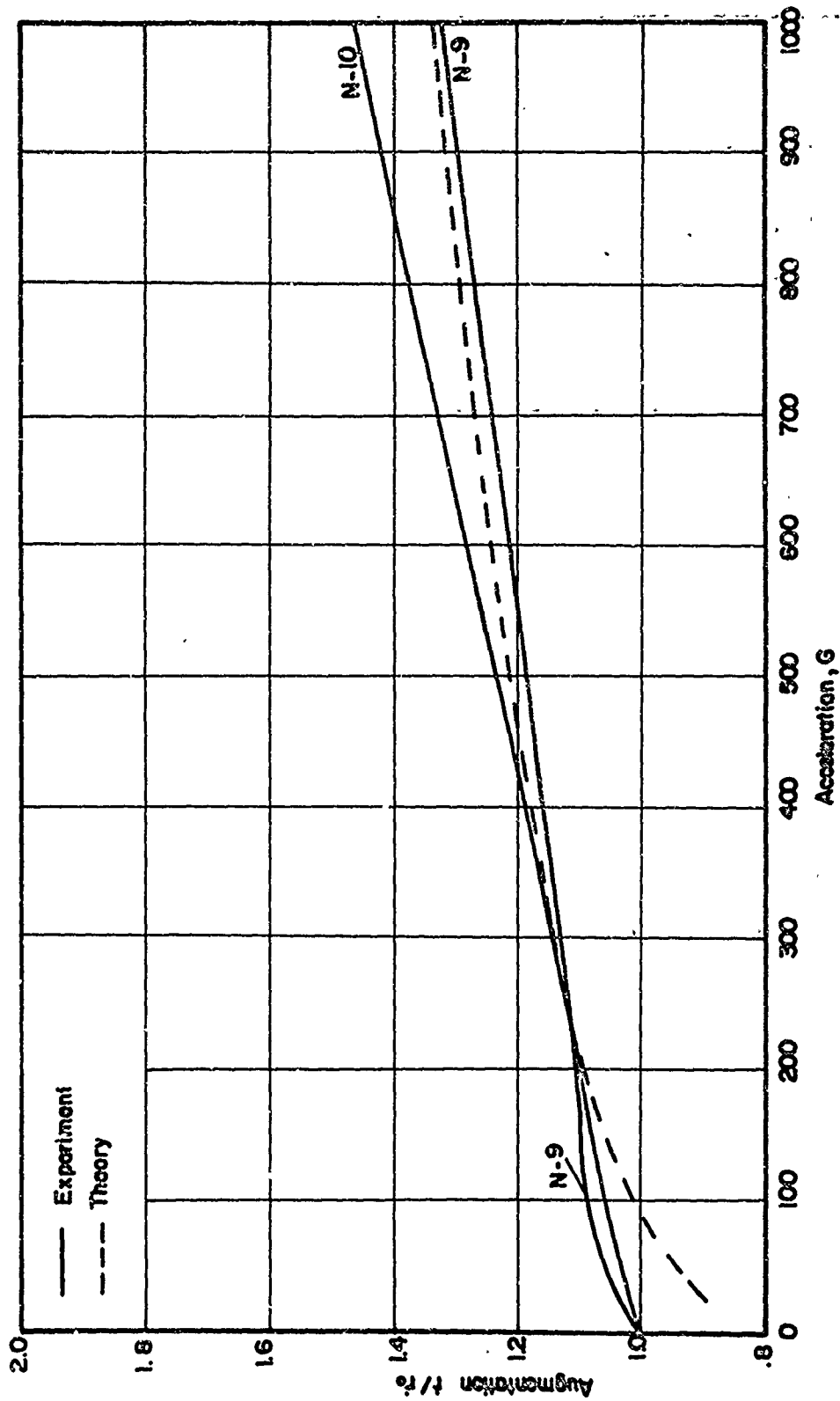


FIGURE 38. COMPARISON OF CROWE MODEL WITH EXPERIMENTAL DATA - CATALYZED PROPELLANTS AT 500 PSIA.

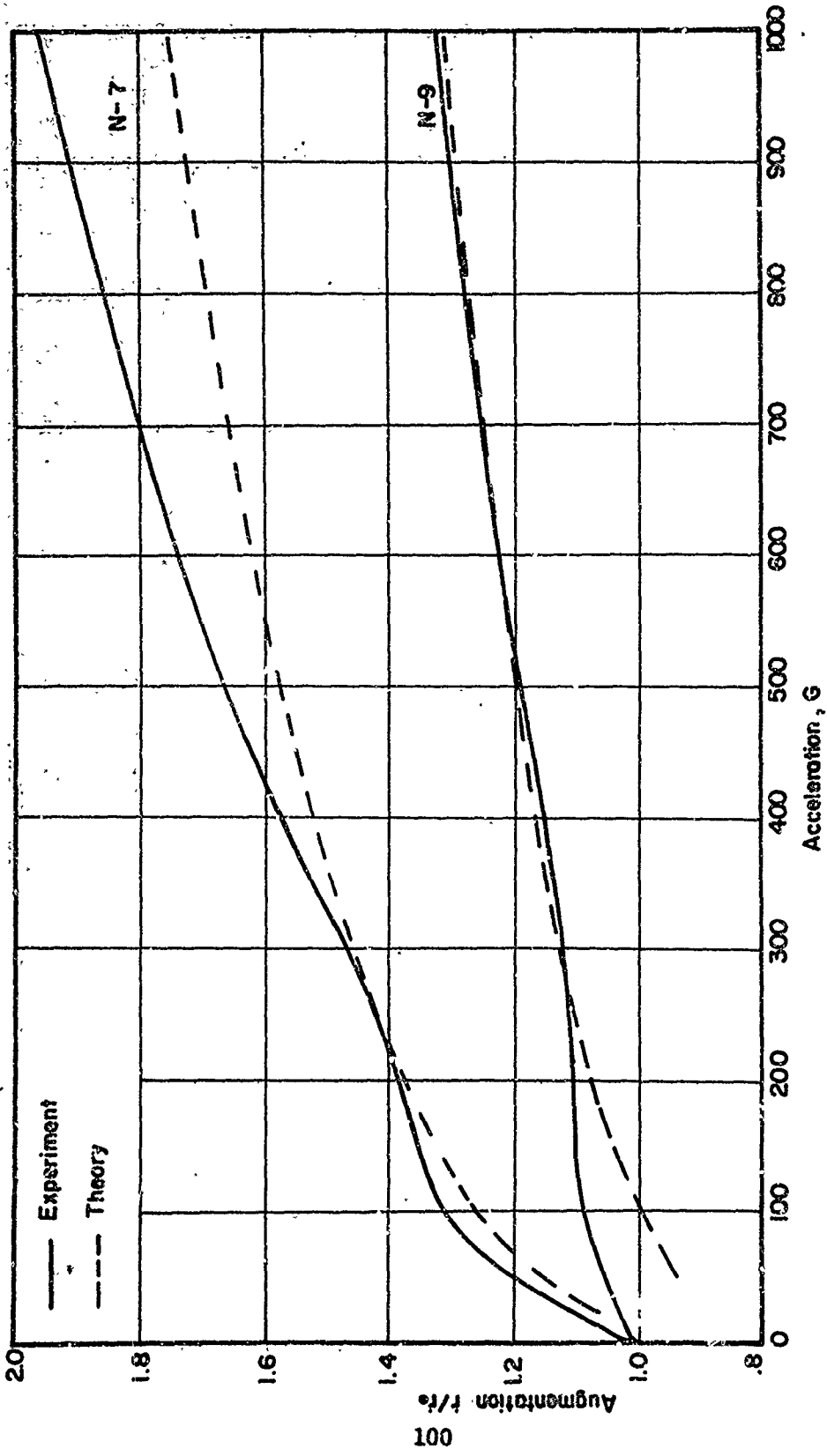


FIGURE 39. COMPARISON OF CROWE MODEL WITH EXPERIMENTAL DATA - EFFECT OF BASE BURNING RATE AT 500 PSIA.

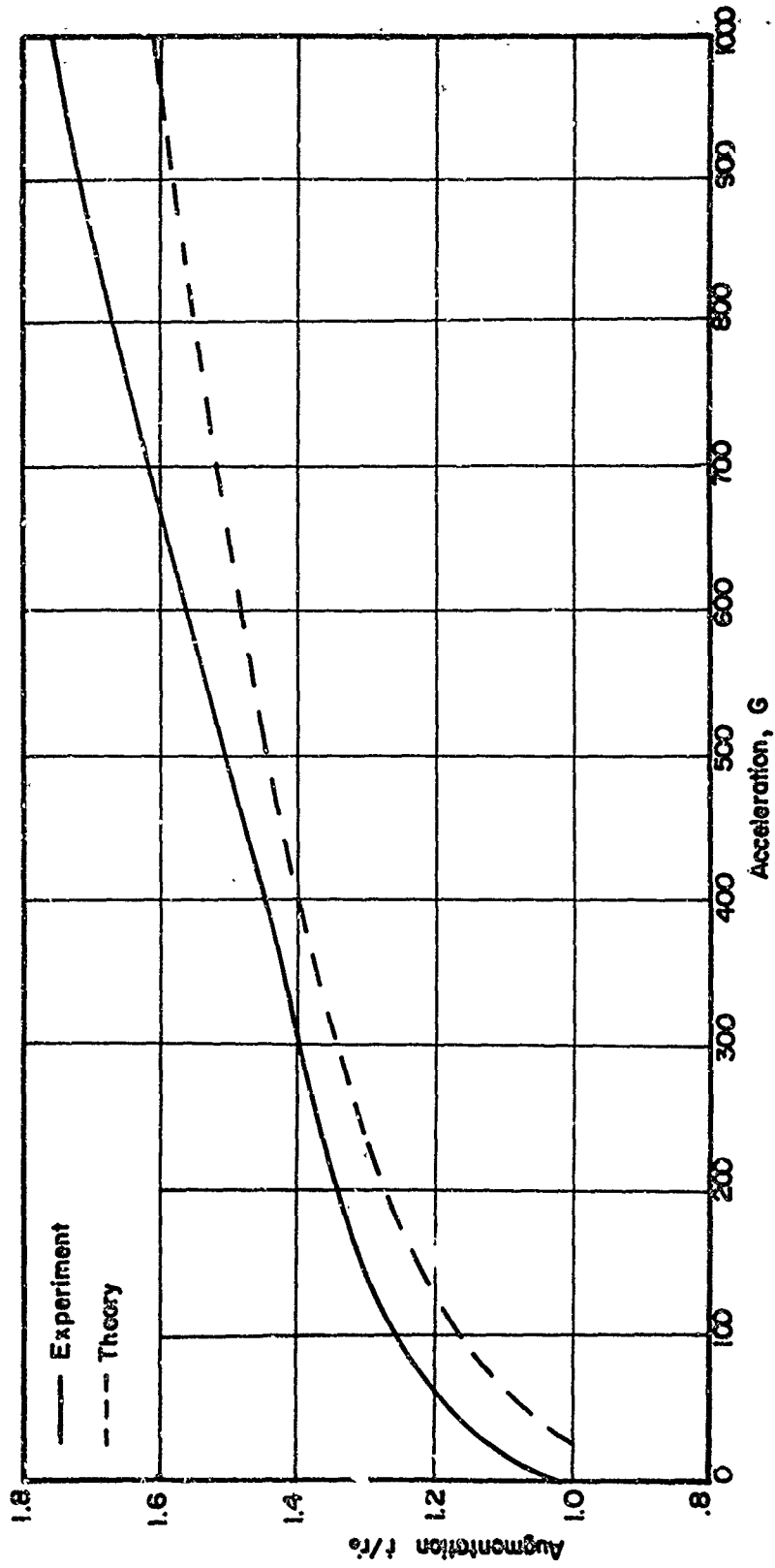


FIGURE 40. COMPARISON OF CROWE MODEL WITH EXPERIMENTAL DATA - PROPELLANT N-7 AT 1000 PSIA.

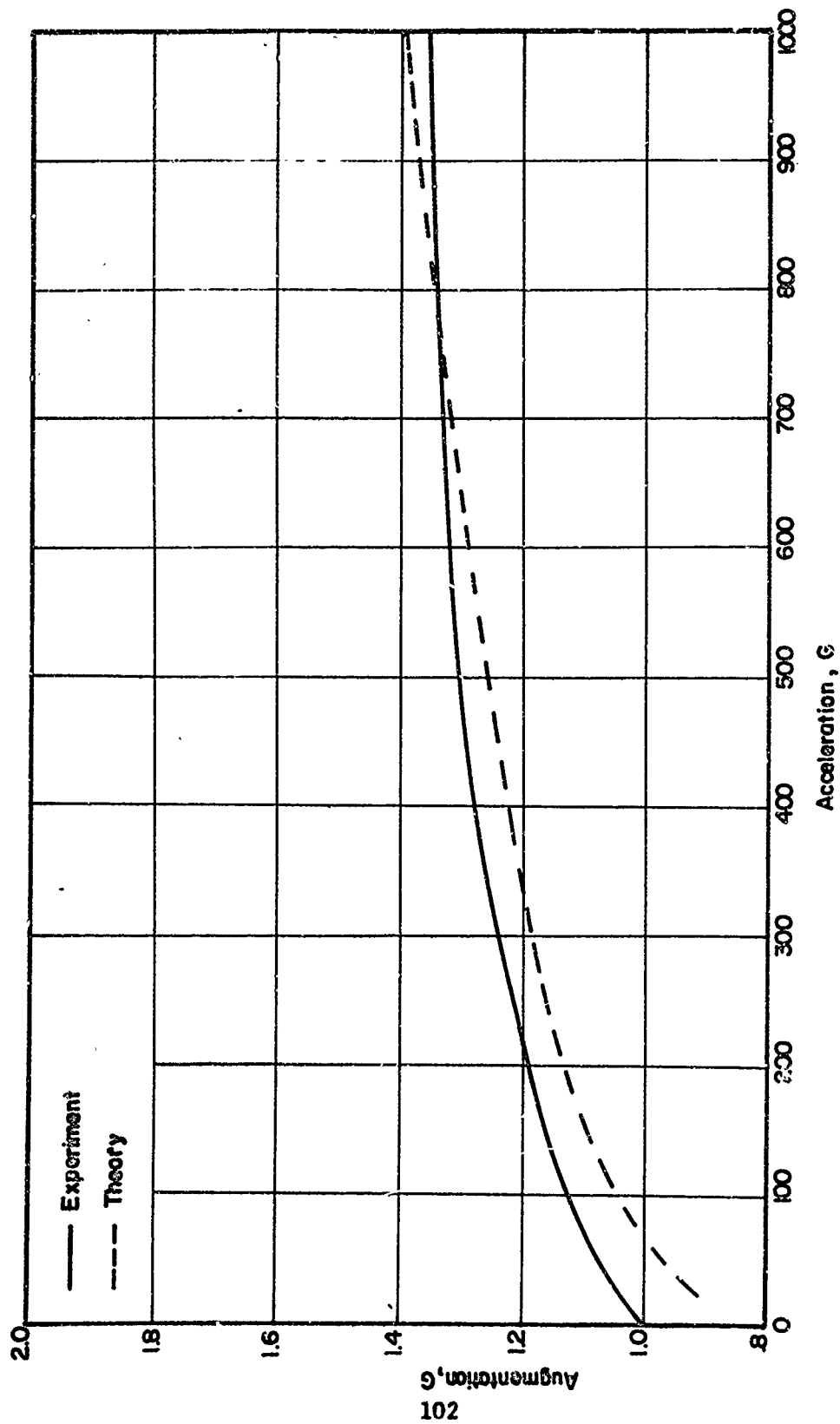


FIGURE 41. COMPARISON OF CROWE MODEL WITH EXPERIMENTAL DATA - PROPELLANT N-6 AT 1005 PSIA.

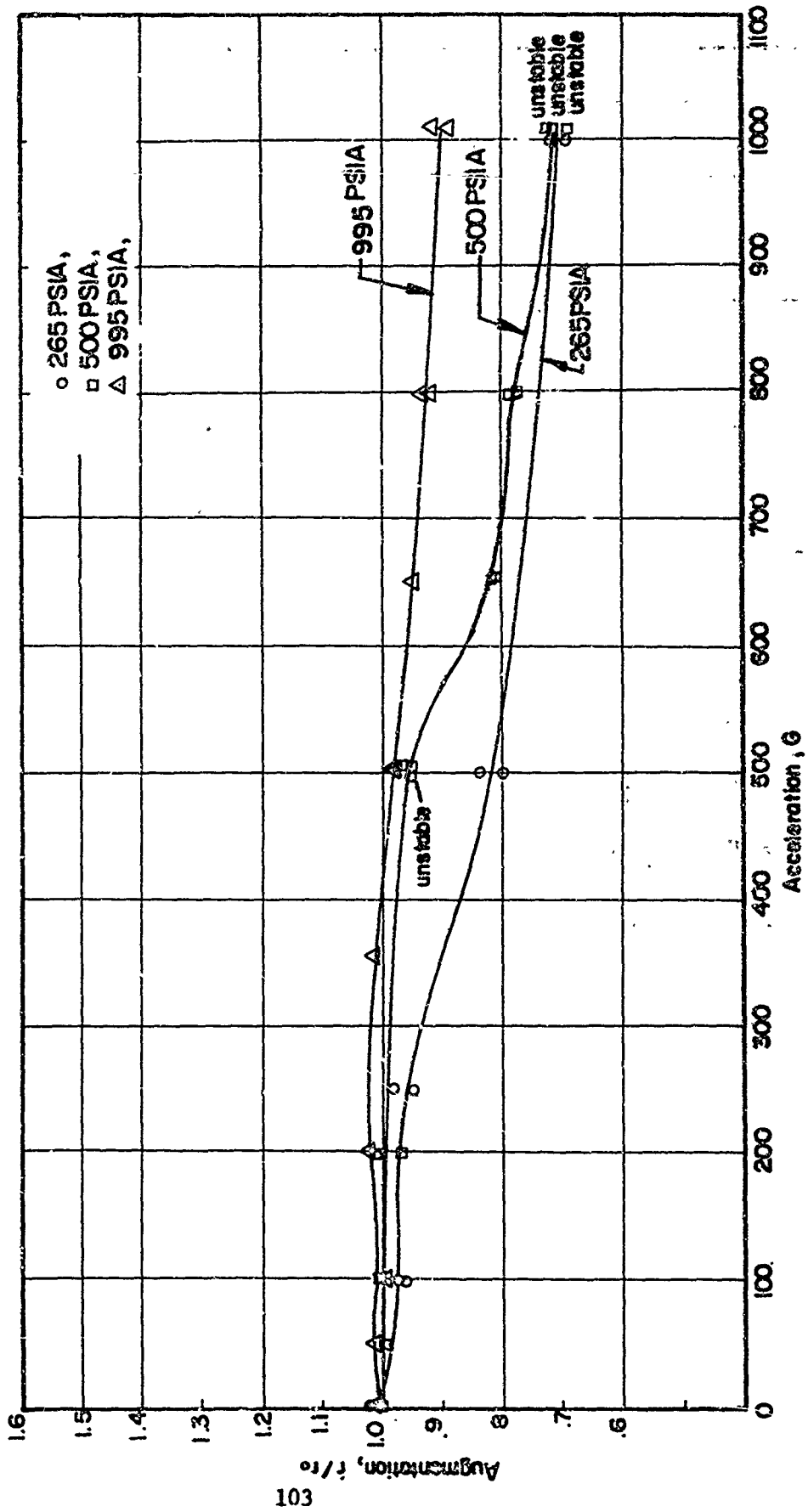


FIGURE 42. EFFECT OF ACCELERATION ON r/r_0 OF DOUBLE-BASE PROPELLANT

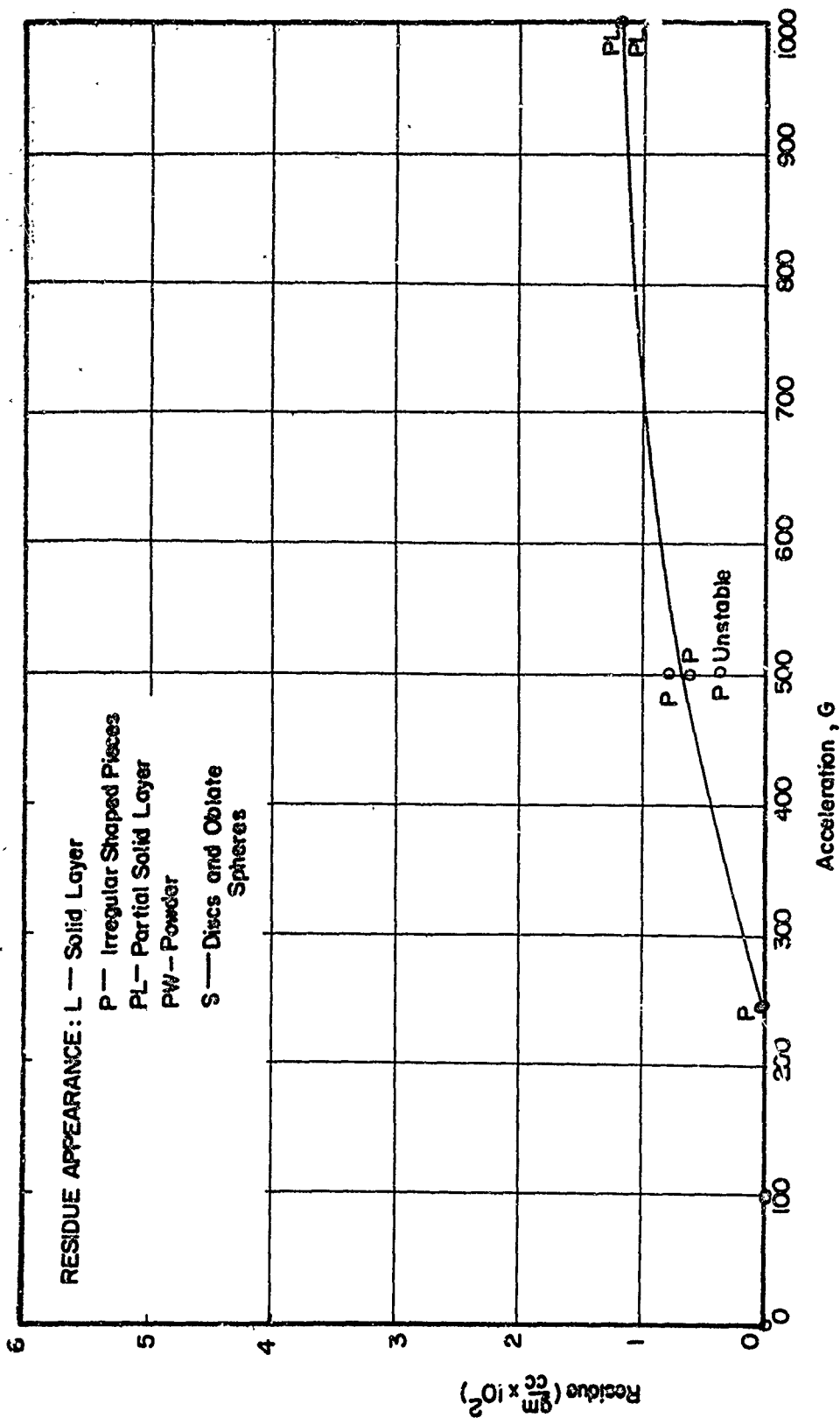


FIGURE 43. EFFECT OF ACCELERATION ON RESIDUE FORMATION OF DOUBLE-BAS PROPELLANT AT 265 PSIA.

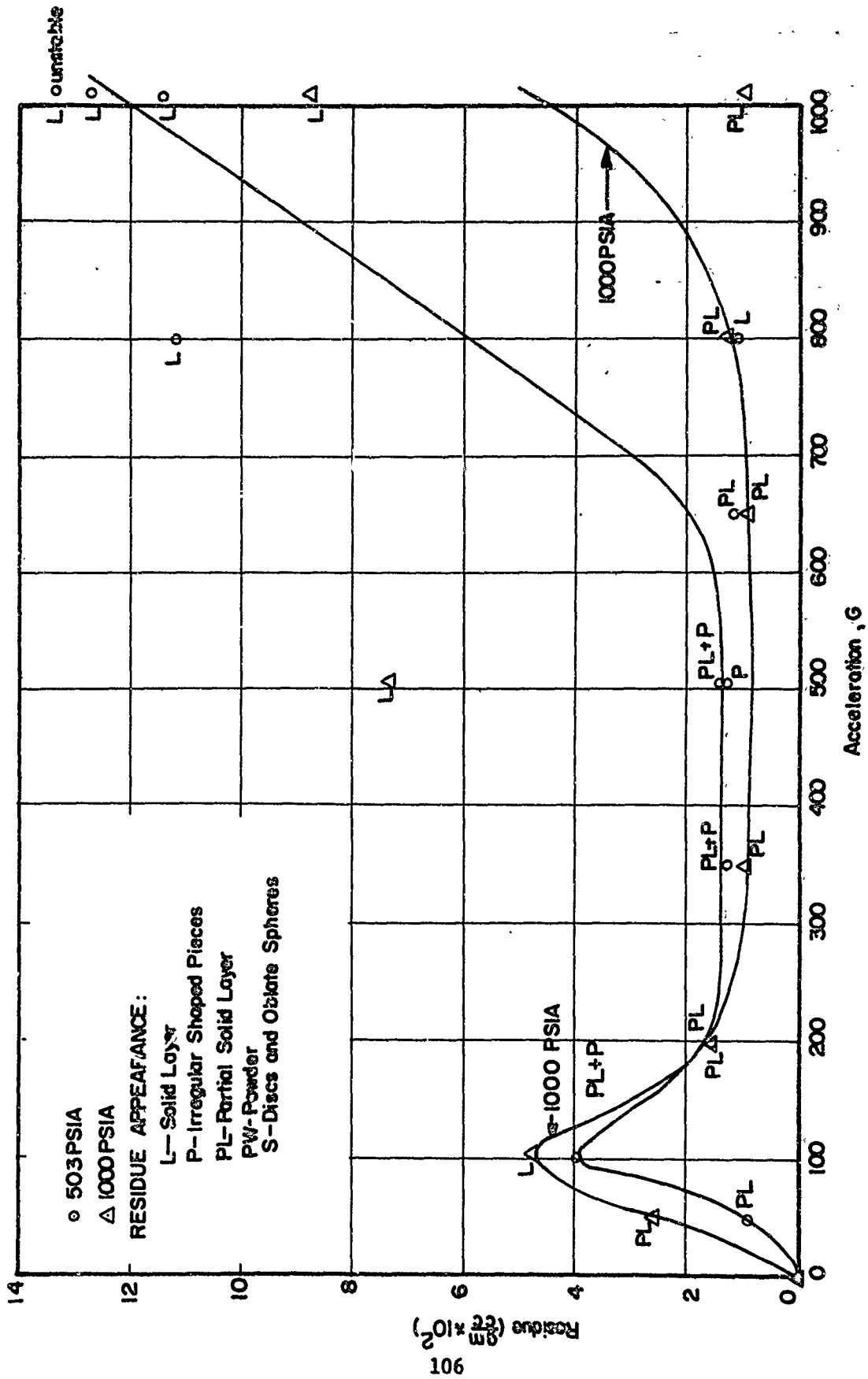


FIGURE 45. EFFECT OF ACCELERATION ON RESIDUE FORMATION OF ALUMINIZED DOUBLE-BASE PROPELLANT

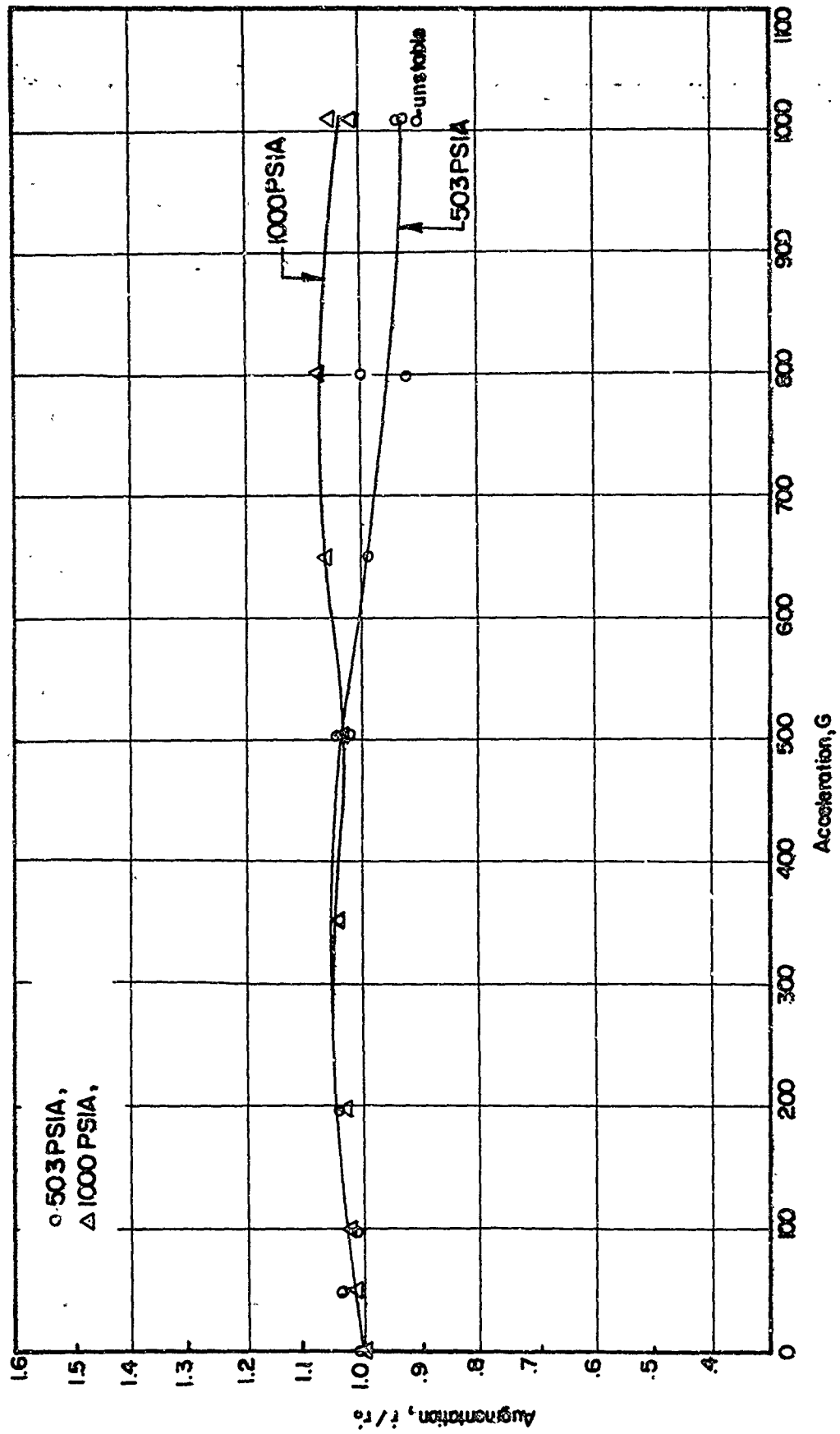


FIGURE 44. EFFECT OF ACCELERATION ON r/r_0 OF ALUMINIZED DOUBLE-BASE PROPELLANT

UNCLASSIFIED

Security Classification

DOCUMENT CONTROL DATA - R & D

(Security classification of title, body of abstract and indexing annotation must be entered when the overall report is classified)

1. ORIGINATING ACTIVITY (Corporate author) Naval Postgraduate School Monterey, California 93940		3a. REPORT SECURITY CLASSIFICATION Unclassified	
		3b. GROUP	
3. REPORT TITLE An Investigation of the Effects of Acceleration on the Burning Rates of Solid Propellants			
4. DESCRIPTIVE NOTES (Type of report and, inclusive dates) Technical Report, 1969			
5. AUTHOR(S) (First name, middle initial, last name) D. W. Netzer, R. C. Bates, W. Bringham Jr., M. J. Bulman			
6. REPORT DATE 1 October 1969	7a. TOTAL NO. OF PAGES 119	7b. NO. OF REFS 22	
8a. CONTRACT OR GRANT NO. ORD-032-135/551-1/P009-06-01	8b. ORIGINATOR'S REPORT NUMBER(S) NPS-57NT9101A		
b. PROJECT NO.	8c. OTHER REPORT NO(S) (Any other numbers that may be assigned this report)		
c.			
d.			
10. DISTRIBUTION STATEMENT This document is subject to special export controls and each transmittal to foreign government or foreign nationals may be made only with prior approval of the Naval Postgraduate School, Monterey, California 93940 (Code 023).*			
11. SUPPLEMENTARY NOTES *Approval granted only upon release by Naval Ordnance Systems Command		12. SPONSORING MILITARY ACTIVITY Naval Ordnance Systems Command	
13. ABSTRACT The acceleration sensitivity of aluminized and nonmetallized composite and double-base propellants were investigated. A review of previous experimental findings and current analytical models was also conducted. Ten composite propellants were tested to accelerations of 1000g and pressures of 1000 psia to determine the effects of AP crystal size, base burning rate, pressure, the form of the molten metal on the burning propellant surface, and temperature on the acceleration sensitivity. The most dominant factor influencing acceleration sensitivity was found to be the base burning rate. The weight and form of the molten metal on the burning surface were found to be important at low accelerations. At high accelerations, the form of the molten metal was found to have more effect on augmentation than the weight. Burn time (web thickness) was also found to have a pronounced effect on the augmentation. The experimental data were compared with current analytical models and qualitative agreement was obtained. A change was proposed for the nonmetallized analytical model which yielded better agreement with the experimental data. An investigation was conducted to determine the cause(s) for the differences in burning rate augmentation data reported by various investigators. Strand length (burn time) was found to be the dominant factor. Lead and copper additives commonly found in double-base propellants were found to decrease the burning rate with increasing acceleration. Burning rate instability was also obtained at high accelerations. The addition of aluminum increased the burning rate at any given acceleration.			

